Challenges and Opportunities for Denitrifying Bioreactors in the Mid-Atlantic

Emily MacLauren Bock

Dissertation submitted to the faculty of the Virginia Polytechnic Institute and State University in partial fulfillment of the requirements for the degree of

Doctor of Philosophy
In
Biological Systems Engineering

Zachary M. Easton, Chair

Matthew J. Eick

W. Cully Hession

Kurt Stephenson

November 29, 2017

Blacksburg, VA

Keywords: denitrifying bioreactor, nitrous oxide, biochar, Mid-Atlantic

Challenges and Opportunities for Denitrifying Bioreactors in the Mid-Atlantic

Emily MacLauren Bock

Academic Abstract

Sustaining the global population depends upon modern agricultural practices reliant on large inputs of nitrogen (N) fertilizer, but export of excess N from agroecosystems has negative environmental consequences, such as accelerated eutrophication and associated water quality degradation. The challenges posed by diffuse and widespread nutrient pollution in agricultural drainage waters necessitate cost-effective, adaptable, and reliable solutions. In this context, enhanced denitrification approaches developed over the last several decades have produced denitrifying bioreactors that harness the ability of ubiquitous soil microorganisms to convert bioavailable N into inert N gas, thereby removing bioavailable N from an ecosystem. Denitrifying bioreactors are edge-of-field structures that consist of organic carbon substrate and support the activity of denitrifying soil bacteria that remove N from intercepted nutrient-enriched drainage waters. The potential to improve bioreactor performance and expand their application beyond the Midwest to the agriculturally significant Mid-Atlantic region was investigated with a three-pronged approach: 1) a pilot study investigating controls on N removal, 2) a laboratory study investigating controls on emission of greenhouse gases nitrous oxide (N_2O), methane (CH_4), and carbon dioxide (CO_2), and 3) a field study of one of the first denitrifying bioreactors implemented in the Atlantic Coastal Plain. The pilot and laboratory studies tested the effect of amending woodchip bioreactors with biochar, an organic carbon pyrolysis product demonstrated to enhance microbial activity. The pilot-scale study provides evidence that either hardwood- of softwood-feedstock biochar may increase N removal in

woodchip bioreactors, particularly under higher N loading. The results from the laboratory experiment suggest the particular pine-feedstock biochar tested may induce greater greenhouse gas emissions, particularly of the intermediate product of denitrification and potent GHG nitrous oxide. The field study evaluated performance of a biochar-amended woodchip bioreactor installed on a working farm. Two years of monitoring data demonstrated that the bioreactor successfully removed N from drainage waters, but at relatively low rates constrained by low N loading that occurred in the absence of fertilizer application during continuous soy cropping at the site (10.0 kg NO_3^--N ha^{-1} yr^{-1} or 4.86 g NO_3^- -N m^{-3} d^{-1} on the basis of bed volume reached the bioreactor.) Removal rates averaged 0.41 g m^{-3} d^{-1} (8.6% removal efficiency), significantly lower than average rates in systems receiving greater N loading in the Midwest, and more similar to installations in the Maryland Coastal Plain. Greenhouse gas fluxes were within the range reported for other bioreactors, and of the N removed an average of only 0.16% was emitted from the bed surface as N_2O. This case study provides useful measurements of bioreactor operation under low N loading that informs the boundaries of bioreactor utility, and may have particular regional relevance. The pilot and field studies suggest that wood-based biochars may enhance N removal and may not produce problematic quantities of greenhouse gases, respectively. However, the laboratory study raises the need for caution when considering the costs and benefits amending woodchip bioreactors with biochar and accounting for the effect on greenhouse gas emissions in this calculation, because the tested pine biochar significantly increased these emissions.

Challenges and Opportunities for Denitrifying Bioreactors in the Mid-Atlantic

Emily MacLauren Bock

General Audience Abstract

Modern agricultural relies on nitrogen (N) fertilizer to produce enough food for the global population, but losses of excess N from farmland has negative environmental consequences. Even with advances in best practices to reduce the environmental impact of agriculture, such as nutrient management planning where the right fertilizer is applied at the right rate at the right time, crops cannot use fertilizer with perfect efficiency and a portion will be lost to the environment. A relatively new agricultural best management practice removes this excess N before it enters surface water bodies by intercepting drainage water with high N levels at the edge of the field, slowing it down, to give the tiny creatures living in the soil the chance to use this N as energy. These naturally occurring soil bacteria remove the N fertilizer from the water by transforming it into harmless N gas that makes up nearly 80% of the atmosphere. These denitrifying bioreactors, named after the microbial N removal mechanism, are becoming established management practices in the Midwest, but they have not yet been widely adopted in other agriculturally significant regions, such as the Mid-Atlantic. In an effort to design more effective and flexible bioreactors, the effect of amending woodchip bioreactors with a charcoal-like material previously shown to increase the activity N-removing bacteria was tested and found to modestly increase N removal with sufficiently high drainage water N concentrations. However, a laboratory test of the effect of biochar on production of a harmful intermediate product of denitrification, the potent greenhouse gas nitrous oxide, found higher emissions from the biochar treatments than the woodchips alone, suggesting the N removal benefits may

not outweigh the costs. To evaluate performance under field conditions, a biochar-amendment woodchip bioreactor was installed in the Virginia Coastal Plain, and monitored for two years. N removal was significantly lower than reported rates, but this was due to a relatively low amount of N in the drainage waters. However, measuring performance under sub-optimal conditions provides useful information for determining the limits to conditions for which bioreactors are useful.

Dedication

To my husband, James W. Bock Jr., and to my mother, Jane E. Corson, for enabling this achievement through your sustaining love and support.

Acknowledgements

Thank you to my husband, James W. Bock Jr., for his unwavering support of my academic endeavors and for all the joy he brings to our life together. I am so thankful that you have been on this journey with me. Thank you to my mother, Jane E. Corson, who has instilled the drive for achievement and confidence in my ability to succeed, and my brother, Daniel C. Lassiter, who constantly inspires me to set goals for myself both personally and professionally. Thank you to Tom Jancowski for your kindness and wisdom. My family has always upheld the value of education as paramount, and left me with no doubt in the value of my pursuits on an engaging, challenging, and rewarding career path. Thank you to my in-laws, Trish and Jim Bock and their daughter Erika, for always believing in me.

Zachary Easton, my mentor and committee chair, continues to encourage my professional growth and inspire me to succeed. His admirable work ethic and record of achievement motivate me as does his confidence in me. I sincerely thank him for his guidance and friendship. Matthew Eick, Cully Hession, and Kurt Stephenson have served as committee members during endeavors and provided valuable encouragement, criticism, and support.

A special thanks to Brady Coleman for his collaborative efforts and friendship, Justin Haber for his assistance in the laboratory and field, and to Easton lab group members for your contributions and comradery. And to Catherine Flemming; you are an inspiration.

Thank you to a very special Labrador retriever, Cornbread Elizabeth Bock, for your unconditional affection.

Funding for this research was provided by a Conservation Innovation Grant from the Natural Resources Conservation Service.

Table of Contents

Attribution

This dissertation is organized in manuscript format, with sections 2, 3, and 4 constituting individual documents. The following describes the contributions of coauthors and publication status of each manuscript. Section 2 is a manuscript by the same title, "Effect of biochar on nitrate removal in a pilot-scale denitrifying bioreactor," published in the Journal of Environmental Quality (2016). The coauthors are Emily Bock, Brady Coleman, and Zachary Easton. Emily Bock, PhD Candidate, Department of Biological Systems Engineering, Virginia Tech, Blacksburg VA, designed the experiment, collected and analyzed samples, conducted statistical analysis, and wrote the manuscript. Brady Coleman, graduate student, Department of Biological Systems Engineering, Virginia Tech, Blacksburg VA, assisted in water sample collection and analysis as well as provided supporting work in the laboratory. Zachary Easton, Associate Professor, Department of Biological Systems Engineering, Virginia Tech, Blacksburg VA, reviewed and edited the manuscript, as well as provided input on experimental design and statistical analysis. This work was funded in part by a grant from the Virginia Tech Institute for Critical Technology and Applied Science, by a grant from the Virginia Secretary of Natural Resources, and by the USDA–NRCS– CIG program.

Section 3 is a manuscript in preparation for submission to the Journal of Environmental Quality in December, 2017. The coauthors are Emily Bock, Brady Coleman, Zachary Easton, and Kurt Stephenson, Professor, Agriculture and Applied Economics, Virginia Tech, Blacksburg, VA. Emily Bock designed the site monitoring equipment system, designed and executed the sampling regime, conducted gas flux measurements in the field, analyzed aqueous samples, processed data, conducted the statistical analysis, and wrote the manuscript. Brady assisted in

sample collection and analysis as well as provided supporting work in the laboratory. Zachary Easton and Kurt Stephenson reviewed and edited the manuscript. This work was funded by the USDA-NRCS-CIG program.

Section 4 is a manuscript in preparation for submission to the Journal of Environmental Quality in December, 2017. The coauthors are Emily M. Bock, Brady Coleman, and Zachary M. Easton. This a study of greenhouse gas (GHG) flux from laboratory-scale bioreactors, which is a companion study to an experiment simultaneously conducted by Brady Coleman, who reports the results of the aqueous analysis in his thesis entitled "Impact of biochar amendment, hydraulic retention time, and influent concentration on N and P removal in horizontal flow-through bioreactors." Emily Bock collaborated in development of experimental design, particularly regarding measurement of GHG flux, assisted with aqueous and gas sampling, conducted analysis of aqueous samples, processed data, calculated gaseous fluxes, performed statistical analysis, and wrote the manuscript. Brady Coleman led the experimental design, conducted most aqueous and gas sampling, performed statistical analysis of aqueous data with assistance from Emily Bock and Zachary Easton. Zachary Easton also contributed to experimental design and reviewed and edited the manuscript.

Citation of published manuscript:

Bock, E. M., B. Coleman, Easton, Z.M., 2016. Effect of biochar on nitrate removal in a pilot-scale denitrifying Bioreactor. 2016. J. Environ. Qual. 45:762–771. doi:10.2134/jeq2015.04. 0179

1 INTRODUCTION

1.1 Problem Statement

Artificial drainage of agricultural land increases productivity and promotes soil conservation, but a large body of research links artificial drainage to increased nutrient export to water bodies, resulting in degradation of water quality as observed on a grand scale as the hypoxic zone in the Gulf of Mexico (Dinnes et al., 2002; Gentry et al., 2000; Ikenberry et al., 2014; Kladivko et al., 1991). With over 36.8 million ha of drained cropland in the US according to the 2012 census of agriculture (USDA NASS, 2012), best management practices (BMPs) are essential tools to mitigate this nonpoint source nutrient pollution, including structural practices such as riparian buffers and non-structural practices such as nutrient management planning. Denitrifying bioreactors (also termed woodchip bioreactors, biofilters, permeable reactive barriers) are a relatively recent addition to the suite of agricultural BMPs to address water quality concerns, developed primarily in the US Midwest to remove excess nitrogen (N) from subsurface (tile) drainage. These edge-of-field practices are lined beds containing organic carbon media, typically woodchips, that intercept N-enriched drainage water and support the activity of denitrifying microorganisms that convert bioavailable nitrate (NO_3^-) to inert dinitrogen gas (N_2) under anaerobic conditions when the bed becomes saturated. Bioreactors have moved beyond proof-of-concept in the last several years (Christianson and Schipper, 2016), as evidenced by recent incorporation into state-level nutrient reduction strategies for Illinois (Illinois Department of Agriculture, 2014), Iowa (Iowa Department of Agriculture, 2016), and Minnesota (Minnesota Pollution Control Agency, 2015). Although bioreactors have been successfully used to remove an average of 35-50% of the N load in drainage waters and

increased adoption is expected to translate into water quality benefits (USDA-NRCS, 2015), the potential negative impacts of widespread bioreactor implementation are emphasized in recent evaluations of pollution swapping potential (Easton et al., 2015; Fenton et al., 2016; Healy et al., 2015, 2012; Weigelhofer and Hein, 2015). Pollution swapping in bioreactors is the trade-off between the environmental benefits of removing excess N and potential negative impacts of harmful byproducts such as greenhouse gas (GHG) emissions, methylmercury production via sulfate reduction, increased biological oxygen demand, or release of ammonium (NH_4^+) or phosphate (PO_4^{3-}). Indeed, a recent meta-analysis of woodchip bioreactor studies emphasizes the need for a holistic assessment of bioreactor systems, considering the production of these byproducts (Addy et al., 2016).

Potential drawbacks of managed denitrification include the release of nitrous oxide (N_2O), an intermediate product of denitrification and powerful GHG with nearly 300 times the global warming potential of carbon dioxide (CO_2); (IPCC, 2007). The potential for GHG emissions motivated investigation into the ability to promote complete denitrification (to N_2) over partial denitrification resulting the release of N_2O with substrate amendment (Bock et al., 2015). A simple benchtop batch experiment demonstrated enhanced N and P removal and reduced N_2O production in woodchip bioreactors with the addition of biochar. Biochar is an organic carbon pyrolysis product previously found to reduce N leaching and GHG emissions from agricultural soils (Clough and Condron, 2010), suggesting that biochar may increase denitrification rates and favor complete denitrification to N_2 over partial denitrification halting at N_2O production and resulting in emissions (Bock et al, 2015). These findings spurred further investigation of the effect of biochar amendment on bioreactor efficiency, which was undertaken with flood-and-

drain experiments of paired woodchip and biochar-amended pilot-scale bioreactors presented in Section 2.

Although N_2O production in bioreactors has been recognized as potentially problematic (e.g., Schipper et al., 2010), and bioreactor GHG fluxes quantified in several laboratory and field studies (Elgood et al., 2010; Feyereisen et al., 2016; Moorman et al., 2010; Warneke et al., 2011c), questions remain regarding the factors controlling GHG production bioreactors. To evaluate the effect of nutrient loading and hydraulic residence time (HRT), factors know to govern N removal in bioreactors (Warneke et al., 2011d), a replicated, full factorial experiment with laboratory-scale column bioreactors was conducted, which is presented in Section 3. Previous work demonstrating the potential to reduce N_2O emissions from woodchip bioreactors motivated with biochar addition (Bock et al., 2015; Easton et al., 2015), this experiment was also designed to test the effect of 10% and 30% volumetric additions of biochar.

As bioreactor technology continues to develop and these systems become more effective at reducing agricultural N export, interest in their application beyond the Corn Belt is growing. Unfortunately, much of the work on drainage and drainage water management conducted in the Midwest and has yet to be suitably tested in other agriculturally significant regions such as the Mid-Atlantic. Thus, substantial as of yet unexplored opportunities with respect to advancing bioreactor design toward more flexible implementation in a variety of agricultural systems remain. To test bioreactor performance in a system more typical of agriculture in the Mid-Atlantic, a full-scale bioreactor was installed in a tile-drained field in the Virginia Coastal Plain in fall 2014 and monitored through the first two-years of its usage. Nutrient removal efficiency and GHG emissions are reported in Section 4.

The subsequently described work aims to support further advancement of bioreactor design through substrate engineering to enhance N removal while reducing unintended pollutant production, namely GHG emissions, and demonstrating the performance of one of the first bioreactors installed in the Atlantic Coastal Plain.

1.2 Research Objectives

This research focuses on opportunities to advance bioreactor design and implementation strategies and improve water quality in agroecosystems by expanding application beyond single-target treatment. The aim of this work is to deepen understanding of factors controlling GHG emissions, and translating this successful best management practice from the US Midwest to the Mid-Atlantic agricultural systems. Substrate engineering is the main approach explored to maximize complete denitrification while minimizing GHG emissions and removing dissolved reactive phosphorus (DRP). These aims are addressed by three individual studies presented in Sections 2-4, which combine laboratory experiments and field methods to evaluate the effect of biochar amendment on woodchip bioreactor performance. The objectives of each study were:

1. Pilot study: to determine the effect of biochar addition on N removal in woodchip bioreactors.
2. Laboratory study: to determine the effect of biochar amendment on emission of N_2O, CH_4, and CO_2 in woodchip bioreactors.
3. Field study: to quantify removal of N and P and measure emissions of N_2O, CH_4, and CO_2 of a biochar-amended woodchip bioreactor installed in the Atlantic Coastal Plain.

1.3 Organization of Thesis

This document consists of an introduction and literature review providing context and motivation (Section 1), a journal article published in the Journal of Environmental Quality describing a pilot-scale experiment assessing effect of biochar amendment to woodchip bioreactors on N removal (Section 2), a manuscript prepared for submission to a peer-reviewed journal describing N removal, GHG emissions, and controlling variables in a field-scale woodchip and biochar bioreactor in the Virginia Coastal Plain (Section 3), a manuscript prepared for submission to a peer-reviewed journal describing the a laboratory experiment to determine effect of biochar-amendment, nutrient loading, and hydraulic residence time in woodchip bioreactors (Section 4), followed by a summary and outlook for future research (Section 5).

1.4 Literature Review

The overarching goal of the proposed work is to improve water quality, with a particular focus on opportunities in the Chesapeake Bay watershed, by contributing to the development of denitrifying bioreactors that can be implemented strategically as part of a broader management scheme to mitigate excess reactive N, as well as phosphorus (P) and GHG emissions, associated with agricultural production. To place these efforts in context, the following literature review includes an overview of agricultural nutrient pollution generation and impacts, the use of denitrifying bioreactors to mitigating this pollution, ongoing concerns regarding pollution swapping, the potential of biochar amendment to improve performance, and status of bioreactor research and application in the Mid-Atlantic.

1.4.1 Anthropogenic nitrogen and denitrification management

Much of the increase in agricultural productivity over the last century is attributable to the increased usage of N fertilizers (Erisman, 2004). Smil (2001) estimated that 40% of the world's population would not have survived if the anthropogenic alteration of the carbon cycle by industrial fertilizer production. However, excess reactive N underlies a suite of environmental and health problems. Environmental degradation resulting from elevated N levels includes eutrophication of receiving water bodies, global acidification, stratospheric ozone depletion, and tropospheric accumulation of ozone and aerosols, which can lead to respiratory illness, cardiac disease, and cancer in humans (Dinnes et al., 2002; Driscoll et al., 2003; Galloway et al., 2003). N can contaminate potable water, high concentrations of NO_3^- being toxic to infants and livestock, resulting in methemoglobinemia, while NO_3^--N reacting with secondary amines forms carcinogenic nitrosamines (Averill and Tiedje, 1982; Ayres, 1997; Gruber and Galloway, 2008; Trudell et al., 1986). Galloway (2003) introduced the term "nitrogen cascade" to describe the accumulating effects that result from temporary storage of reactive N in its various chemical forms as it is transported through the environment by water and air, each atom resulting in multiple, and potentially deleterious, consequences. Disruption of the global N cycle also has a multitude of potential impacts on the other major chemical cycles of carbon, P, and sulfur, which have become a topic of increasing study, particularly with respect to global climate change (Ayres, 1997; Gruber and Galloway, 2008; Rabalais et al., 2009). Mitigating the effects of anthropogenic N inputs is vital to protection of our health and natural resources while continuing to produce food and energy for a growing population. Appropriately, the National Academy of Engineering has cited management of the global N

cycle as one of the 14 Grand Challenges for Engineering in the 21st century (NAE, 2016). This priority is echoed by the N pollution control goals set by both the United States and Europe (Melillo and Cowling, 2002).

The global nitrogen cycle consists of biochemical and physiochemical processes that transform as well as the hydrologic and atmospheric mechanisms that transport N species. Historically, most ecosystems have been N limited because the largest reservoir of N is inert dinitrogen gas (N_2), comprising 78% of the atmosphere (Galloway et al., 1995); few organisms are capable of fixing nitrogen, converting N_2 to biologically available, reactive forms (N_r) (Ayres, 1997; Galloway et al., 1995). Drastic increases in anthropogenic reactive N inputs to the environment have resulted from the doubling of the conversion of atmospheric N to reactive N through the combustion of fossil fuels, intense cultivation of legumes and other crops that depend on N fixation in the rhizosphere (e.g. rice), and the use of industrial fertilizer produced by the Haber-Bosch process, primarily in agriculture (Gruber and Galloway, 2008; Seitzinger et al., 2006). Denitrification is the link completing the N cycle by converting reactive N back to N_2, the only ability to remove N from the reactive pool other than the relatively recently discovered anaerobic oxidation of ammonium (anammox) (Burgin and Hamilton, 2007). Delwiche (1970) concluded that the transformation between the reactive and nonreactive pools of N was balanced prior human activities, but today we face a different reality. Denitrification has not kept pace with increased inputs of reactive N, and has often been spatially separated from reactive N sources through the destruction of ecosystems in which denitrification naturally occurs, such as riparian buffers and wetlands (Schipper et al., 2010a). As a result, net

accumulation of reactive N is occurring and projected to increase with the human population (Ayres, 1997; Galloway et al., 2003).

Denitrification is the microbially mediated stepwise reduction of NO_3^- to N_2 gas. Organic carbon serves as an energy source and the electron donor for this reduction-oxidation reaction, and a N oxyanion (NO_3^-, NO_2^-) or oxide (NO, N_2O) serves as the terminal electron acceptor in the absence of oxygen: $NO_3^- \Rightarrow NO_2^- \Rightarrow NO \Rightarrow N_2O \Rightarrow N_2$, utilizing an organic source and producing CO_2 and H_2O at each step (Istok et al., 1997). Excluding anammox, denitrification is the only transformation that removes reactive N from an ecosystem by transforming reactive N to its inert form. Denitrification is conducted mainly by heterotrophic bacteria, but also by some chemolithic and autotrophic bacteria, Archaea, and fungi (Mateju et al., 1992; Zumft, 1997). The heterotrophic denitrifying bacteria are taxonomically diverse and ubiquitous in surface water and the subsurface, both soil and groundwater (Rivett et al., 2008). Denitrification serves as the basis for N removal in traditional municipal wastewater treatment, coupled nitrification-denitrification being the single most common method to reduce N in wastewater (Mulder et al., 1995).

Denitrification management, harnessing this naturally occurring microbial process promoting reactive N removal throughout the cascade, is increasingly recognized as an essential component of managing the global N cycle, especially with respect to diffuse pollution (Kumar and Lin, 2010; Seitzinger et al., 2006). Denitrification management is thought to have some of the highest potential in agro-ecosystems, the single largest source of reactive N entry into the cascade (Seitzinger et al., 2006, Schipper et al., 2010a). Globally, 75% of anthropogenic N_r is utilized in agro-ecosystems, of which approximately half is lost to the atmosphere (NH_3,

NO, N_2O, N_2) or to water (NO_3), and produces harmful effects as it moves through the environment in its bioavailable form; complete denitrification to N_2 only accounts for a minor portion (Galloway et al., 2003). Most of the N that is lost from agro-ecosystems is leached to groundwater and ultimately discharged into surface water bodies, contributing to downstream eutrophication (Mitch et al., 2001). The form most often associated with water quality problems is NO_3^- (Novotny, 2003), because it is easily transported by water and due to its negative charge is not appreciably adsorbed to soil colloids like ammonium (Mitsch et al., 2001). Even with the extensive implementation of agricultural BMPs such as nutrient management plans dictating the appropriate rates and timing of fertilizer applications for a given crop, fertilizer use efficiency will never reach 100%, so additional management is required. Consequently, managing agricultural landscapes to increase denitrification is gaining momentum (Schipper et al., 2010). Examples include preserving ecosystems that support naturally high rates of denitrification in saturated soil environments, such as wetlands and riparian buffers. However, land conservation or ecological engineering, e.g. creating constructed wetlands, has a substantial footprint that my take land out of production and consequently may not be a viable option. This need to harness the biochemical process of denitrification in agricultural landscapes with a smaller footprint drove the development of denitrifying bioreactors.

Denitrifying bioreactors are edge-of-field structures designed to remove excess N from agricultural drainage by provide habitat favorable to anaerobic heterotrophic denitrification, which consists of an organic carbon substrate saturated with intercepted, nutrient-rich drainage water. Indeed, artificial drainage of agricultural systems, which is necessary to

increase productivity of poorly drained soils and has been historically significant in creating some of the most agronomically productive land in the United States, exacerbates nutrient export. Yet these relatively concentrated flows provide a unique opportunity for treatment that denitrifying bioreactors are designed to exploit.

1.4.2 Denitrifying bioreactors

Fundamentally, a bioreactors consist of organic carbon substrate that becomes saturated with sufficient duration and frequency to develop anoxic conditions and support the activity of denitrifying microorganisms. Denitrification has been confirmed to be the main mechanism of NO_3^- removal, as opposed to temporary immobilization or cycling between bioavailable forms, in both laboratory (Gibert et al., 2008; Warneke et al., 2011) and field studies (Greenan et al., 2006; Robertson, 2010; Warneke et al., 2011). A large variety of carbon substrates for use in bioreactors have also been tested in the laboratory setting, including maize cobs, green waste, wheat straw, and a variety of cellulose based media (Cameron and Schipper, 2010; Gibert et al., 2008; Greenan et al., 2006; Saliling et al., 2007). However, wood-based media is by far the most common carbon media that has been utilized in the field (Blowes et al., 1994; Elgood et al., 2010; Long et al., 2011; Moorman et al., 2010; Robertson and Cherry, 1995; Schipper and Vojvodić-Vuković, 2000). Several hydraulic designs, reported by Schipper et al. (2010b), have been implemented including streambed structures, upflow bioreactors, layers that receive effluent from above, unlined walls receiving shallow groundwater, and lined beds where the influent and effluent are piped. Field-scale applications have included various sources of NO_3^--laden waters such as greenhouse effluent (Warneke et al., 2011a), septic system effluent (Rambags et al., 2016; Robertson et al., 2008; Robertson and

Cherry, 1995), wastewater (Christianson et al., 2016), shallow groundwater (Robertson et al., 2000; Schipper et al., 2005), aquaculture (Lepine et al., 2016). However, treatment of agricultural drainage is the most common use of bioreactors (e.g. Blowes et al., 1994; Christianson et al., 2013a; David et al., 2016; Hartz et al., 2017; Woli et al., 2010). Denitrifying bioreactors have been successfully implemented in agricultural settings to intercept shallow groundwater flow, treat subsurface (tile), and, more recently, interfaced with ditch drainage systems (Rosen and Christianson, 2017). Lined woodchip beds receiving subsurface (tile) drainage have emerged as the dominant bioreactor design for agricultural systems, having proven to sustain N removal rates up to 15 years with minimal maintenance while receiving variable influent flow rates and N concentrations (Robertson et al., 2000).

Factors controlling the N removal rates in denitrifying bioreactors have widely been studied in field and laboratory and include temperature, influent NO_3^- concentration, hydraulic residence time (HRT), bed dimensions, pH, dissolved oxygen concentration, cycles of wetting and drying, and properties of the organic carbon media, specifically the age, type carbon to N ratio, substrate particle size, hydraulic conductivity (Addy et al., 2016; Christianson et al., 2013b; David et al., 2016; Greenan et al., 2009; Pluer et al., 2016; Schmidt and Clark, 2013; Sharrer et al., 2016; Warneke et al., 2011e). A recent meta-analysis of woodchip bioreactors emphasized the importance of HRT, bed age, and N limitation, and temperature as within-bed constraints N removal (Addy et al., 2016). Addy et al. (2016) also emphasized that both field- and watershed-scale factors also affect bioreactor performance, particularly the amount of flow received by the bioreactor, as bypass flows can be substantial but essential for maintaining functionality of drainage systems as demonstrated by Christianson et al. (2013a). In sum, the

controls on N removal in bioreactors are relatively well understood and bioreactors are moving beyond proof of concept based upon a foundation of research establishing achievable N removal (Christianson and Schipper, 2016).

1.4.3 Bioreactor pollution swapping potential

Earlier work focused on robust quantitative assessments of performance, as defined by N removal efficiency, but more recent efforts are taking a broader perspective that considers opportunities to expand the functionality of bioreactors to target other pollutants or to minimize production of harmful byproducts. These aims can be synergistic. For example, leveraging bioreactors to remove P from drainage water, both in response to the P export observed in some woodchip beds (e.g. Healy et al., 2012) and to treat high P loads often occurring concurrently with excess N in drainage waters (King et al., 2015), is a natural extension of the technology.

The accumulation of any of intermediates denitrification products (NO_2, NO, and N_2O), although generally thought to occur only in low levels, is worthy of consideration because of their severe consequences, NO_2 reacting to form a carcinogen and NO and N_2O being potent GHGs. Significant GHG production has been observed in other N removal systems utilizing denitrification including constructed wetlands, which have been shown to act as both sources and sinks of N gases, occasionally producing high emissions of N_2O (Søvik and Mørkved, 2007). Although the production of GHGs has been cited as a potential drawback to bioreactor implementation (Robertson, 2010; Schipper et al., 2010b), only four studies have attempted to quantify N_2O emissions from field-scale in situ bioreactors: (Elgood et al., 2010; Mooreman et al., 2010; Warneke et al., 2011; Woli et al., 2010)

The factors controlling accumulation and release of denitrification intermediate products have yet to be fully identified. Initial evidence from laboratory testing does suggest that bioreactor GHG emissions are low under the appropriate conditions. Mooreman et al. (2010) presented encouraging findings that nitrous oxide emissions from bioreactors are lower than those from agricultural land or N polluted streams. However, a soil core study by Warneke (2011) showed that factors such as increased temperature and certain substrate types, likely due to the higher labile carbon content (e.g. maize cobs), can increase N_2O production via denitrification (Warneke et al., 2011), although significant N_2O production was not observed in the woodchip treatment. Although these emissions were low in the relatively stable laboratory environment, in the field where influent NO_3^- concentrations and saturation conditions fluctuate with precipitation events and seasonality of the water table, emissions cannot be predicted and warrant investigation in situ (Moorman et al., 2010). Investigation of novel organic carbon substrates in bioreactors may provide an opportunity to mitigate N_2O emissions. The application of biochar has been found to reduce N_2O production, as well as reducing leaching of N and P in agricultural soils.

1.4.4 Biochar to enhanced bioreactor performance

Biochar, as defined by the International Biochar Institute (IBI), is “a solid material obtained from thermochemical conversion of biomass in an oxygen limited environment” which is distinguished from charcoal by its intended application as a soil amendment (IBI, 2014, McLaughlin et al., 2009, Verheijhen et al., 2010). Biochar is also associated with energy production during low temperature pyrolysis (burning at less than 700 C with little to no oxygen present) of biomass, in which the gasses given off are used to produce heat, electricity or

biofuel (Lehmann et al,. 2011). Long-term carbon sequestration is cited as a driving application of biochar and excites interest in its ability to mitigate climate change (Clough and Condron, 2010; IBI, 2014; Lehmann et al., 2011; Singh et al., 2010). Biochar is termed carbon net-negative because more CO_2 is removed from the atmosphere during biomass growth and then is released during pyrolysis, transforming the biomass into more stable biochar, which can remain in the soil for hundreds to thousands of years (Fruth and Ponzi, 2010; Renner, 2007).

Biochar application is also associated with improvement of soil function via increased cation exchange capacity (CEC), soil water retention, and enhanced microbial growth (Christianson et al., 2011; Lehmann et al., 2011; McLaughlin et al., 2009), as well as increased crop yields in some cases (Beck et al., 2011). General characteristics of biochars underlying induced soil properties include high specific surface area and high micropore volume, which cause biochar to be an effective sorbent (Kookana et al., 2011). Logically, biochar amendment also impacts N and P cycling by changing the physiochemical soil environment and consequently altering the structure and activity of the microbial community (Anderson et al., 2011), although the effects on nutrient transformations and interrelated mechanisms are incompletely understood (Clough and Condron, 2010; Nelson et al., 2011). However, biochar application to soil has been shown to reduce leaching of N, P, and organic carbon (Beck et al., 2011).

In a review "Biochar and the Nitrogen Cycle: Introduction" Clough and Condron (2010) summarize the findings of studies on biochar and N:

> "studies have suggested or shown that biochar has the ability (i) to retain N within soils by enhancing ammonia (NH_3) and ammonium (NH_4) retention, (ii) to reduce nitrous

oxide (N_2O) and nitrate leaching (NO_3-) fluxes, and (iii) to enhance biological N fixation and beneficially influence soil microbial communities."

For example, Singh et al. (2010) demonstrated that biochar reduces emissions of N_2O emissions and ammonium leaching after four months. Independently, oxidation of biochar has been shown to increase cation exchange capacity, which could account for the retention of ammonium (Clough and Condron, 2010). Raising the soil pH with the addition of alkaline biochar may also contribute to reduced N_2O emissions (Clough and Condron, 2010), as increasing pH has been shown to favor the production of N_2 over the accumulation of N_2O during denitrification (Firestone et al., 1980). Other studies have shown that biochar amendment has increased N_2O emissions (Yanai et al., 2007), which is likely due to the resultant increase in water holding capacity that allows anaerobic microsites supporting denitrification to persist longer. Factors identified in the literature impacting N_2O:N_2 during denitrification include soil water content as a function of soil type, pH, microbial respiration rates, available carbon, and soil NO_3- content (Clough and Condron, 2010; Firestone et al., 1980; Parton et al., 1996).

Consequently, biochar amendment can reduce runoff quantity while improving the water quality and potentially reduce GHG emissions. However, due to the variety of feedstocks (biomass) and pyrolysis conditions utilized, biochars are in practice a heterogeneous group of materials (Kookana et al., 2011). Many researchers point out the futility of reporting responses to biochar addition without sufficient characterization of the material (McLaughlin et al., 2009). The IBI (2014) has developed both a biochar certification program for biochars which meets the IBI Biochar Standards, which "provide[s] common reporting requirements for biochar that will

aid researchers in their ongoing efforts to link specific functions of biochar to its beneficial soil and crop impacts."

Biochar is of particular in interest for application in denitrifying bioreactors not only for its capacity to reduce nutrient leaching, but also because its organic matter is more resistant to degradation than the original biomass and can provide a long-term carbon source for the heterotrophic denitrifying microbes. However, its half-life is the subject of debate and likely varies with feedstock and pyrolysis conditions (Lehmann et al., 2011). The utility of bioreactors relies on supplying sufficient labile (easily degraded) organic carbon so that the rate of denitrification is not reduced due to carbon limitation, but also maintaining a stock of organic carbon over the long-term (on the order of decades) for the system to remain self-reliant and maintenance free. Therefore, biochar may hold promise for both reducing nutrient export from bioreactors and increasing their lifespans.

Currently, only one study has been published that addresses the use of biochar in a bioreactor. Christianson et al. (2011) examined the effect of fresh biochar addition to a seven-year-old woodchips (*Pinus radiata*) in a laboratory-scale column experiment, hypothesizing that amendment would increase NO_3^- removal while decreasing the ammonium loss. Two application rates, 7% and 14% by dry weight, of *P. radiata* biochar prepared at three pyrolysis temperatures were compared. No significant differences between the biochar treatments and the control (woodchips only) were observed during this trial. However, the effect of biochar amendment in a bioreactor at the field scale should not be extrapolated from the results of this incubation experiment due to the short duration of the study (3 days), the freshness of the biochar, and differences in environmental conditions between a controlled laboratory and

fluctuating field conditions. Christianson et al. (2011) acknowledge that the aging effect of biochar may increase adsorption capacity that would be expected to result in increased retention of NH_4^+ and other cations. Biochar incorporation into bioreactors merits further investigation.

1.4.5 Adapting bioreactors to the Mid-Atlantic

Adaptation of denitrifying bioreactors to the Mid-Atlantic region is driven by water quality improvement goals for the Chesapeake Bay, and a nascent yet strong interest in incorporating these practices into management strategies exists (Christianson et al., 2017). However, agricultural systems in the Mid-Atlantic differ substantially from those in the Midwest, particularly with regard to agricultural drainage. Midwestern agriculture is largely reliant on poorly drained Mollisols that require extensive drainage to cultivate. Most fields are drained with a patterned tile network feeding large mains that provide obvious opportunities for bioreactors. In contrast, cropping systems in the Mid-Atlantic are much more variable, fields tend to be smaller, and drainage, if required, is accomplished mainly with ditching and to a small extent subsurface tile drainage. The tile drainage systems that do exist tend to target saturated areas in the field rather than uniformly drain the entire field. Consequently, adapting bioreactors to the Mid-Atlantic is more complex than transplanting bioreactors designed to treat tile drainage. Early work has begun to design bioreactors that treat ditch drainage in the Maryland Coastal Plain, but modifying bioreactor design for use with surface drainage networks in areas with nearly flat slopes (<2%) and shallow water tables presents a challenge (Christianson et al., 2017; Rosen and Christianson, 2017). Christianson et al. (2017) point out that while Midwestern drainage systems also have relatively low gradients, the larger size of

the drainage networks provides sufficient head differences to interface bioreactors with tile drainage outlets. Furthermore, expected flowrates from tile systems can easily be calculated for the purposes of bioreactor sizing. In contrast to the piped influent supplied to tile bioreactors, drainage ditch networks are fed by runoff and shallow groundwater and design innovations are required to interface bioreactors with these networks.

Three approaches to incorporating bioreactors into ditch drainage systems were evaluated by Christianson et al. (2017) to determine their suitability for application in the Mid-Atlantic Coastal Plain. The three designs were a ditch diversion bioreactor, which receives ditch drainage via the same type of water control structure used in tile bioreactors and subsurface drainage water management, an in-ditch bioreactor, where woodchips and gravel are installed in the excavated bottom of a drainage ditch, and a sawdust wall running parallel to a drainage ditch intercepting shallow groundwater. All designs demonstrated feasibility of bioreactor implementation in surface drained agricultural systems typical of the Mid-Atlantic, but performance assessment is only preliminary for the in-ditch and sawdust wall bioreactors, where only concentration reductions, as opposed to the more comprehensive metric loading reductions, with 65% and over 90% of influent N removed, respectively. For the ditch diversion bioreactor, which followed the design methods developed for tile bioreactors, both flow through the bioreactor and bypass flow were measured in addition to N concentrations of the influent and effluent, establishing a 25% reduction in N load with removal rates averaging 0.97 g NO_3^--N m^{-3} d^{-1}. Rosen and Christianson (2017) also provide a positive proof of concept for bioreactor application in the Mid-Atlantic Coastal Plain with a comprehensive assessment of three bioreactors treating tile effluent from networks draining approximately 25 to 40 ha,

reporting rates of 0.21 to 5.36 g NO_3^--N m^{-3} d^{-1} with removal efficiencies of 9.0 to 62%. These mass removal rates are comparable to the mean N removal of 4.7 g NO_3^--N m^{-3} d^{-1} reported for denitrifying beds in a recent meta-analysis by Addy et al. (2016), and closely aligned with rates reported for low influent concentrations (< 10 mg NO_3^--N l^{-1}) of 1.0 to 4.9 g NO_3^--N m^{-3} d^{-1}.

Significant opportunities for denitrifying bioreactors in the Mid-Atlantic are increasingly recognized and supported by examples of successful application, but the main challenges are refining design of bioreactors for use in ditch drainage networks while anticipating the need for site-specific flexibility (Christianson et al., 2017), and overcoming barriers to voluntary adoption, namely high initial costs of installation combined with a lack of direct incentive payments for N removal in the absence of nutrient trading programs (DeBoe et al., 2017). Developing standard design criteria like those available for tile bioreactors a more complex endeavor given the diversity in hydraulic designs needed to treat ditch drainage in different scenarios. For example, quantifying N removal is requisite to establishing design standards but for bioreactor walls passively fed by shallow groundwater consistent calculations of load removal are not possible without standardized regional estimates of groundwater flowrates (Christianson et al., 2017). Maintenance challenges have already been identified for in-ditch bioreactors with respect to sediment deposition and clogging, suggesting more applied research and design iterations are needed to translate the success of bioreactors to the Mid-Atlantic. However, meeting the first challenge of developing flexible and well-supported design standards for different types of ditch system bioreactors may create additional opportunities for incentivizing adoption, such as cost-sharing through the Natural Resources Conservation Service.

1.5 References

Addy, K., Gold, A.J., Christianson, L.E., David, M.B., Schipper, L.A., Ratigan, N.A., 2016. Denitrifying bioreactors for nitrate removal: a meta-analysis. J. Environ. Qual. 45(3):873–881. doi:10.2134/jeq2015.07.0399

Anderson, C., Condron, L., Clough, T., Fiers, M., Stewart, A., Hill, R., Sherlock, R., 2011. Biochar induced soil microbial community change: Implications for biogeochemical cycling of carbon, nitrogen and phosphorus. Pedobiologia. 54(5-6):309-320. doi: 10.1016/j.pedobi.2011.07.005

Averill, B., Tiedje, J., 1982. The chemical mechanism of microbial denitrification. FEBS Lett. 138(1):8-12. doi: 10.1016/0014-5793(82)80383-9

Ayres, R., 1997. Integrated assessment of the grand nutrient cycles. Environ. Model. Assess. 2(3):17-128. doi: 10.1023/A:1019057210374

Beck, D., Johnson, G., Spolek, G., 2011. Amending greenroof soil with biochar to affect runoff water quantity and quality. Environ. Pollut. 159(8-9):2111-2118. doi: 10.1016/j.envpol.2011.01.022

Blowes, D.W., Robertson, W.D., Ptacek, C.J., Merkley, C., 1994. Removal of agricultural nitrate from tile-drainage effluent water using in-line bioreactors. J. Contam. Hydrol. 15(3):207–221. doi:10.1016/0169-7722(94)90025-6

Bock, E., Smith, N., Rogers, M., Coleman, B., Reiter, M., Benham, B., Easton, Z.M., 2015. Enhanced nitrate and phosphate removal in a denitrifying bioreactor with biochar. J. Environ. Qual. 44(2):605-613. doi:10.2134/jeq2014.03.0111

Bock, E.M., Coleman, B., Easton, Z.M., 2016. Effect of biochar on nitrate removal in a pilot-scale denitrifying bioreactor. J. Environ. Qual. 45(3):762-771. doi:10.2134/jeq2015.04.0179

Bruun, E.W., Müller-Stöver, D., Ambus, P., Hauggaard-Nielsen, H., 2011. Application of biochar to soil and N_2O emissions: potential effects of blending fast-pyrolysis biochar with anaerobically digested slurry. Eur. J. Soil Sci. 62(4):581–589. doi:10.1111/j.1365-2389.2011.01377.x

Burgin, A., Hamilton, S., 2011. Have we overemphasized the role of denitrification in aquatic ecosystems? A review of nitrate removal pathways. Front. Ecol. Environ. 5(2):89-96. doi: 10.1890/1540-9295(2007)5[89:HWOTRO]2.0.C

Burke, P.M., Hill, S., Iricanin, N., Douglas, C., Essex, P., Tharin, D., 2002. Evaluation of preservation methods for nutrient species collected by automatic samplers. Environ. Monit. Assess. 80(2):149–173. doi:10.1023/A:1020660124582

Cameron, S., Schipper, L., 2010. Nitrate removal and hydraulic performance of organic carbon for use in denitrification beds. Ecol. Eng. 36(11):1588-1595. doi: 10.1016/j.ecoleng.2010.03.010

Case, S.D.C., McNamara, N.P., Reay, D.S., Stott, A.W., Grant, H.K., Whitaker, J., 2015. Biochar suppresses N_2O emissions while maintaining N availability in a sandy loam soil. Soil Biol. Biochem. 81:178-185. doi:10.1016/j.soilbio.2014.11.012

Christianson, L.E., Bhandari, A., Helmers, M.J., 2011. Pilot-scale evaluation of denitrification drainage bioreactors: reactor geometry and performance. J. Environ. Eng. 137(4):213–220. doi:10.1061/(ASCE)EE.1943-7870.0000316

Christianson, L.E., Bhandari, A., Helmers, M.J., 2011b. Potential design methodology for agricultural drainage denitrification bioreactors. World Environmental and Water Resources Congress 2011. American Society of Civil Engineers, Reston, VA, pp. 2740–2748. doi:10.1061/41173(414)285

Christianson, L.E., Hedley, M., Camps, M., Free, H., Saggar, S., 2011c. Influence of biochar amendements on denitrificaiton bioreactor performance. Report. Massey University.

Christianson, L.E., Christianson, R., Helmers, M., Pederson, C., Bhandari, A., 2013a. Modeling and calibration of drainage denitrification bioreactor design criteria. J. Irrig. Drain. Eng. 139(9): 699–709. doi:10.1061/(ASCE)IR.1943-4774.0000622

Christianson, L.E., Helmers, M., Bhandari, A., Moorman, T., 2013b. Internal hydraulics of an agricultural drainage denitrification bioreactor. Ecol. Eng. 52:298–307. doi:10.1016/j.ecoleng.2012.11.001

Christianson, L.E., Lepine, C., Sharrer, K.L., Summerfelt, S.T., 2016. Denitrifying bioreactor clogging potential during wastewater treatment. Water Res. 105:147-156. doi:10.1016/j.watres.2016.08.067

Christianson, L.E., Schipper, L.A., 2016. Moving denitrifying bioreactors beyond proof of concept: introduction to the special section. J. Environ. Qual. 45(3):757-761. doi:10.2134/jeq2016.01.0013

Christianson, L.E., Lepine, C., Sibrell, P.L., Penn, C., Summerfelt, S.T. 2017. Denitrifying woodchip bioreactor and phosphorus filter pairing to minimize pollution swapping. Water Res. 121, 129–139. doi:10.1016/J.WATRES.2017.05.026

Chun, J.A., Cooke, R.A., Eheart, J.W., Kang, M.S., 2009. Estimation of flow and transport parameters for woodchip-based bioreactors: I. laboratory-scale bioreactor. Biosyst. Eng. 104(3):384–395. doi:10.1016/j.biosystemseng.2009.06.021

Clough, T.J., Condron, L.M., 2010. Biochar and the nitrogen cycle: introduction. J. Environ. Qual. 39(4):1218-1223. doi:10.2134/jeq2010.0204

Collier, S.M., Ruark, M.D., Oates, L.G., Jokela, W.E., Dell, C.J., 2014. Measurement of greenhouse gas flux from agricultural soils using static chambers. J. Vis. Exp. 90:e52110. doi:10.3791/52110

David, M.B., Flint, C.G., Gentry, L.E., Dolan, M.K., Czapar, G.F., Cooke, R.A., Lavaire, T., 2015. Navigating the socio-bio-geo-chemistry and engineering of nitrogen management in two

illinois tile-drained watersheds. J. Environ. Qual. 44(2):368-381. doi:10.2134/jeq2014.01.0036

David, M.B., Gentry, L.E., Cooke, R.A., Herbstritt, S.M., 2016. Temperature and substrate control woodchip bioreactor performance in reducing tile nitrate loads in East-Central Illinois. J. Environ. Qual. 45(3):822-829. doi:10.2134/jeq2015.06.0296

DeBoe, G., Bock, E., Stephenson, K., Easton, Z., 2017. Nutrient biofilters in the Virginia Coastal Plain: nitrogen removal, cost, and potential adoption pathways. J. Soil Water Conserv. 72(2): 139–149. doi:10.2489/jswc.72.2.139

De Klein, C.A.M., Harvey, M.J., 2012. Nitrous oxide Chamber Methodology Guidelines--Version 1.1. Global Reserch Alliance on Agricultural Greenhouse Gases. Available: <https://globalresearchalliance.org/wp-content/uploads/2015/11/Chamber_Methodology_Guidelines_Final-V1.1-2015.pdf> (accessed December 10, 2017)

Delwiche, C.C., Steyn, P.L., 1970. Nitrogen isotope fractionation in soils and microbial reactions. Environ. Sci. Technol. 4(11):929-935. doi: 10.1021/es60046a004

Dinnes, D.L., Karlen, D.L., Jaynes, D.B., Kaspar, T.C., Hatfield, J.L., Colvin, T.S., Cambardella, C.A., 2002. Nitrogen management strategies to reduce nitrate leaching in tile-drained Midwestern soils. Agron. J. 94:153–171.

Driscoll, D., Whitall, D., Aber, J., Boyer, E., Castro, M., Cronan, C., Goodale, C., Groffman, P., Hopkinson, C., Lambert, K., Lawrence, G., Ollinger, S., 2003. Nitrogen pollution in the Northeastern United States: sources, effects, and management options. Biosci. 53(4). doi:10.1641/0006-3568(2003)053[0357:NPITNU]2.0.CO;2

Duran, B.E.L., Kucharik, C.J., 2013. Comparison of Two Chamber Methods for Measuring Soil Trace-Gas Fluxes in Bioenergy Cropping Systems. Soil Sci. Soc. Am. J. 77:1601. doi:10.2136/sssaj2013.01.0023

Easton, Z.M., Rogers, M., Davis, M., Wade, J., Eick, M., Bock, E., 2015. Mitigation of sulfate reduction and nitrous oxide emission in denitrifying environments with amorphous iron oxide and biochar. Ecol. Eng. 82:605-613. doi:10.1016/j.ecoleng.2015.05.008

Elgood, Z., Robertson, W.D., Schiff, S.L., Elgood, R., 2010. Nitrate removal and greenhouse gas production in a stream-bed denitrifying bioreactor. Ecol. Eng. 36:1575–1580. doi: 10.1016/j.ecoleng.2010.03.011

Erisman, J.W., 2004. The Nanjing declaration on management of reactive nitrogen. BioSci. 54(4):286-287.

Fenton, O., Healy, M.G., Brennan, F.P., Thornton, S.F., Lanigan, G.J., Ibrahim, T.G., 2016. Holistic evaluation of field-scale denitrifying bioreactors as a basis to improve environmental sustainability. J. Environ. Qual. 45(3):788-795. doi:10.2134/jeq2015.10.0500

Feyereisen, G.W., Moorman, T.B., Christianson, L.E., Venterea, R.T., Coulter, J.A., Tschirner, U.W., 2016. Performance of agricultural residue media in laboratory denitrifying

bioreactors at low temperatures. J. Environ. Qual. 45(3):779-787. doi:10.2134/jeq2015.07.0407

Firestone, M., Firestone, R., Tiedje, J., 1980. Nitrous oxide from Soil Denitrification: Factor Controlling Its Biological Production. Science. 208(4445):749-751. doi:10.1126/science.208.4445.749

Florinsky, I. V, McMahon, S., Burton, D.L., 2004. Topographic control of soil microbial activity: a case study of denitrifiers. Geoderma 119(1):33–53. doi:10.1016/s0016-7061(03)00224-6

Fruth, D., Ponzi, J., 2010. Adjusting carbon management policies to encourage renewable, net-negative projects such as biochar sequestration. William Mitch Law Rev. 36(3):992-1013

Galloway, J., Schlesinger, W., Levy, H., Michaels, A., Schnoor, J., 1995. Global Biogeochem. Cy. 9(2):235-252. doi: 10.1029/95GB00158

Galloway, J., Aber, J., Erisman, J., Seitzinger, S., Howarth, R., Cowling, E., Cosby, B. 2003. The nitrogen cascade. BioSci. 53(4):341-356. doi: 10.1641/0006-3568(2003)053[0341:TNC]2.0.CO;2

Gentry, L.E., David, M.B., Smith-Starks, K.M., Kovacic, D.A., 2000. Nitrogen fertilizer and herbicide transport from tile drained fields. J. Environ. Qual. 29(1):232-240. doi:10.2134/jeq2000.00472425002900010030x

Gibert, O., Pomierny, S., Rowe, I., Kalin, R., 2008. Selection of organic substrates as potenial reactive materials for use in a denitnification permeable reactive barrier (PRB). Bioresource Technol. 99(16):7587-7596. doi: 10.1016/j.biortech.2008.02.012

Greenan, C., Moorman, T., Kaspar, T., Parkin, T., Jaynes, D., 2006. Comparing carbon substrates for denitrification of subsurface drainage water. J. Environ. Qual. 35(3):824-829. doi: 10.2134/jeq2005.0247

Greenan, C.M., Moorman, T.B., Parkin, T.B., Kaspar, T.C., Jaynes, D.B., 2009. Denitrification in wood chip bioreactors at different water flows. J. Environ. Qual. 38(4):1664-1671. doi:10.2134/jeq2008.0413

Gruber, N., Galloway, J., 2008. An Earth-system perspective of the global nitrogen cycle. Nature. 451(7176):293-296. doi: 10.1038/nature06592

Hartz, T., Smith, R., Cahn, M., Bottoms, T., Bustamante, S.C., Tourte, L., Johnson, K., Coletti, L., 2017. Wood chip denitrification bioreactors can reduce nitrate in tile drainage. Calif. Agric. 71(1):41–47. doi:10.3733/ca.2017a0007

Healy, R.W., Striegl, R.G., Russell, T.F., Hutchinson, G.L., Livingston, G.P., 1996. Numerical evaluation of static-chamber measurements of soil—atmosphere gas exchange: identification of physical processes. Soil Sci. Soc. Am. J. 60(3):740-747. doi:10.2136/sssaj1996.03615995006000030009x

Healy, M.G., Ibrahim, T.G., Lanigan, G.J., Serrenho, A.J., Fenton, O., 2012. Nitrate removal rate, efficiency and pollution swapping potential of different organic carbon media in laboratory

denitrification bioreactors. Ecol. Eng. 40:198–209. doi:10.1016/j.ecoleng.2011.12.010

Healy, M.G., Barrett, M., Lanigan, G.J., João Serrenho, A., Ibrahim, T.G., Thornton, S.F., Rolfe, S.A., Huang, W.E., Fenton, O., 2015. Optimizing nitrate removal and evaluating pollution swapping trade-offs from laboratory denitrification bioreactors. Ecol. Eng. 74:290–301. doi:10.1016/j.ecoleng.2014.10.005

Hua, G., Salo, M.W., Schmit, C.G., Hay, C.H., 2016. Nitrate and phosphate removal from agricultural subsurface drainage using laboratory woodchip bioreactors and recycled steel byproduct filters. Water Res. 102:180-189. doi:10.1016/j.watres.2016.06.022

IA EPA. 2015. Illinois nutrient loss reduction strategy. Springfield, IL. http://www.epa.illinois.gov/assets/iepa/water-quality/watershed-management/nlrs/nlrs-final-revised-083115.pdf (accessed 11 Dec. 2017).

IDALS. 2014. Iowa nutrient reduction strategy: A science and technology-based framework to assess and reduce nutrients to Iowa waters and the Gulf of Mexico. Iowa Department of Agriculture and Land Stewardship, Iowa Department of Natural Resources, and Iowa State University. http://www.nutrientstrategy.iastate.edu/ (accessed 11 Dec. 2016).

Ikenberry, C.D., Soupir, M.L., Schilling, K.E., Jones, C.S., Seeman, A., 2014. Nitrate-nitrogen export: magnitude and patterns from drainage districts to downstream river basins. J. Environ. Qual. 43(6):2024-2033. doi:10.2134/jeq2014.05.0242

Istok, J., Humphrey, M., Schroth, M., Hyman, M., O'Reily, K., 1997. Single-well, "push-pull" test for in situ determination of microbial activites. Ground Water. 35(4):619-631. doi: 10.1111/j.1745-6584.1997.tb00127.x

King, K.W., Williams, M.R., Fausey, N.R., 2015. Contributions of systematic tile drainage to watershed-scale phosphorus transport. J. Environ. Qual. 44(2):486-494. doi:10.2134/jeq2014.04.0149

Kladivko, E.J., Van Scoyoc, G.E., Monke, E.J., Oates, K.M., Pask, W., 1991. Pesticide and nutrient movement into subsurface tile drains on a silt loam soil in Indiana. J. Environ. Qual. 20(1):264-270. doi:10.2134/jeq1991.00472425002000010043x

Kookana, R.S., Sarmah, A.K., Van Zwieten, L., Krull, E., Singh, B., Donald L. Sparks, 2011. Chapter three - Biochar Application to Soil: Agronomic and Environmental Benefits and Unintended Consequences. pp. 103–143. Elsevier Academic Press Inc. San Diego, CA.

Kumar, M., Lin, J., 2010. Co-existence of anammox and denitrification for simultaneous nitrogen and carbon removal--strategies and issues. J. Hazard. Mater. 178(1-3):1-9. doi: 10.1016/j.jhazmat.2010.01.077

Kutzbach, L., Schneider, J., Sachs, T., Giebels, M., Nykänen, H., Shurpali, N.J., Martikainen, P.J., Alm, J., Wilmking, M., 2007. CO_2 flux determination by closed-chamber methods can be seriously biased by inappropriate application of linear regression. Biogeosciences 4, 1005–1025.

Lehmann, J., Rillig, M., Thies, J., Masiello, C., Hockaday, W., Crowley, D., 2011. Soil Biol. Biochem. 43(9):1812-1836. doi: 10.1016/j.soilbio.2011.04.022

Lepine, C., Christianson, L., Sharrer, K., Summerfelt, S., 2016. Optimizing hydraulic retention times in denitrifying woodchip bioreactors treating recirculating aquaculture system wastewater. J. Environ. Qual. 45(3):813-821. doi:10.2134/jeq2015.05.0242

Liu, B., Mørkved, P.T., Frostegård, Å., Bakken, L.R., 2010. Denitrification gene pools, transcription and kinetics of NO, N_2O and N_2 production as affected by soil pH. FEMS Microbiol. Ecol. 72(3):407–417. doi:10.1111/j.1574-6941.2010.00856.x

Livingston, G.P., Hutchinson, G.L., Spartalian, Kevork, N.D. Trace gas emission in chambers: a non-steady-state diffusion model. Soil Sci. Soc. Am. J. 70:1459-1469. doi:10.2136/sssaj2005.0322

Long, L.M., Schipper, L.A., Bruesewitz, D.A., 2011. Long-term nitrate removal in a denitrification wall. Agr. Ecosyst. Environ. 140(3-4):514-520. doi: 10.1016/j.agee.2011.02.005

Mateju, V., Cizinska, S., Krejci, J., Janock, T., 1992. Biological water denitrificaiton - a reivew. Enzyme Microb. Technol. 14(3):170–183. doi:10.1016/0141-0229(92)90062-S

Mathieu, O., Lévêque, J., Hénault, C., Milloux, M.-J., Bizouard, F., Andreux, F., 2006. Emissions and spatial variability of N_2O, N_2 and nitrous oxide mole fraction at the field scale, revealed with ^{15}N isotopic techniques. Soil Biol. Biochem. 38(5):941–951. doi:10.1016/j.soilbio.2005.08.010

McLaughlin, H., Anderson, P., Shields, F., Reed, T., 2009. All biochars are not created equal and how to tell them apart. North Amer. Biochar. 2:1-36.

Melillo, J., Cowling, E., 2002. Reactive nitrogen and public policies for environmental protection. AMBIO. 31(2):150-158.

MN PCA. 2014. The Minnesota nutrient reduction strategy. Minnesota Pollution Control Agency, St. Paul, MN. https://www.pca.state.mn.us/sites/default/files/wq-s1-80.pdf (accessed 11 Dec. 2016).

Moorman, T.B., Parkin, T.B., Kaspar, T.C., Jaynes, D.B., 2010. Denitrification activity, wood loss, and N_2O emissions over 9 years from a wood chip bioreactor. Ecol. Eng. 36:1567–1574. doi: 10.1016/j.ecoleng.2010.03.012

Mulder, A., van de Graaf, A., Robertson, L., Kuenen, J. 1995. Anaerobic ammonium oxidation discovered in a denitrifying fluidized bed reactor. FEMS Microbiol. Ecol. 16(3):177-183. doi: 10.1016/0168-6496(94)00081-7

Nelder, J.A., 1994. The statistics of linear models: back to basics. Stat. Comput. 4(4):221–234. doi:10.1007/BF00156745

Oertel, C., Matschullat, J., Zurba, K., Zimmermann, F., Erasmi, S., 2016. Greenhouse gas emissions from soils—a review. Chemie der Erde - Geochemistry 76(3):327–352. doi:10.1016/j.chemer.2016.04.002

Parton, W., Mosier, A., Ojima, D., Valentine, D., Schime, D., Weier, K., Kulmala, A., 1996. Generalized model for N_2 and N_2O production from nitrification and denitrification. Global Biogeochem. Cy. 10(3):401-412. doi:10.1029/96GB01455

Pluer, W.T., Geohring, L.D., Steenhuis, T.S., Walter, M.T., 2016. Controls influencing the treatment of excess agricultural nitrate with denitrifying Bioreactors. J. Environ. Qual. 45(3):772-778. doi:10.2134/jeq2015.06.0271

Rabalias, N., Turner, R., Diaz, R., Justic, D., 2009. Global change and eutrophication of coastal waters. ICES J. Mar. Sci. 66(7):1528-1537. doi:10.5539/enrr.v3n2p37

Rambags, F., Tanner, C.C., Stott, R., Schipper, L.A., 2016. Fecal bacteria, bacteriophage, and nutrient reductions in a full-scale denitrifying woodchip bioreactor. J. Environ. Qual. 45(3):847-854. doi:10.2134/jeq2015.06.0326

Renner, R., 2007. Rethinking biochar. Environ. Sci. Technol. 41(17):5932-5933. doi: 10.1021/es0726097

Rivett, M., Buss, S., Morgan, P., Smith, J., Bemment, C., 2008. Nitrate attenuation in groundwater: a review of biogeochemical controlling processes. Water Res. 42(16):4215-4232. doi: 10.1016/j.watres.2008.07.020

Robertson, W.D., 2010. Nitrate removal rates in woodchip media of varying age. Ecol. Eng. 36, 1581–1587. doi:10.1016/j.ecoleng.2010.01.008

Robertson, W.D., Blowes, D.W., Ptacek, C.J., Cherry, J.A., 2000. Long-term performance of in situ reactive barriers for nitrate remediation. Ground Water 38(5):689–695. doi:10.1111/j.1745-6584.2000.tb02704.x

Robertson, W.D., Cherry, J.A., 1995. In situ denitrification of septic-system nitrate using reactive porous media barriers: field trials. Ground Water 33(1):99–111. doi:10.1111/j.1745-6584.1995.tb00266.x

Robertson, W.D., Vogan, J.L., Lombardo, P.S., 2008. Nitrate removal rates in a 15-year-old permeable reactive barrier treating septic system nitrate. Ground Water Monit. Remediat. 28(3):65–72. doi:10.1111/j.1745-6592.2008.00205.x

Rosen, T., Christianson, L., 2017. Performance of denitrifying bioreactors at reducing agricultural nitrogen pollution in a humid subtropical coastal plain climate. Water 9(2): [112]. doi:10.3390/w9020112

Saarnio, S., Heimonen, K., Kettunen, R., 2013. Biochar addition indirectly affects N_2O emissions via soil moisture and plant N uptake. Soil Biol. Biochem. 58:99-106. doi:10.1016/j.soilbio.2012.10.035

Salilling, W., Westerman, P., Losordo, T., 2007. Wood chips and wheat straw as alternative biofilter media for denitrification reactors treating aquaculture and other wastewaters with high nitrate concentrations. Aquac. Eng. 37(3):222-233. doi: 10.1016/j.aquaeng. 2007.06.003

Schipper, L.A., Vojvodic-Vukovic, M., 2001. Five years of nitrate removal, denitrification and carbon dynamics in a denitrification wall. Water Res. 35(14):3473-3477. doi: 10.1016/S0043-1354(01)00052-5

Schipper, L.A., Barkle, G.F., Vojvodic-Vukovic, M., 2005. Maximum rates of nitrate removal in a denitrification wall. J. Environ. Qual. 34(4):1270–1276. doi:10.2134/jeq2005.0008

Schipper, L.A., Gold, A.J., Davidson, E.A., 2010a. Managing denitrification in human-dominated landscapes. Ecol. Eng. 36:1503–1506. doi:10.1016/j.ecoleng.2010.07.027

Schipper, L.A., Robertson, W.D., Gold, A.J., Jaynes, D.B., Cameron, S.C., 2010b. Denitrifying bioreactors—An approach for reducing nitrate loads to receiving waters. Ecol. Eng. 36:1532–1543. doi:10.1016/j.ecoleng.2010.04.008

Schmidt, C.A., Clark, M.W., 2013. Deciphering and modeling the physicochemical drivers of denitrification rates in bioreactors. Ecol. Eng. 60:276-288. doi:10.1016/j.ecoleng.2013.07.041

Seitzinger, S., Harrison, J., Bohlke, J., Bouwman, A., Lowrance, R., Peterson, B., Tobias, C., Van Drecht, G., 2006. Denitrification across landscapes and waterscapes: a synthesis. Ecol. Appl. 16(6):2064-2090. doi:10.1890/1051-0761(2006)016[2064:DALAWA]2.0.CO;2

Sharrer, K.L., Christianson, L.E., Lepine, C., Summerfelt, S.T., 2016. Modeling and mitigation of denitrification “woodchip” bioreactor phosphorus releases during treatment of aquaculture wastewater. Ecol. Eng. 93:135-143. doi:10.1016/j.ecoleng.2016.05.019

Singh, B.P., Hatton, B.J., Singh, B., Cowie, A.L., Kathuria, A., 2010. Influence of biochars on nitrous oxide emissions and nitrogen leaching from two contrasting soils. J. Environ. Qual. 39(4):1224-1235. doi: 10.2134/jeq2009.0138

Smil, V., 2001. Enriching the Earth: Fritz Haber, Carl Bosch, and the Transformation of World Food. MIT Press, Cambridge (2001), pp. 339

Sohi, S., Krull, E., Lopez-Capel, E., Bol, R., 2010. A review of biochar and its use and function in soil. Adv. Agron. 105:47-82. doi:10.1016/S0065-2113(10)05002-9

Sovik, A., Morkved, P., 2008. Use of stable nitrogen isotope fractionation to estimate denitrification in small constructed wetlands treating agricultural runoff. Sci. Total Environ. 392(1):157-165. doi:10.1016/j.scitotenv.2007.11.014

Trudell, M., Gillham, R., Cherry, J., 1986. An in-situ study of the occurrence and rate of denitrification in a shallow unconfined sand aquifer. J. Hydro. 83(3-4):251-268. doi: 10.1016/0022-1694(86)90155-1

USDA NASS, 2012 Census of Agriculture, Ag Census Web Maps. Available at: www.agcensus.usda.gov/Publications/2012/Online_Resources/Ag_Census_Web_Maps/Overview/Warneke, S., Schipper, L.A., Bruesewitz, D.A., Baisden, W.T., 2011a. A comparison of different approaches for measuring denitrification rates in a nitrate removing bioreactor. Water Res. 45(14):4141–4151. doi:10.1016/j.watres.2011.05.027

USDA-NRCS. 2015. Conservation practice standard denitrifying bioreactor code 605 (605-CPS-

1). USDA-NRCS, Washington, DC.

Verheijen, F., Jeffery, S., Bastos, A., Van Der Velde, M., Diafas, I., 2010. Biochar application to soils: a critical review of effects on soil properties, processes and functions. JRC Scientific and Technical Report. doi:10.2788/472

Warneke, S., Schipper, L.A., Bruesewitz, D.A., McDonald, I., Cameron, S., 2011a. Rates, controls and potential adverse effects of nitrate removal in a denitrification bed. Ecol. Eng. 37:511–522. doi:10.1016/j.ecoleng.2010.12.006

Warneke, S., Schipper, L.A., Matiasek, M.G., Scow, K.M., Stewart Cameron, Bruesewitz, D.A., McDonald, I.R., 2011b. Nitrate removal, communities of denitrifiers and adverse effects in different carbon substrates for use in denitrification beds. Water Res. 45(17):5463–5475. doi:doi: 10.1016/j.watres.2011.08.007

Weigelhofer, G., Hein, T., 2015. Efficiency and detrimental side effects of denitrifying bioreactors for nitrate reduction in drainage water. Environ. Sci. Pollut. Res. 22(17):13534–13545. doi:10.1007/s11356-015-4634-0

Williams, M.R., King, K.W., Fausey, N.R., 2015. Drainage water management effects on tile discharge and water quality. Agric. Water Manag. 148:45-51. doi:10.1016/j.agwat.2014.09.017

Woli, K.P., David, M.B., Cooke, R.A., McIsaac, G.F., Mitchell, C.A., 2010. Nitrogen balance in and export from agricultural fields associated with controlled drainage systems and denitrifying bioreactors. Ecol. Eng. 36:1558–1566. doi:10.1016/j.ecoleng.2010.04.024

Yanai, Y., Toyota, K., Okazaki, M., 2007. Effects of charcoal addition on N_2O emissions from soil resulting from rewetting air-dried soil in short-term laboratory experiments. Soil Sci. Plant Nutr. 53(2):181–188. doi:10.1111/j.1747-0765.2007.00123.x

Zumft, W. 1997. Cell biology and molecular basis of denitrification. Microbiol. Mol. Biol. R. 61(4):533-616.

2 EFFECT OF BIOCHAR ON NITRATE REMOVAL IN A PILOT-SCALE DENITRIFYING BIOREACTOR

Emily M. Bock, Brady Coleman, and Zachary M. Easton*

Department of Biological Systems Engineering, Virginia Tech, Blacksburg, VA 24061

*Corresponding author: zeaston@vt.edu

Full citation:

Effect of biochar on nitrate removal in a pilot-scale denitrifying Bioreactor. 2016. Bock, E. M., B. Coleman, and Z. M. Easton. J. Environ. Qual. 45:762–771. doi:10.2134/jeq2015.04. 0179

2.1 Abstract

Denitrifying bioreactors (DNBRs) harness the natural capacity of microorganisms to convert bioavailable nitrogen (N) into inert nitrogen gas (N_2) by providing a suitable anaerobic habitat and an organic carbon energy source. Woodchip systems are reported to remove 2 to 22 g N m^{-3} d^{-1}, but the potential to enhance denitrification with alternative substrates holds promise. The objective of this study was to determine the effect of adding biochar, an organic carbon pyrolysis product, to an in-field, pilot-scale woodchip DNBR. Two 25-m^3 DNBRs, one with woodchips and the other with woodchips and a 10% by volume addition of biochar, were installed on the Delmarva Peninsula, Virginia. Performance was assessed using flood-and drain batch experiments. An initial release of N was observed during the establishment of both DNBRs, reflecting a start-up phenomenon observed in previous studies. Nitrate (NO_3^--N) removal rates observed during nine batch experiments 4 to 22 mo after installation were 0.25 to 6.06 g N m^{-3} d^{-1}. The presence of biochar, temperature, and influent NO_3^--N concentration were found to have significant effects on NO_3^--N removal rates using a linear mixed effects model. The model predicts that biochar increases the rate of N removal when influent concentrations are above approximately 5 to 10 mg L^{-1} NO_3^--N but that woodchip DNBRs outperform biochar-amended

DNBRs when influent concentrations are lower, possibly reflecting the release of N temporarily stored in the biochar matrix. These results indicate that in high N–yielding systems the addition of biochar to standard woodchip DNBRs has the potential to significantly increase N removal.

2.2 Introduction

Denitrifying bioreactors (DNBRs) have emerged as an innovative approach to mitigating the impacts of excess anthropogenic nitrogen (N), particularly in agricultural systems. Agricultural production sustained by application of N fertilizer represents the largest share of N input to the environment (Galloway et al., 2008) and results in unavoidable export of N despite implementation of various best management practices, such as nutrient management planning or riparian buffers (Seitzinger et al., 2006). Oversupply of bioavailable N to natural systems results in a suite of environmental impacts, including algal blooms and subsequent anoxic conditions that affect aquatic organisms in receiving waters (Canfield et al., 2010; Jickells, 2005). These negative consequences develop because ecosystems have adapted to recycle and conserve N, which is often the limiting factor for primary production (Galloway et al., 2003). Therefore, the natural rate of denitrification, the microbial process that removes bioavailable N from an ecosystem by converting nitrate-nitrogen (NO_3^--N) to inert atmospheric nitrogen (N_2), cannot counterbalance these anthropogenic N inputs (Seitzinger et al., 2006).

Denitrifying bioreactors are designed to serve as artificial N sinks that can increase the magnitude of denitrification within the landscape and are strategically placed to intercept NO_3^--enriched groundwater or concentrated flows such as tile drainage (Gold et al., 2013). They function by supporting the activity of denitrifying microorganisms by supplying an organic carbon energy source that, as the system becomes saturated, provides an anaerobic environment

favoring the biochemical conversion of NO_3^--N to N_2. Denitrifying bioreactors have been implemented in tile-drained agricultural systems in the Midwest and have demonstrated N removal efficiencies of 33 to 100% (Christianson et al., 2012; Woli et al., 2010) at a rate of 2 to 22 g N m^{-3} d^{-1} (Schipper et al., 2010a). Interim conservation standards for DNBR construction in Iowa published by the USDA Natural Resource Conservation Service reflect the growing body of research evidencing the effectiveness of these systems for NO_3^--N removal and their potential to mitigate the impacts of anthropogenic N (NRCS, 2009).

Although woodchip media dominates field-scale DNBR applications due to its low cost, availability, and established performance, the potential for substrate engineering to enhance denitrification rates remains largely untested at the field scale. Various alternative substrates investigated at the laboratory scale have been shown to outperform woodchips, but their increased capacity for N removal has not yet been translated to the field (e.g., Bock et al., 2015; Gibert et al., 2008; Warneke et al., 2011; Hunter, 2001). Often the high removal rates observed in laboratory testing are not sustained for longer than a few months because they are supported by the rapid degradation of the most labile portion of the organic carbon, after which removal rates decline (e.g., Cameron and Schipper, 2010; Greenan et al., 2006; Saliling et al., 2007). In contrast, woodchip DNBRs can maintain N removal rates for up to 15 yr in the field (Robertson et al., 2008). Therefore, optimizing denitrification rates in DNBRs by manipulating the substrate composition requires a balance between the lability and longevity of the organic carbon media.

Biochar, an organic carbon pyrolysis product, shows promise as an amendment to woodchip DNBRs based on laboratory testing (Bock et al., 2015) and a larger body of research on biochar as an agricultural soil amendment (e.g., Kookana et al., 2011; Sohi et al., 2010). When

applied to agricultural soils, biochar reduces leaching of N from the soil profile (Beck et al., 2011; Clough and Condron, 2010; Coumaravel et al., 2011; Nelson et al., 2011). Additionally, biochar induces an increase in total microbial activity (e.g., Ding et al., 2013; Lehmann et al., 2011) as well as an increase in the abundance and activity of denitrifying microorganisms specifically (Anderson et al., 2011; Cayuela et al., 2013). Laboratory testing conducted by Bock et al. (2015) provides preliminary evidence that an addition of biochar to woodchip DNBRs at a rate of 10% by volume results in increased permanent N removal via denitrification. Importantly, biochar is more stable in the soil than the feedstock from which it was created (Lehmann et al., 2006), and consequently woodbased-feedstock biochar may have a suitable longevity in DNBRs to have a sustained effect on N removal rates.

The objective of this study was to determine the effect of biochar addition to traditional woodchip DNBRs on NO_3^--N removal. Nitrogen removal was compared between two identical pilot-scale DNBRs, one with woodchips and one with woodchips and a 10% by volume biochar addition. Batch experiments were conducted in the field by introducing a single bed volume of influent containing a concentration of NO_3^--N within an environmentally relevant range and observing the change in concentration over time. Monitoring was conducted at various times during the year to encompass differing seasonal conditions. This work aims to assist in defining optimum operating conditions, substrate composition, and residence times for field-scale DNBRs. However, this novel flood-and-drain bioreactor contrasts with commonly used flow-through systems, and there is uncertainty in the ability of batch experiments to capture the dynamics of flow-through designs. Although we acknowledge this uncertainty, the experimental design

enables comparative assessment of nutrient removal in woodchip bioreactors with and without biochar.

2.3 Materials and Methods

2.3.1 Site Description

Two pilot-scale DNBRs were installed in October 2012 at the Virginia Tech Eastern Shore Agricultural Research and Extension Center located in Painter, Virginia on the Delmarva Peninsula. The 226-acre research farm includes 26 acres of tile-drained row crops. Cultivated crops include corn, wheat, soy, and various vegetables, which receive substantial fertilizer application. Shallow ground water samples collected at the site at a depth of 0.5 to 2 m contained concentrations up to 29.5 mg L^{-1} NO_3^--N, averaging 8.3 mg L^{-1} NO_3^-–N (Lassiter and Easton, 2013), which approaches the maximum contaminant level for drinking water of 10 mg L^{-1} NO_3^--N set by the USEPA (1996).

2.3.2 Denitrifying Bioreactor Design and Materials

The two separate DNBRs were plumbed into the tile drain system near the tile outfall. Each DNBR measures 4.3 m in length and width by 1.4 m in depth. These compartments are filled with approximately 25 m^3 of woodchips, and one compartment received 2.5 m^3 of biochar. Biochar did not increase the total volume of the DNBR because it filled some of the interstitial pore spaces between the woodchips. The biochar, obtained from Biochar Solutions Inc., was created from a pine feedstock and was produced using a two-stage process whereby the pine feedstock is first carbonized under low O_2 conditions at 500 to 700°C for <1 min and then held for up to 14 min at 300 to 550°C in a hot gas environment where O_2 is unavailable. The final

product consists of two size fractions after passing through an augur: 80% of the material is approximately 1.5 cm by 1 cm by 0.5 cm (0.75 cm^3), and 20% is a fine dust fraction 10 to 100 µm in length. The woodchips were comprised of mixed hardwood ranging approximately 2.5 by 2.5 by 0.3 cm to 6 by 6 by 0.6 cm. The woodchips and biochar were added alternately and mixed by shovel during installation to create homogenous media. Upgradient of the DNBRs, a three-compartment Agri Drain flow control unit was installed to divert water from the tile into each DNBR (Agri Drain Corp.). The two DNBRs are located on either side of the tile and lined with a 30-mL landfill liner to prevent shallow groundwater from influencing the experiments. Each DNBR compartment is connected to the inlet flow control structure by 6-in corrugated HDPE plastic piping that extends from the inlet structure through a hole in the liner at the bottom corner into the bed approximately 0.5 m. Leakage around the HDPE piping is prevented by securing the liner to the piping with waterproof tile tape and sealing with bentonite. Backflow valves between the Agri Drain inlet structure and each bed prevent mixing of the treatment volume in the DNBRs. Two outlet drainage control structures were also installed to control the water height in the DNBRs. Similar to the inlet, the HDPE piping connected the downgradient bottom corner of each DNBR to the outlet flow control structures. Permeable geotextile fabric was installed on the ends of the outlet piping protruding into the DNBRs to prevent export of substrate. Large wells made from 12-in perforated corrugated HDPE piping were placed near the center of each DNBR for the purpose of collecting water samples and measuring water chemistry parameters.

2.3.3 Nutrient Addition, Sampling, and Analysis

Observation of the removal of NO_3^--N in the DNBRs was conducted during 12 artificial storm events between November 2012 and August 2014 (Table 1). Each experiment was

conducted as a batch, where the water was retained within the DNBRs rather than allowed to flow through, the latter occurring in field-scale applications in practice. Water drawn from an irrigation pond on site was pumped into the DNBRs through the inlet drainage control structure until they reached capacity while the outlets were closed. Simultaneously, a concentrated solution of dissolved $Ca(NO_3^-)_2$ was slowly added to the inlet structure while mixing with the irrigation water in an effort to approximate influent with a uniform N concentration. For these experiments, NO_3^--N was introduced in the form of $Ca(NO_3^-)_2$, as opposed to ammonium nitrate $(NH_4)(NO_3)$, to reflect that NO_3^--N is the dominant form of dissolved N encountered in shallow groundwater and tile drainage on the Delmarva (Smiciklas and Moore, 2008). Controlled NO_3^--N introduction was chosen for the purpose of manipulating initial concentrations to represent a range of environmentally relevant values. This experimental design was used to examine nutrient removal processes in an effort to define management approaches for biochar-amended DNBRs. The batch design was intended to estimate NO_3^--N removal rates and to facilitate comparison of the woodchip and biochar treatments for a range of design residence times while conducting fewer replications by using the time elapsed during each event as a proxy for residence time in a flow-through system. However, with significant uncertainty in equating the elapsed time in a batch experiment to the residence time of a flow-through DNBR, the results of this experiment can only suggest how biochar amendment would affect NO_3^--N removal in systems receiving continuous flow. A potentially significant departure of the flood-and-drain experimental design from typical operation of existing installations was that the DNBRs were allowed to dry out for extensive periods between events. Consequently, the denitrifying activity of the microbial population may have been suppressed relative to the flow-through systems more typically used

due to the presence of oxygen. Alternatively, more rapid cycling between saturated and unsaturated conditions or sustained inflow via tile drainage would be expected to sustain higher NO_3^--N removal rates. Therefore, the observed removal rates likely underestimate the performance of flowthrough or more actively managed flood-and-drain designs.

Table 1. Dates of batch experiments with initial NO_3^--N concentrations, average water temperatures, and the standard deviation of the temperatures.

Dates	Initial NO_3^--N (mg L^{-1})†		Water Temp. (˚C)		Air Temp (˚C)
	Biochar	Woodchips	Avg.	SD	Monthly avg. ‡
26-30 Nov. 2012	> 0.1	> 0.1	10.8	2.3	9.1
20 Feb.-4 Mar. 2013	8.3	20.5	9.6	2.5	3.1
18-25 Apr. 2013	22.2	15.9	-§	-	11.2
25-29 June 2014	NA¶	33.3	-	-	23.1
12-14 Aug. 2014	9.8	25.3	23.6	0.1	24.8
14-15 Aug. 2014	0.5	3.1	23.9	0.2	25.5

† Initial NO_3^--N concentrations were determined from samples collected immediately on filling.
‡ Average air temperature during 30 d preceding the event
§ Temperature data were unavailable for the April and June events.
¶ NA indicates omission of poor quality data.

Water samples were collected from the sampling wells in the DNBRs every 0.5 to 3 h after NO_3^--N introduction, with decreasing frequency over the course of each event. Initial NO_3^--N concentrations were determined from samples collected immediately on filling from the monitoring wells in the middle of each DNBR. Taking these measured values as the initial concentration assumed homogenous mixing and the absence of dead zones within the DNBRs. The method of flooding the DNBRs with pumped irrigation water while simultaneously adding the $Ca(NO_3^-)_2$ solution was intended to ensure adequate mixing. However, measured initial

concentrations in the woodchip- and biochar-amended DNBRs were less similar than anticipated (Table 1), possibly due to differing quantities of $Ca(NO_3^-)_2$ diverted to the two DNBRs through the inlet control structure due to the presence of a slight gradient between the woodchip- and biochar-amended beds. Additionally, rapid sorption reactions may have affected the measured concentrations in the monitoring well, given that biochar can have significant anion exchange capacity (AEC) and the opportunity for the influent to interact with the substrate. Duration of sample collection corresponded to the initial concentration and temperature, with longer monitoring periods for higher initial concentrations and lower temperatures, in anticipation of longer removal times. Samples were stored in HDPE bottles, either field filtered through 0.45-mm nylon filters or chilled on ice, and transported to the lab where they were filtered if they had not been previously and stored at 4°C until analysis. Samples were analyzed for NO_3^--N and NH_4^+-N using flow injection analysis (Lachat QuikChem 8500 series 2) methods 10-107-01-1-A and 10-107-06-2-L for NO_3^--N and NH_4^+-N, respectively.

A portable multiparameter sonde (Hach HQ40d) with pH, oxidation reduction potential (ORP) with gel-electrolyte reference, and optical dissolved oxygen (DO) probes was used to measure these water quality parameters as well as temperature in the sampling wells during a subset of the events

2.3.4 Statistical analysis

The effect of the presence of biochar, temperature, time, and initial concentration on NO_3^--N removal was determined using a linear mixed effects (LME) model. Linear mixed effects models are commonly used to analyze data with multiple measurements per subject, particularly observations spaced unequally over time (Verbeke et al., 2010). Using an LME for this analysis

enables the inclusion of all of the data points, whereas a repeated measures ANOVA would necessitate the comparison of data only at identical time points, consequently losing much data from trials with differing duration and sampling intervals. The underlying assumptions of the LME include linearity, absence of collinearity, homoscedasticity, and normality of the residuals (Gelman and Hill, 2009). Collinearity was not present based on the selection of uniquely predictive model parameters (presence of biochar, initial concentration, temperature, and time). Homoscedasticity, the equal variance of residuals across groups, was verified graphically by observing the absence of a trend between the fitted data and the residuals and with the Studentized Breush-Pagan test in R (p = 0.1971) (R Core Team, 2014). Although the model residuals were not normally distributed as determined by the Bartlett test ($p < 0.001$) (R Core Team, 2014), the LMEs are relatively robust against this assumption (Winter, 2013).

The LMEs were developed and run in R (R Core Team, 2014) using the 'nlme' package (Pinheiro et al., 2014). Two separate models were fit with the NO_3^--N and NH_4^+-N concentrations as the respective dependent variables by restricted maximum likelihood method. A continuous autoregressive variance–covariance matrix was specified in the model to account for the temporal autocorrelation of the independent variable (i.e., the higher correlation of N concentrations closer in time than measurements more distant in time). Nine events were analyzed with this procedure: four from the DNBR with biochar and five from the DNBR without biochar. The first event in each of the treatments was excluded as not representative of long-term performance; net export of N was observed as a result of the "first flush," an initial release of nutrients associated with rapid decomposition of the most labile organic carbon from fresh substrate, which is a recognized aspect of DNBR performance. The June 2013 event conducted in

the biochar DNBR was also excluded from LME analysis due to poor data quality as a result of instrument failure.

Each event consisted of a time sequence of nutrient concentrations in water samples, collected from the time of introduction of the irrigation water with dissolved NO_3^--N into the DNBR. The dosing events were considered to be independent because the experimental unit was the water with dissolved NO_3^--N pumped into the DNBRs. This assumption allowed for increased power to estimate the difference between the woodchip and biochar treatments. The independent variables included in the LME were the presence of biochar (e.g., treatment), initial concentration with respect to the dependent variable (either NO_3^--N or NH_4^+-N), temperature, and time elapsed from addition of influent. The temperature variable was treated as categorical, assigned as high during the summer months (June–August) and low during the late winter and spring (February–April). Incorporation of water temperature into the predictive model as a categorical rather than a continuous variable provided greater ability to distinguish the effect of biochar addition on N removal by grouping comparable conditions as high- and low-temperature categories (23.9 ± 0.3°C and 9.6 ± 1.5°C, respectively) instead of emphasizing temperature as a predictive variable. The models were fit with random slopes supplied by an estimated error term to reflect the variation in initial concentrations for each of the events. The model included all interaction effects (i.e., multiplicative combinations of two or more independent variables) but only the main effects of time and initial concentration as predictors. The main effects of treatment and temperature were omitted to prevent them from influencing the predicted value of the intercept, a boundary condition of the model representing the initial N concentration. The fit of the model with the main effects of treatment and temperature omitted was not significantly

different from the model including all main effects, as evidenced by an ANOVA comparing the two models (p = 0.1028), demonstrating that the added predictors in the larger model have coefficients statistically equal to zero (Gelman and Hill, 2009). An ANOVA was also used to determine which parameters in the LME were significant predictors of N concentration (Gelman and Hill, 2009).

2.4 Results and Discussion

Both the woodchip- and biochar-amended DNBRs successfully removed NO_3^--N from enriched influent during the nine batch experiments conducted 4 to 22 mo after installation (Table 1). After the initial export of N observed within 1 mo of installation (Fig. 1), the systems achieved removal rates ranging from 0.25 to 6.06 g N m^{-3} d^{-1}. Removal rates were determined using the slopes of linear regressions on aqueous concentration over time and calculated on the basis of saturated volume assuming an effective porosity of 0.7 (van Driel et al., 2006). That is, the slope of the regression as g N $m^{-3}(H_2O)$ d^{-1} was multiplied by 0.7 to obtain g N m^{-3}(media) d^{-1}. Ultimately, the beds removed 53 to 99% of influent NO_3^--N concentration given sufficient elapsed time, up to nearly a week for high-influent concentrations at low temperatures (Fig. 2). Although removal rates and mass reductions observed in these batch experiments largely fell within the range of values reported in the literature for flow-through systems (2–22 g N m^{-3} d^{-1} [Schipper et al., 2010a] and 33–100% [Christianson et al., 2012; Woli et al., 2010]), the residence times required to reach these removal efficiencies were generally higher than those reported in the literature (6–24 h for 50% removal) (Moorman et al., 2015). Temperature, treatment, and initial NO_3^--N concentration were found to have significant effects on the NO_3^--N concentration over time with LME analysis (Table 2). According to predictions from this LME, biochar addition

induced greater N removal than woodchips alone for higher NO_3^--N influents (Fig. 3). However, the woodchip system outperformed the biochar-amended system when influent NO_3^--N concentrations were below approximately 5 mg L^{-1} at low temperatures and 10 mg L^{-1} at high temperatures (Fig. 3). Predicted N removal rates for the DNBRs receiving influent ranging from 5 to 20 mg L^{-1} were 0.41 to 4.08 g N m^{-3} d^{-1} (Table 3), similar to the observed removal rates.

Microbial denitrification was concluded to be responsible for the majority N removal for three reasons: (i) observing pH, ORP, and DO levels suitable for denitrification within the DNBRs (Fig. 4); (ii) the absence of significant levels of dissimilatory reduction of nitrate to ammonium (DNRA) as evidenced by the stable levels of NH_4^+-N during the events (p = 0.1253, data not shown); and (iii) finding that higher temperatures increase N removal rates, supplying further evidence that the NO_3^--N reductions were the result of a temperature-dependent biological process.

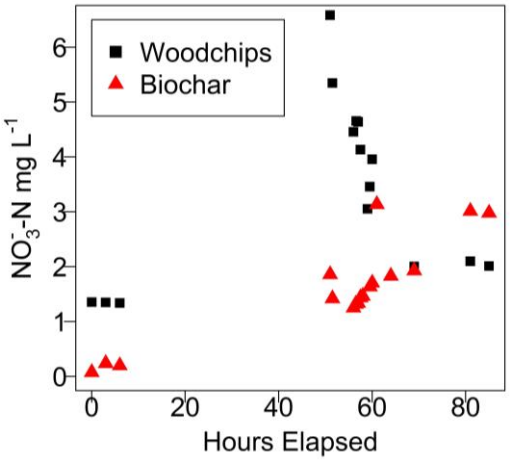

Figure 1. Concentrations of NO_3^--N observed in the woodchip- and biochar-amended denitrifying bioreactors dura a first flush event within 1 mo of installation, November 2012. Influent NO_3^--N concentrations were <0.1 mg L^{-1}.

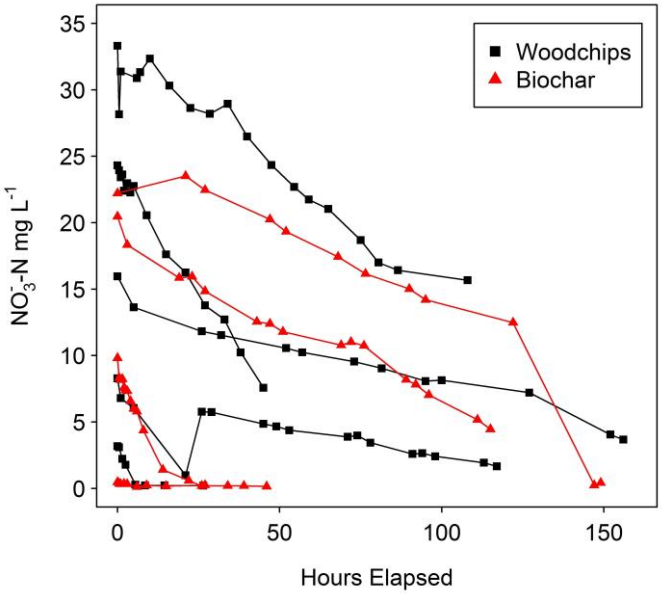

Figure 2. Concentrations of NO_3^--N in the woodchip and biochar-amended denitrifying bioreactors during nine artificial storm events. Note that the first flush is not included.

Table 2. Results from an ANOVA on the output of a linear mixed effects model showing the significance of the independent variables (presents of biochar, initial concentration, temperature, and time) and their interaction effects on the dependent variable, NO_3^--N concentration.

Effect	**DFn†**	**DFd‡**	**F statistic**	***p* Value**
Intercept	1	109	133.04	<0.0001*
Time	1	109	306.66	<0.0001*
Initial N	1	7	110.89	<0.0001*
Time:Initial N	1	109	61.71	<0.0001*
Time:Treatment	1	109	4.55	0.0352*
Time:Temperature	1	109	16.62	0.0001*
Time:Initial N:Treatment	1	109	3.47	0.0651
Time:Initial N:Temperature	1	109	1.46	0.2286
Time:Treatment:Temeprature	1	109	0.08	0.7788
Time:Initial N:Treatment:Temperature	1	109	0.17	0.6853

†DFn Degrees of freedom of the numerator.
‡DFd Degrees of freedom of the denominator.
* Significance at the 0.05 probability level.

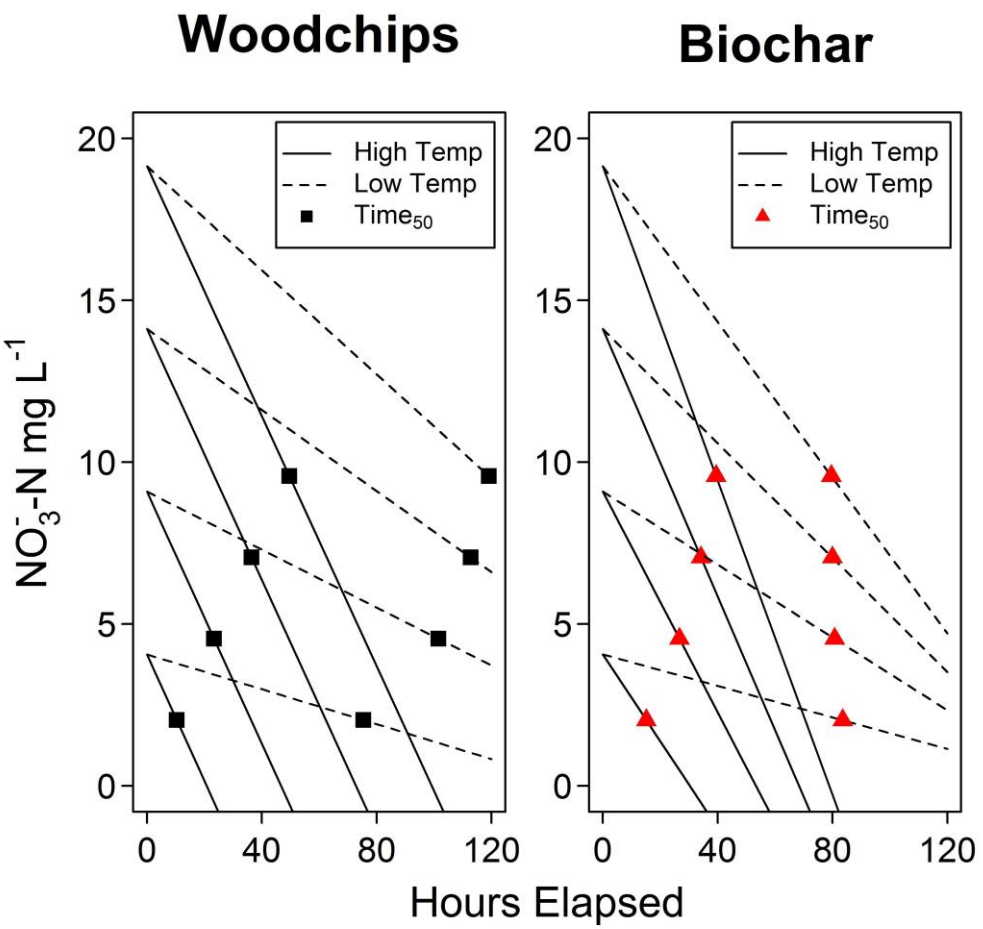

Figure 3. Predicted NO_3^--N removal from a linear mixed effects model fit for woodchip only and biochar-amended denitrifying bioreactors operating under different temperatures and with a range of NO_3^--N influent concentrations.

Table 3. Predicted residence times required for 50% and 90% of influent NO_3^--N removal and removal rates from a linear mixed effects model for a woodchip only and a biochar-amended denitrifying bioreactor operating under a range of influent NO_3^--N concentrations and two temperature conditions, high and low temperatures, averaging 23.9 and 9.6 ˚C respectively. Q^{10} indicates the factor by which the rate of removal is predicted to increase for an increase in temperature of 10 ˚C for a given influent NO_3^--N concentration. A single Q_{10} is reported for each initial concentration as calculated from the paired predicted removal rates at high and low temperature.

Temp	**Influent NO_3^--N (mg L^{-1})**	**$T_{50\%}$ † hours**		**$T_{90\%}$ ‡ hours**		**Removal Rate g N m^{-3} d^{-1}**		**Q_{10} §**	
		Biochar	**Wood**	**Biochar**	**Wood**	**Biochar**	**Wood**	**Biochar**	**Wood**
High	5	15.1	10.4	27.2	18.7	3.22	4.70	3.0	3.6
	10	26.7	23.3	48.0	42.0	4.09	4.67	2.1	2.6
	15	34.2	36.4	61.5	65.5	4.96	4.65	1.7	2.1
	20	39.4	49.6	71.0	89.2	5.83	4.63	1.6	1.8
Low	5	83.5	75.4	150.4	135.6	0.58	0.65	-	-
	10	80.7	101.5	145.3	182.7	1.35	1.07	-	-
	15	79.9	112.8	143.9	203.0	2.12	1.50	-	-
	20	79.6	119.0	143.2	214.3	2.89	1.93	-	-

† Time required for removal of 50% of the initial NO_3^--N concentration.
‡ Time required for removal of 90% of the initial concentration.
§ Q_{10}

2.4.1 First Flush

The first filling event was conducted approximately 1 mo after installation, where introducing low NO_3^--N influent (<0.1 mg L^{-1}) resulted in net export of NO_3^--N. Previously, the DNBRs had remained unsaturated and aerobic. The concentration of NO_3^--N increased over time in both treatments (Fig. 1). This export of nutrients from DNBRs has been observed within the first 3 to 6 mo after installation (and described as the “first flush” phenomenon associated with the export of dissolved organic carbon) in several studies conducted in both field and laboratory

settings, which were cited in a review by Schipper et al. (2010a) (Greenan et al., 2009; Robertson and Cherry, 1995; Robertson et al., 2005; Schipper et al., 2010b; Schmidt and Clark, 2012).

The woodchip DNBR produced a greater maximum NO_3^--N concentration (6.6 mg L^{-1}) during the 80-h observation period than the biochar-amended DNBR (3.1 mg L^{-1}). However, the biochar DNBR maintained an approximately linear increase in NO_3^--N concentration over time, whereas the woodchip NO_3^--N concentration peaked at around 50 h and decreased to about 2.0 mg L^{-1} by hour 80. The differing behavior between the treatments suggests that differing mechanisms in the woodchip- and biochar-amended DNBRs influence the NO_3^-–N concentrations. The lower maximum NO_3^--N concentration observed in the biochar treatment may result from the sorption of the NO_3^--N released from the woodchips (or dissolved in the influent) to the biochar surface. Although biochar is most often associated with an increase in cation exchange capacity (Kookana et al., 2011; Lehmann et al., 2011; McLaughlin et al., 2009), the retention of nutrients (NO_3^--N and PO_4^{3-}) in soils with biochar amendments (Beck et al., 2011; Nelson et al., 2011) suggests the presence of a mechanism for anion sorption. Inyang et al. (2010) reported the first detection of AEC associated with a biochar produced from sugarcane bagasse and proposed AEC as the means for the reported increase in nutrient-holding capacity in soils. Recent work by Lawrineko (2015) indicates that the AEC of biochars created from three feedstocks (alfalfa meal, corn stover, and cellulose derived from hardwood) varies between 0.602 to 27.76 cmol kg^{-1} and is largely attributable to oxonium functional groups. Even in a study noting the absence of significant AEC in biochar, Mukherjee et al. (2011) suggest that “biochars may still sorb phosphate and nitrate by bridge binding using the residual charge of electrostatically attracted or ligand bonded divalent cations such as Ca^{2+} and Mg^{2+} or other metals including Al^{3+}

and Fe^{3+}." The capacity of biochar for anion adsorption through one of these mechanisms could explain the observed extended release of NO_3^--N at a lower concentration in the biochar DNBR compared with the woodchips alone. The delayed onset of NO_3^--N removal in the woodchip DNBR after initial export of NO_3^--N is likely attributable to a lag in denitrifier activity associated with the transition from an aerobic to an anaerobic environment occurring during the first filling of the DNBR. In contrast, the onset of denitrification resulting in NO_3^--N removal in the biochar-amended DNBR could be masked by the extended release of the labile NO_3^--N desorbing from the biochar exchange complex.

The impact of the first flush in DNBRs during start-up includes increased biological oxygen demand and the export of nutrients, which can contribute to the very water quality issues DNBRs attempt to remedy (Schmidt and Clark, 2012). Biochar may be a useful amendment with respect to the first flush phenomenon because lowering the NO_3^--N concentration of the effluent is beneficial even if the total mass of NO_3^--N exported on startup remains the same. Although dissolved organic carbon was not monitored as part of this study, additional contribution from the biochar amendment is not anticipated given its recalcitrance relative to woodchips. Although interesting and informative for field-based applications and environmental implications, these two events were omitted from the dataset used to fit the LME because they were not considered representative of long-term performance. Further research is required to determine the extent of the ability of biochar amendment to mitigate the first flush in DNBRs.

The rate of N removal was found to increase with increasing initial concentration independently of treatment and temperature, which reflects the findings of Christianson et al. (2012) and Chun et al. (2010). In contrast, the majority of DNBRs can be described by zero-order

kinetic reactions, maintaining similar removal rates independently of the influent concentration (Schipper et al., 2010a). Unmeasured site-specific parameters may account for the discrepancy between the governing kinetics of denitrification in the literature as well as the conflicting conclusions of other studies that have yet to be resolved and warrant further investigation. Visual examination of Fig. 3 suggests that the correlation between initial NO_3^--N concentration and removal rate is greater in the biochar treatment than in the woodchip control because the slopes become steeper (e.g., faster removal) with increasing concentration.

The LME predicts that biochar addition results in greater N removal when influent NO_3^--N concentrations are greater than approximately 5 mg L^{-1} under low-temperature conditions (water temperatures averaging 9.6°C) and >10 mg L^{-1} under high-temperature conditions (averaging 23.9°C) but may reduce the rate of N removal relative to woodchips alone when the initial concentration is lower (Table 3; Fig. 3). Based on these results, biochar addition to woodchip DNBRs is hypothesized to induce both increased denitrification and NO_3^--N sorption under higher concentrations, but subsequent desorption of NO_3^--N can occur under lower concentrations. That is, the AEC associated with the biochar acts as a temporary N sink, storing N sorbed under high influent concentrations and releasing bound N under low influent concentrations in an equilibrium process. In addition to the reports of biochar's anion sorption capacity discussed above (Inyang et al., 2010; Lawrineko, 2015; Mukherjee et al., 2011) and the well-established reduction in NO_3^-–N leaching in biochar-amended soils (Beck et al., 2011; Nelson et al., 2011), this hypothesis is supported by adsorption tests conducted by the Soil Control Lab, Watsonville, CA, on samples of the biochar used in this study, which indicate that 23.3% of NO_3^--

N in an initial solution of 409 mg L^{-1} was retained after 20 pore volume additions of deionized water.

The question remains as to what proportion of the biochar-induced removal is permanent NO_3^--N removal via denitrification and what is temporary storage via sorption. Although this study did not differentiate these removal mechanisms, many laboratory-scale investigations have demonstrated that biochar addition to soil results in a change in the microbial community structure and biological N cycling, specifically increasing the relative abundance of denitrifying enzymes (Anderson et al., 2011; Ducey et al., 2013; Harter et al., 2014). Therefore, increased rates of denitrification in response to biochar amendment represents a plausible explanation for the observed increase in NO_3^--N removal in biochar-amended woodchip DNBRs under higher relative concentrations. However, future studies should examine the contribution of biochar sorption to NO_3^--N removal, assess the stability of this surface interaction, and isolate the effect of biochar on denitrification both chemically and microbially.

Higher temperatures resulted in more rapid NO_3^--N removal in both the woodchip and biochar DNBRs (p = 0.0039). Water temperatures averaged 23.9 and 9.6°C in the high and low categories, respectively. That N removal increases at higher temperatures independently of the presence of biochar is unsurprising if N removal is attributed to denitrification because microbial activity generally increases with temperature over the range to which organisms are adapted (Seitzinger et al., 2006). These results corroborate previous research and reflect the conclusions drawn by Schipper et al. (2010a) based on a review of published DNBR research: N removal increases with average annual temperature when NO_3^--N is nonlimiting with a Q_{10} (the factor by which the rate of removal is predicted to increase for an increase in temperature of 10°C) value

of approximately 2. Table 3 reports the Q_{10} values calculated from the predicted NO_3^-–N removal rates using the average water temperatures for the high and low categories. Calculated Q_{10} values of 1.3 to 2.0 aligned with previous studies (Schipper et al., 2010a) and indicated slightly greater values for the woodchip DNBR (Table 3).

Observed rates of NO_3^-–N removal of 0.25 to 6.06 g N m^{-3} d^{-1} and predicted rates of 0.41 to 4.08 g N m^{-3} d^{-1} track with average removal rates achieved by similarly designed woodchip denitrification beds of 1.8 to 5.1 g N m^{-3} d^{-1}, which were reported by seven of the eight studies reviewed by Schipper et al. (2010a). However, removal rates during some of the events with low influent concentrations under low temperature conditions fell below the typical range. Figure 3 and Table 3 indicate the predicted residence times to achieve 50 and 90% reduction in NO_3^--N relative to initial concentration for each of the treatments under both temperature conditions over a range of influent concentrations (5–20 mg L^{-1}). A recent article by Moorman et al. (2015) summarized selected estimates of hydraulic residence times required to reach 50% removal in various field studies and concluded that 6 to 24 h was required to reduce influent concentrations of 10 to 25 mg L^{-1} by half. In contrast, the LME suggests that to achieve 50% NO_3^-–N removal with influent concentrations of 5 to 20 mg L^{-1}, residence times of 15.1 to 89.7 h for the biochar-amended DNBR and 10.4 to 119 h for the woodchip DNBR are required (Table 3). However, given that the N removal expressed as a function of elapsed time in a batch experiment is not directly equivalent to removal as a function of residence time in flow-through systems, this operational difference may provide some explanation for the differing time scales of removal. A principle difference of the flood-and-drain operations is the unsaturated condition between batch events, which likely inhibits the denitrifying population, whereas the flow-through design can maintain

anaerobic conditions and sustain denitrifying microorganisms. Consequently, the removal rates in these pilot-scale DNBRs would be expected to increase if operated under flow-through conditions. Nonetheless, the LME output emphasizes that biochar DNBRs could be potentially beneficial in agricultural areas with higher influent NO_3^-–N concentrations or perhaps, as demonstrated in this experiment, biochar addition could significantly reduce the residence time required to achieve a given reduction in NO_3^--N (T_{50} or T_{90}) when influent NO_3^--N concentrations are greater than 5 to 10 mg L^{-1} (Fig. 3; Table 3).

2.4.2 Ammonium Analysis by the Linear Mixed Effects Model

The only significant factor in the LME predicting NH_4^+-N concentration was the initial NH_4^+-N concentration (p = 0.0132). Treatment and time were not significant predictors of NH_4^+-N concentration, which provides evidence that biochar did not affect the rate of DNRA, an alternative mechanism of NO_3^--N transformation that can occur under anaerobic conditions. Interpretation of differences in NO_3^--N between the treatments is simplified because DNRA results in NO_3^--N removal, which could be misinterpreted as denitrification. These observations agree with previous work indicating the marginal activity of DNRA in DNBRs (Greenan et al., 2006; Schipper and Vojvodic-Vukovic, 2000).

2.4.3 Water Chemistry: pH, Oxidation Reduction Potential, and Dissolved Oxygen

Qualitative evidence for biological removal of NO_3^--N via denitrification included measurements of ORP, DO, and pH indicating that conditions were suitable for denitrification: ORP <300 mV, DO <2 mg L^{-1}, and pH between 6 and 8 (Trudell et al., 1986; Vymazal, 2007). Observed concentrations of DO were <0.1 to 0.4 mg L^{-1} at steady state, ORP values were -90 to 440 mV, and pH ranged from 5.87 to 7.15. Figure 4 displays pH, ORP, and DO observations for

one low-temperature event and one high-temperature event that are reflective of the other high- and low-temperature events. Significant differences for any of these parameters between the treatments were not observed based on a paired *t* test on the mean values.

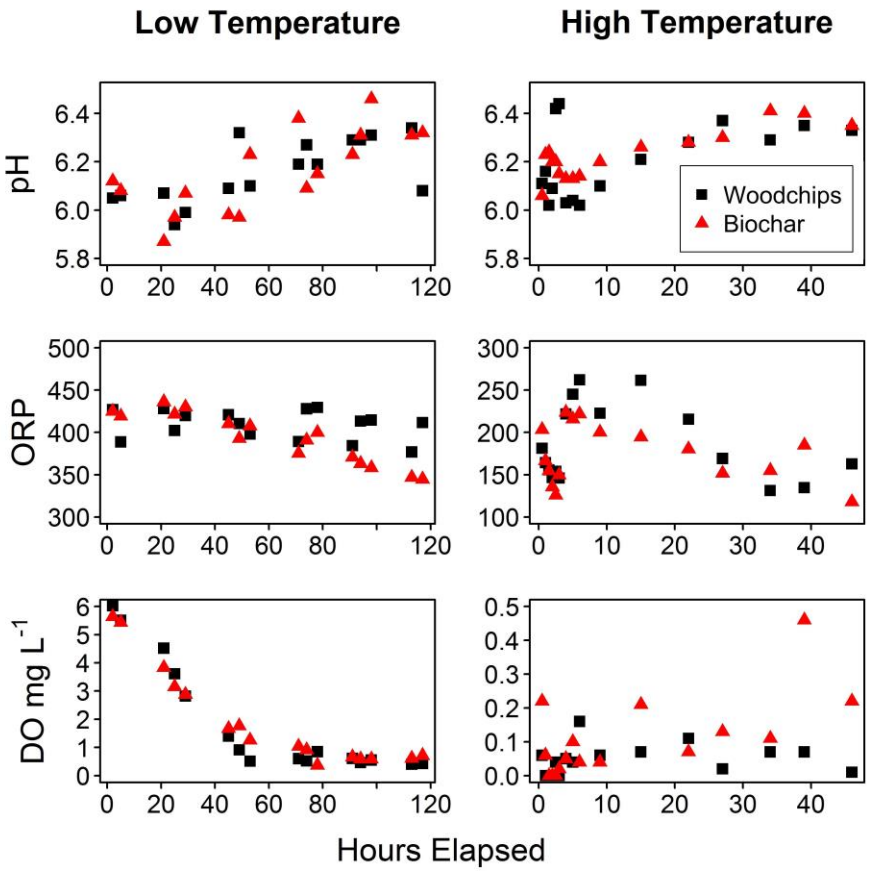

Figure 4. Comparison of pH, oxidation reduction potential (ORP) and dissolved oxygen (DO) levels in woodchip only and biochar-amended denitrifying bioreactors recorded during a low temperature event during the non-growing season and a high temperature event during the growing season.

Values of pH generally increased over the course of an event. A comparable increase in pH was observed during the events in both treatments at both high and low temperatures, likely a result of the alkalinity produced by the $Ca(NO_3)_2$ with a possible contribution of the process of denitrification itself via the release of hydroxyl anions as oxygen atoms are sequentially stripped from NO_3^- (McBride, 1994). Similarly, Warneke et al. (2011) observed an increase in pH from

about 6 to 7 over the length of a flow-through DNBR. A thorough review of the influence of pH on denitrification by Simek and Cooper (2002) concludes that "in acidic soil [the rates of denitrification] are less than in neutral or slightly alkaline soils." Therefore, buffering pH at or above neutral conditions within DNBRs could potentially increase NO_3^--N removal. Although a difference in pH between the treatments was not observed, previous research demonstrates that biochar can induce a liming effect cited as responsible for the agronomic improvement in nutrient availability and retention associated with its application in soils (Ippolito et al., 2012). Therefore, the relationship between biochar, pH, and NO_3^--N removal rates in DNBRs deserves further investigation.

Observed values of ORP remained below the approximate limiting maximum value for denitrification of 300 mV (Vymazal, 2007) in the biochar-amended bed and approached this limiting value in the woodchip bed. However, interpreting ORP values as an indication of suitable conditions to support denitrification is severely limited by the convoluting effects of site-specific characteristics, such as the concentrations of other redox active constituents, soil heterogeneity, and system disequilibrium (McBride, 1994). A net decrease in ORP occurred in both treatments, albeit from a higher initial value and much more slowly under low temperature. A decrease in ORP over time is associated with oxygen consumption during denitrification (Cey et al., 1999; Schilling et al., 2007) and is further indicative of the occurrence of denitrification. The difference in initial ORP between the high- and low-temperature events is at least partially due to the difference in oxygen content of the influent for the low- and high-temperature events, given that oxygen is a major driver of ORP (McBride, 1994). Low-temperature events received influent

saturated with dissolved oxygen, whereas the oxygen content of the influent water for the high-temperature event had already been depleted of oxygen to <0.2 mg L^{-1}.

The level of DO limiting environmental denitrification rates remains uncertain within a range of values (0.5–4.5 mg L^{-1}), as reported by Warneke et al. (2011). Variability in limiting concentrations is likely due to substrate heterogeneity and the presence of microsites creating anaerobic environments (Seitzinger et al., 2006; Warneke et al., 2011). Even in the context of woodchip DNBRs, differing levels of limiting DO are frequently reported. Warneke et al. (2011) demonstrated that DO levels up to 1.7 mg L^{-1} did not limit removal, whereas Healy et al. (2006) reported uninhibited denitrification up to 3.7 mg L^{-1}. Oxygen-induced inhibition of denitrification is another possible mechanism for the lower N removal rates at low temperatures where DO concentrations as high as 6 mg L^{-1} were measured; conversely, under high temperatures DO was <0.5 mg L^{-1} (Fig. 4).

2.4.4 Implications

This study provides pilot-scale evidence that biochar has the potential to enhance NO_3^--N removal in woodchip DNBRs receiving sufficiently NO_3^--N-enriched influent at concentrations likely to be encountered in agricultural drainage. By achieving a given level of removal with a shorter residence time than a woodchip bed, biochar amendment could either allow for smaller bed designs or the treatment of larger flows with high NO_3^--N concentrations. Therefore, determining the cost-effectiveness of biochar amendment to DNBRs deserves further investigation, acknowledging that biochar is a more expensive substrate than woodchips. However, the addition of biochar can change the porosity and alter the hydraulic conductivity of the bed, perhaps necessitating a greater bed volume to accommodate design flows. Determining

the effect of biochar addition on the hydraulic properties of DNBRs will be necessary before recommendation of design and management of DNBRs using biochar. In sum, although these data suggest that biochar may not improve performance of DNBRs receiving less than 5 to 10 NO_3^--N mg L^{-1}, further investigation of biochar applied to field-scale DNBRs is warranted by the potential for biochar to be beneficial under high N loadings and the laboratory findings of increased phosphate removal and reduced N_2O emission associated with biochar amendment (Bock et al., 2015).

2.5 References

Anderson, C.R., L.M. Condron, T.J. Clough, M. Fiers, A. Stewart, R.A. Hill, and R.R. Sherlock. 2011. Biochar induced soil microbial community change: Implications for biogeochemical cycling of carbon, nitrogen and phosphorus. Pedobiologia 54:309–320. doi:10.1016/j.pedobi.2011.07.005

Beck, D.A., G.R. Johnson, and G.A. Spelok. 2011. Amending greenroof soil with biochar toaffect runoff water quantity and quality. Environ. Pollut. 159:2111–2118. doi:10.1016/j.envpol.2011.01.022

Bock, E., N. Smith, M. Rogers, B. Coleman, M. Reiter, B. Benham, and Z. Easton. 2015. Enhanced nitrate and phosphate removal in a denitrifying bioreactor with biochar. J. Environ. Qual. 44:605–613. doi:10.2134/ jeq2014.03.0111

Cameron, S., and L. Schipper. 2010. Nitrate removal and hydraulic performance of organic carbon for use in denitrification beds. Ecol. Eng. 36:1588–1595. doi:10.1016/j.ecoleng.2010.03.010

Canfield, D.E., A.N. Glazer, and P.G. Falkowski. 2010. The evolution and future of the Earth's nitrogen cycle. Science 330:192–196. doi:10.1126/ science.1186120

Cayuela, M.L., M.A. Sanchez-Monedero, A. Roig, K. Hanley, A. Enders, and J. Lehmann. 2013. Biochar and denitrificaiton in soils: When, how much and why does biochar reduce N2O emissions? Sci. Rep. 3:1732–1739. doi:10.1038/srep01732

Cey, E.E., D.L. Rudolph, R. Aravena, and G. Parkin. 1999. Role of the riparian zone in controlling the distribution and fate of agricultural nitrogen near a small stream in southern Ontario. J. Contam. Hydrol. 37:45–67. doi:10.1016/S0169-7722(98)00162-4

Christianson, L., A. Bhandari, M. Helmers, K. Kult, T. Sutphin, and R. Wolf. 2012. Performance evaluation of four field-scale agricultural drainage denitrification bioreactors in Iowa. Trans. ASABE 55:2163–2174. doi:10.13031/2013.42508

Chun, J.A., R.A. Cooke, J.W. Eheart, and J. Cho. 2010. Estimation of flow and transport parameters for woodchip-based bioreactors: II. field scale bioreactor. Biosyst. Eng. 105:95–102. doi:10.1016/j.biosystemseng.2009.09.018

Clough, T.J., and L.M. Condron. 2010. Biochar and the nitrogen cycle: Introduction. J. Environ. Qual. 39:1218–1223. doi:10.2134/jeq2010.0204

Coumaravel, K., R. Santhi, V.S. Kumar, and M.M. Mansour. 2011. Biochar: A promising soil additive. Agric. Rev. 32:134–139.

Ding, Y., J. Liu, and Y. Wang. 2013. Effects of biochar on microbial ecology in agricultural soil: A review. Chin. J. Appl. Ecol. 11:3311–3317.

Ducey, T.F., J.A. Ippolito, K.B. Cantrell, J.M. Novak, and R.D. Lentz. 2013. Addition of activated switchgrass biochar to an aridic subsoil increases microbial nitrogen cycling gene abundances. Appl. Soil Ecol. 65:65–72. doi:10.1016/j.apsoil.2013.01.006

Galloway, J.N., J.D. Aber, J.W. Erisman, S.P. Seitzinger, R.W. Howarth, and E.B. Cowling. 2003. The nitrogen cascade. Bioscience 53:341–356. doi:10.1641/0006 3568(2003)053(0341:TNC]2.0.CO;2

Galloway, J.N., A.R. Townsend, J.W. Erisman, M. Bekunda, Z. Cai, J.R. Freney, L.A. Martinelli, S.P. Seitzinger, and M.A. Sutton. 2008. Transformations of the nitrogen cycle: Recent trends, questions, and potential solutions. Science 320:889–892. doi:10.1126/science.1136674

Gelman, A., and J. Hill. 2009. Data analysis using regression and multilevel/hierarchical models. 11th ed. Cambridge Univ. Press, New York.

Gibert, O., S. Pomierny, I. Rowe, and R.M. Kalin. 2008. Selection of organic substrates as potential reactive materials for use in a denitrification permeable reactive barrier (PRB). Bioresour. Technol. 99:7587–7596. doi:10.1016/j.biortech.2008.02.012

Gold, A.J., K. Addy, M.B. David, L.A. Schipper, and B.A. Needelman. 2013. Artificial sinks: Opportunities and challenges for managing offsite nitrogen losses. J. Contemp. Water Res. Educ. 151:9–19. doi:10.1111/j.1936-704X.2013.03147.x

Greenan, C.M., T.B. Moorman, T.C. Kaspar, T.B. Parkin, and D.B. Jaynes. 2006. Comparing carbon substrates for denitrification of subsurface drainage. J. Environ. Qual. 35:824 829. doi:10.2134/jeq2005.0247

Greenan, C.M., T.B. Moorman, T.B. Parkin, T.C. Kaspar, and D.B. Jaynes. 2009. Denitrification in wood chip bioreactors at different water flows. J. Environ. Qual. 38:1664–1671. doi:10.2134/jeq2008.0413

Harter, J., H. Drause, S. Schuettler, R. Ruser, M. Fromme, T. Scholten, A. Kappler, and S. Behrens. 2014. Linking N2O emissions from biochar-amended soil to the structure and function of the N-cycling microbial community. ISME J. 8:660–674 doi:10.1038/ismej.2013.160

Healy, M.G., M. Rodgers, and J. Mulqueen. 2006. Denitrification of a nitrate-rich synthetic wastewater using various wood-based media materials. J. Environ. Sci. Health Part A 41:779–788. doi:10.1080/10934520600614371

Hunter, W.J. 2001. Use of vegetable oil in a pilot-scale denitrifying bioreactor. J. Contam. Hydrol. 53:119–131. doi:10.1016/S0169-7722(01)00137-1

Inyang, M., B. Goa, P. Pullammanapppallili, W. Ding, and A.R. Zimmerman. 2010. Biochar from anaerobically digested sugarcane bagasse. Bioresour. Technol. 101:8868–8872. doi:10.1016/j.biortech.2010.06.088

Ippolito, J.A., D.A. Laird, and W.J. Busscher. 2012. Environmental benefits of biochar. J. Environ. Qual. 41:967–972. doi:10.2134/jeq2012.0151

Jickells, T. 2005. External inputs as a contributor to eutrophication problems. J. Sea Res. 54:58 69. doi:10.1016/j.seares.2005.02.006

Kookana, R.S., A.K. Sarmah, L. Van Zwieten, E. Krull, B. Singh, and D.L. Sparks. 2011. Biochar application to soil: Agronomic and environmental benefits and unintended consequences. Adv. Agron. 112:103–143. doi:10.1016/B978-0-12-385538-1.00003-2

Lassiter, E., and Z.M. Easton. 2013. Denitrifying bioreactors: An emerging best management practice to improve water quality. BSE-55P. pubs.ext.vt.edu/ BSE/BSE-55/BSE-55 PDF.pdf (accessed 15 Apr. 2015).

Lawrineko, M., and D.A. Laird. 2015. Anion exchange capacity of biochar. Green Chem. 17:4628–4636.

Lehmann, J., J. Gaunt, and M. Rondon. 2006. Bio-char sequestration in terrestrial ecosystems: A review. Mitigation Adapt. Strat. Glob. Change. 11:395– 419. doi:10.1007/s11027-005 9006-5

Lehmann, J., M.C. Rilig, J. Thies, C.A. Masiello, W.C. Hockaday, and D. Crowley. 2011. Biochar effects on soil biota: A review. Soil Biol. Biochem. 43:1812–1823 doi:10.1016/j.soilbio.2011.04.022

McBride, M.B. 1994. Environmental chemistry of soils. Oxford Univ. Press, New York.

McLaughlin, H., P.S. Anderson, F.E. Shields, and T.B. Reed. 2009. All biochars are not created equal and how to tell them apart. North American Biochar. 2:1–36.

Moorman, T.B., M.D. Tomer, D.R. Smith, and D.B. Jaynes. 2015. Evaluating the potential role of denitrifying bioreactors in reducing watershed-scale nitrate loads: A case study comparing three Midwestern (USA) watersheds. Ecol. Eng. 75:441–448. doi:10.1016/ j.ecoleng.2014.11.062

Mukherjee, A., A.R. Zimmerman, and W. Harris. 2011. Surface chemistry variations among a series of laboratory-produced biochars. Geoderma 163:247–255. doi:10.1016/ j.geoderma.2011.04.021

Nelson, N.O., S.C. Agudelo, W. Yuan, and J. Gan. 2011. Nitrogen and phosphorus availability in biochar amended soils. Soil Sci. 176:218–226.

Natural Resource Conservation Service. 2009. Conservation standard practice denitrifying bioreactor. Interim IA-747-1. NRCS, Des Moines, IA.

Pinheiro, J., and D. Bates, S. DebRoy, and R Core Team. 2014. NLME: Linear and nonlinear mixed effects models. R package version 3.1-117. cran.rproject.org/web/ packages /nlme/nlme.pdf (accessed 15 Apr. 2015).

R Core Team. 2014. R: A language and environment for statistical computing. R Foundation for Statistical Computing, Vienna, Austria. www.R-project. org/ (accessed 15 Apr. 2015).

Robertson, W., and J. Cherry. 1995. In situ denitrification of septic-system nitrate using reactive porous media barriers: Field trials. Ground Water 33:99–111. doi:10.1111/ j.17456584.1995.tb00266.x

Robertson, W., G. Ford, and P. Lombardo. 2005. Wood-based filter for nitrate removal in septic systems. Trans. ASABE 48:121–128. doi:10.13031/2013.17954

Robertson, W.D., J.L. Vogan, and P.S. Lombardo. 2008. Nitrate removal rates in a 15-year-old permeable reactive barrier treating septic system nitrate. Ground Water Monit. Rev. 28:65–72. doi:10.1111/j.1745-6592.2008.00205.x

Saliling, W.J.B., P.W. Westerman, and T.M. Losordo. 2007. Wood chips and wheat straw as alternative biofilter media for denitrification reactors treating aquaculture and other wastewaters with high nitrate concentrations. Aquacult. Eng. 37:222–233. doi:10.1016/j.aquaeng.2007.06.003

Schilling, K.E., M.D. Tomer, Y.K. Zhang, T. Weisbrod, P. Jacobson, and C.A. Cambardella.

2007. Hydrogeologic controls on nitrate transport in a small agricultural catchment, Iowa. J. Geophys. Res. Biogeosci. 112. doi:10.1029/2007JG000405

Schipper, L.A., and M. Vojvodic-Vukovic. 2000. Nitrate removal from groundwater and denitrification rates in a porous treatment wall amended with sawdust. Ecol. Eng. 14:269–278. doi:10.1016/S0925-8574(99)00002-6

Schipper, L.A., W.D. Robertson, A.J. Gold, D.B. Jaynes, and S.C. Stewart. 2010a. Denitrifying bioreactors: An approach for reducing nitrate loads to receiving waters. Ecol. Eng. 36:1532–1543. doi:10.1016/j.ecoleng.2010.04.008

Schipper, L.A., S. Cameron, and S. Warneke. 2010b. Nitrate removal from three different effluents using large-scale denitrification beds. Ecol. Eng. 36:1552–1557. doi:10.1016/j.ecoleng.2010.02.007

Schmidt, C.A., and M.W. Clark. 2012. Evaluation of a denitrification wall to reduce surface water nitrogen loads. J. Environ. Qual. 41:724–731. doi:10.2134/jeq2011.0331

Seitzinger, S., J.A. Harrison, J.K. Bohlke, A.F. Bouwman, R. Lowrance, B. Peterson, C. Tobias, and G. Van Drecht. 2006. Denitrification across landscapes and waterscapes: A synthesis. Ecol. Appl. 16:2064–2090. doi:10.1890/1051-0761(2006) 016[2064:DALAWA] 2.0.CO;2

Simek, M., and J.E. Cooper. 2002. The influence of soil pH on denitrification: Progress towards the understanding of this interaction over the last 50 years. Eur. J. Soil Sci. 53:345–354. doi:10.1046/j.1365-2389.2002.00461.x

Smiciklas, K.D., and A.S. Moore. 2008. Tile drainage nitrate concentrations in response to nitrogen application. J. Agron. 7:163–169 doi:10.3923/ ja.2008.163.169

Sohi, S., E. Krull, E. Lopez-Capel, and R. Bol. 2010. A review of biochar and its use and function in soils. Adv. Agron. 105:47–82. doi:10.1016/ S0065-2113(10)05002-9

Trudell, M., R.W. Gillham, and J.A. Cherry. 1986. An in-situ study of the occurrence and rate of denitrification in a shallow unconfined sandy aquifer. J. Hydrol. 83:251–268.doi:10.1016 /0022-1694(86)90155-1

USEPA. 1996. Safe Drinking Water Act. National primary drinking water regulations. 40 CFR Part 141–149.

van Driel, P.W., W.D. Robertson, and L.C. Merkley. 2006. Upflow reactors for riparian zone denitrification. J. Environ. Qual. 35:412–420. doi:10.2134/ jeq2005.0027

Verbeke, G., G. Molenberghs, and D. Rizopoulos. 2010. Random effects models for longitudinal

data. In: K. van Montfort, J.H.L. Oud, and A. Satorra, editors, Longitudinal research with latent variables. 11th ed. Springer My Copy, UK. doi:10.1007/978-3-642-11760-2-2

Vymazal, J. 2007. Removal of nutrients in various types of types of constructed wetlands. Sci. Total Environ. 380:48–65. doi:10.1016/j. scitotenv.2006.09.014

Warneke, S., L.A. Schipper, D.A. Bruesewitz, I. McDonald, and S. Cameron. 2011. Rates, controls, and potential adverse effects of nitrate removal in a denitrification bed. Ecol. Eng. 37:511–522. doi:10.1016/j. ecoleng.2010.12.006

Winter, B. 2013. Linear models and linear missed effects models in R with linguistic applications. arXiv:1308.5499. arxiv.org/pdf/1308.5499.pdf (accessed 15 Apr. 2015).

Woli, K.P., M.B. David, R.A. Cooke, G.G. McIsaac, and C.A. Mitchell. 2010. Nitrogen balance in and export from agricultural fields associated with controlled drainage systems and denitrifying bioreactors. Ecol. Eng. 36:1558–1566. doi:10.1016/j.ecoleng.2010.04.024

3. EFFECT OF BIOCHAR, HYDRAULIC RESIDENCE TIME, AND NUTRIENT LOADING ON N_2O, CH_4, and CO_2 EMISSIONS FROM LABORATORY-SCALE DENITRIFYING BIOREACTORS

3.1 Abstract

Increased adoption of woodchip denitrifying bioreactors to mitigate nutrient export in agricultural drainage creates opportunities for improving water quality but also raises concerns about potential unintended consequences of widespread implementation. Greenhouse gas (GHG) emissions, particularly as nitrous oxide (N_2O) produced during denitrification, are of particular concern. To gain understanding of the controls on GHG emissions in bioreactors, the effects of nutrient loading, hydraulic residence time (HRT), and biochar addition were tested in laboratory-scale woodchip bioreactors, as biochar amendment to agricultural soils has previously been reported to reduce GHG emissions. A full factorial experiment with three media types (woodchips, 10% biochar, and 30% biochar), three HRTs (3, 6, and 12 h), and four influent formulations, all combinations of high and low nitrogen (16.1 and 4.5 mg l^{-1} NO_3^--N) and phosphorus (1.9 and 0.6 PO_4^{3-}-P), tested the effect of these variables on GHG flux in 6050 cm^3 bioreactor columns, with three replicates of every experimental treatment. Nitrous oxide, methane (CH_4), and carbon dioxide (CO_2) fluxes were measured using the closed dynamic chamber technique with a cavity ring-down spectrometer. N_2O was found to contribute substantially to total GHG emissions assessed in terms of CO_2 equivalents, accounting for 20.9% of warming potential on average and up to 84.5%, with a mean flux of 2.92 mg N_2O-N m^{-2} d^{-1} and a maximum of 77.3 mg N_2O-N m^{-2} d^{-1}. Emissions factors, the proportion of NO_3^- removed by the bioreactor released as N_2O, ranged -0.1 to 9.5%. Treatment effects were assessed with

linear mixed effects models, and biochar addition was found to significantly increase GHG emissions under most tested conditions.

3.2 Introduction

The establishment of denitrifying bioreactors as an accepted agricultural best management practice (BMP) to reduce nitrogen (N) export in drainage waters is underpinned by a growing body of research establishing expected N removal efficiencies (e.g. Addy et al., 2016) and relating performance to design parameters including bed sizing, dimensions, and target hydraulic residence time (HRT) (Christianson et al., 2013c; Christianson et al., 2011; Sharrer et al., 2016). Maximizing N removal has been the primary focus of bioreactor studies, but increasingly pollution swapping potential, the trade-off between increasing N removal and increasing environmentally harmful byproducts such as greenhouse gases (GHGs), methylmercury (CH_3Hg^+), or excess dissolved organic carbon is acknowledged, quantified, and incorporated into assessment of bioreactor performance (Christianson and et al., 2017; Healy et al., 2012, 2015; Warneke et al., 2011a, 2011b). Indeed, bioreactor GHG emissions, specifically nitrous oxide (N_2O) emissions produced via incomplete denitrification, were among the earliest identified concerns regarding widespread bioreactor implementation (Schipper et al., 2010), and have since been quantified in several laboratory- (Bock et al., 2015), pilot- (Warneke et al., 2011b), and field-scale systems (Elgood et al., 2010; Moorman et al., 2010; Warneke et al., 2011a; Woli et al., 2010). Although problematic rates of N_2O flux have not been reported, given the high variability of GHG emissions from agricultural soils (Mathieu et al., 2006; Oertel et al., 2016), a similarly spatially and temporally dynamic fluxes could be expected in denitrifying bioreactors and complicate efforts to estimate average or cumulative emissions. Given the

expense and technical challenges of measuring GHG flux with high temporal resolution, controlled experiments of the factors influencing GHG emissions in bioreactors have not been conducted. However, such experiments could provide valuable insight into the mechanisms of bioreactor GHG emissions and potentially inform refinement of bioreactor design guidelines aimed at minimizing emissions.

Substrate engineering is one approach to mitigating bioreactor GHG emissions. Use of biochar, an organic carbon pyrolysis product developed as a soil amendment, in denitrifying bioreactors merits investigation because it has been widely reported to reduce GHG emissions when incorporated into agricultural soils (Florinsky et al., 2004; Kookana et al., 2011; Saarnio et al., 2013; Sohi et al., 2010), although instances of biochar increase N_2O emissions have been observed as well (Bruun et al., 2011; Yanai et al., 2007). Additionally, biochar has also been shown to reduce leaching of N, phosphorus (P), and organic carbon from soils (Beck et al., 2011), potentially providing additional opportunities to mitigate pollution swapping in bioreactors. General characteristics of biochars underlying induced soil properties include high specific surface area, micropore volume, cation exchange capacity, and water holding capacity (Kookana et al., 2011; Lehmann et al., 2011; McLaughlin et al., 2009). Different mechanisms of N_2O suppression related to these characteristics have been reported, Clough and Condron (2010) describe the ability of alkaline biochar to raise pH which favors production of N_2 over the accumulation of N_2O during denitrification. Saarnio et al. (2013) found that biochar indirectly decreased N_2O emissions through its effect on increasing soil moisture. However, Case et al. (2015) reported that biochar suppressed N_2O emissions even in a completely saturated sandy loam, suggesting a mechanism unrelated to the effect on soil water holding capacity. Perhaps

unsurprisingly, the effect of biochar on GHG emissions in woodchip bioreactors has been mixed. Simple batch experiments showed that biochar-amended woodchips produced less N_2O than woodchips alone in batch experiments with gastight bioreactor columns (Bock et al., 2015; Easton et al., 2015), whereas no differences in N_2O production between woodchips with or without biochar amendment by Christianson et al. (2011). Aside from its effect on GHG flux, biochar may hold potential to increase N removal in bioreactors. Pluer et al. (2016) and Bock et al. (2015; 2016) observed greater N removal rates in both laboratory and field bioreactors amended with biochar than for the woodchips alone. Furthermore, an economic analysis based on the relationship between biochar and added N removal developed in a pilot-scale experiment (Bock et al., 2016) suggests that increasing N removal efficiency with biochar addition may be cost-effective given sufficient drainage area and N loading to the bioreactor (DeBoe et al., 2017), although as pointed out by Christianson et al. (2016), these results require validation in field testing. Nonetheless, additional investigation of the effect of biochar on nutrient removal and GHG emissions in denitrifying bioreactors is warranted.

The objective of this study was to evaluate the effect of biochar amendment to woodchip bioreactors, HRT, and nutrient loading, both N and P, on emission of N_2O, CH_4, and CO_2. A longitudinal factorial experiment with 6560 cm^3 laboratory bioreactor columns tested the hypothesis that biochar addition lowers GHG emissions relative to woodchips alone across different HRTs and nutrient loading rates; simultaneously, the effect of biochar on N and P removal was also examined and is reported elsewhere.

3.3 Methods

A full factorial experiment tested the effect of media type, HRT, and N and P influent concentration on the GHG flux (N_2O, CH_4, and CO_2) in a flow through laboratory scale denitrifying bioreactor. The three media types tested were woodchips (W), woodchips with a 10% volumetric biochar addition (B_{10}), and woodchips with 30% volumetric biochar addition (B_{30}). Three target HRTs, 3, 6, and 12 h encompassed the reported target range of 4-8 h to meet a target load reduction of 45% (Christianson et al., 2011; Christianson et al., 2013b). Twelve horizontal, flow through columns were used to test each treatment combination of media, HRT, and N loading in triplicate over the course of nine trials. A single combination of media and HRT was tested in each trial, while four different nutrient solutions, all combinations of the selected high (16.1 mg l^{-1} NO_3^--N and 1.9 mg l^{-1} PO_4^{3-}-P) and low (4.5 mg l^{-1} N and 0.6 mg l^{-1} P) N and P concentrations representative of agricultural drainage, were pumped through the four sets of columns in triplicate. In addition to the description in 3.3.1, details of the experimental design can be found for a companion study of nutrient removal in Coleman (2017).

3.3.1 Column design

Bioreactor columns with a volume of 6560 +/- 30 cm^3 were constructed from 10.22 cm inner diameter (ID) schedule 40 PVC pipe (4 in), with a 45° wye with a 5.25 cm ID branch with socket connections (4 in by 4 in by 2 in) inserted approximately 70% of the length toward the outlet to function as a gas sampling port. A short section of 5.25 cm PVC was cemented to the branch of the wye to accommodate a removable socket cap to isolate the headspace during GHG flux measurement. Endcaps with removable threaded plugs were affixed to each end with PVC primer and cement, and pipe thread sealant (RectorSeal) maintained a watertight

connection between the endcaps and plugs. Couplings with barbed tube fitting adaptors were installed in the threaded plugs and attached to tubing supplying the column-bioreactors with nutrient solution and freely draining effluent. The inlet coupling was located near the top of the column when placed horizontally, at a height of 9.75 cm from the bottom of the column, and the outlet coupling was at a height of 7.5 cm, just above the fill media, setting the volume of water contained in the column. Nutrient solution was pumped through the columns using two peristaltic pumps (Masterflex, Cole-Parmer, Vernon Hills, IL).

3.3.2 Experimental treatments

Organic carbon media included locally-sourced woodchips of mixed hardwood species, produced as mulch and biochar (Biochar Now, Carbondale, CO) produced from pine (*Pinus sp*.) feedstock. The biochar was produced by a two-stage pyrolysis process where low oxygen conditions are maintained and the feedstock is held briefly (<1 min) between 500 and 700 °C followed by an extended period at 300 to 550 °C, up to 14 min. The formulation consisted of two size fractions, 80% with dimensions approximately 1.5 cm by 1 cm by 0.5 cm and the remaining 20% a fine dust fraction ranging 10 to 100 µm. For each trial, 5,000 cm^3 of woodchips were measured out for each column, and combined with either 500 cm^3 or 1500 cm^3 of biochar for the B_{10} and B_{30} treatments, respectively. The total volume of woodchips was held constant across treatments to maintain comparable headspace volumes within the columns, as the biochar filled the interstitial spaces between the woodchips, to reduce difference in GHG flux measurements between the columns due to differences in headspace geometry, an important component of the calculation of flux from direct measurements of headspace concentration. The biochar-amended media were combined thoroughly to produce a homogeneous mixture.

Prior to the start of each trial, the columns were filled with fresh media and primed with the same nutrient solution as would be tested experimentally by filling and draining three times over five days and flushed three times in short succession with deionized water.

Flow rates for the peristaltic pumps were selected to achieve HRTs of 3, 6, and 12 h and determined by measuring the time between beginning to pump water through the columns and the first drainage at the outlet. Due to differences in porosity between the media treatments, being reduced in proportion to the volume of biochar added, the flow rates to achieve the same HRTs differed between media treatments. Porosities of the media, determined using volumetric displacement, were 0.66 for the woodchips, 0.61 for B_{10}, and 0.52 for B_{30}; porosity of the woodchips was within the range of 0.60 to 0.86 cm^3 cm^{-3} for woodchips used in other bioreactors reported in the literature (Chun et al., 2009; Robertson, 2010; Woli et al., 2010). Differing flow rates between media types to achieve comparable HRTs confounded the assessment of the effect of influent N and P concentration, but examining N and P loading as a continuous variable allowed the effects of media and loading rate to be distinguished as described in section 2.5.

Table 1. Flow rates, measured hydraulic residence time (HRT), and NO_3^--N loading rates between for each media type, woodchips (W), 10% biochar (B_{10}), and 30% biochar (B_{30}), for each target HRT.

HRT	**3 h**			**6 h**			**12 h**		
Media Type	**W**	**B_{10}**	**B_{30}**	**W**	**B_{10}**	**B_{30}**	**W**	**B_{10}**	**B_{30}**
Flow rate (ml min^{-1})	18.3	16.9	14.4	9.2	8.5	7.2	4.6	4.2	3.6
HRT (h)	3.3	3.1	3.4	6.0	5.8	6.6	11.8	12.5	13.1
N loading (g N m^{-3} $d^{-1)}$	84.9	78.4	66.8	42.7	39.4	33.4	21.3	19.5	16.6

Four nutrient solutions simulating agricultural drainage were prepared for each trial, all combinations of representative high (16.1 mg l^{-1} NO_3^--N and 1.9 mg l^{-1} PO_4^{3-}-P) and low (4.5 mg l^{-1} N and 0.6 mg l^{-1} P) N and P concentrations. Solutions consisted of tap water, previously determined to have consistently low N and P concentrations, and weighed quantities of granular calcium nitrate ($Ca(NO_3)_2$) and potassium phosphate monobasic (KH_2PO_4) mixed in 113 L plastic tanks. During the trials, each of the four nutrient solutions was pumped at the prescribed rate directly to the columns via silicone tubing, a 4-channel peristaltic pump supplying one replicate of each nutrient loading rate and an 8-channel peristaltic pump supping the remaining two replicates.

3.3.3 Greenhouse gas flux measurement

Fluxes of N_2O, CH_4, and CO_2 were quantified using the closed dynamic chamber technique with a cavity ring-down mass spectrometer (CRDS, Picarro G2508, Santa Clara, CA), whereby a closed system is created by isolating the column headspace, which is pumped through the inline analyzer and returned to the column (Collier et al., 2014). For each trial, measurements were taken from each of the 12 columns beginning when the columns were saturated and the first effluent began to drain at 0, 2, 4, 6, 9, and 12 h, then every 6 h through the second day of the trial, every 12 h on the third day, and every 24 hours on the fourth and fifth days. Sampling frequencies accommodated the parallel objective of evaluating treatment effects on N and P removal by the bioreactors, based on preliminary testing of the stability of effluent concentrations and previous laboratory-scale bioreactor experiments (Bock et al., 2015; Easton et al., 2015). Column headspace GHG concentrations were quantified by capping the open branch of the wye to create a closed system and recirculating the headspace between

the CRDS analyzer and the column. A socket cap was modified with two brass bulkhead unions, with rubber gaskets on the inside of the cap to prevent leakage, which were connected with compression fittings the inlet and exhaust lines of the analyzer, two 3 m lengths of 3.2 mm ID inert, polyethylene lined tubing with a vinyl acetate shell. The exhaust union was also fitted with an elbow connector inside the cap to expel the recirculated headspace away from the intake to minimize short circuiting of the flow. Prior to taking a measurement the exhaust line was disconnected from the cap and reattached only after the cap was placed onto the sampling port, venting to minimize the disruption of the headspace pressure gradient and diffusive flux from the media (De Klein and Harvey, 2012). Headspace concentrations of N_2O, CH_4, and CO_2 were recorded for two minutes for each column, a relatively short duration to avoid changing the analyte concentration gradients to the point where the rate of diffusive flux is appreciably affected (Collier et al., 2014). Ambient air was pumped through the instrument for at least two minutes between each measurement to allow return to background concentration. Barometric pressure (+/- 0.8 kPa) and ambient air temperature (+/- 0.2 ˚C) were recorded for each time point for conversion of dry molar fractions to gravimetric concentrations.

GHG fluxes were calculated from chamber headspace concentration measurements over time using least squares linear regression (LR), the most common approach to quantifying gas flux with chamber methodologies (Collier et al., 2014), using the equation:

$$F = S \cdot V \cdot A^{-1} \quad (1)$$

where S is the slope of the analyte concentration regressed over time, V is total volume of the recirculating system (column headspace, tubing volume, instrument internal volume, 0.00221 m^3), and A is the contained surface area (the horizontal plane determined by height of media

and column dimensions, 0.0749 m^2). Measurement start and end times were recorded and manually adjusted after visual examination of the data; several of the total 1,632 individual measurements were eliminated due to poor data quality (n=7, n=16, and n=2 for N_2O, CH_4, and CO_2, respectively.) The first 30% and last 10% of the recorded response for each measurement were removed prior to LR to ensure that differing background headspace concentrations would not bias the flux calculations; GHG accumulation in the headspace likely occurred, since exchange with ambient air occurred only through the 5.25 cm ID gas sampling port. If the background headspace concentration is elevated relative to ambient conditions, and measurements of ambient concentrations are included in the regression interval, fluxes would be overestimated by fitting a steeper slope. Additionally, selecting this inner subset of concentration measurements avoided error due to uncertainty in the start and stop times of the measurement interval.

3.3.4 Statistical analysis

The purpose of the empirical flux models described as follows was to differentiate and estimate the effects of experimental treatments (media type, HRT, N and P loading) on GHG flux in order to hypothesize the impact of these variables on bioreactor function at the field scale. Although the experimental design was factorial, all variables except for media type were treated as continuous to included differences between measured HRTs, and, more importantly, to use N loading rather than influent concentration an explanatory variable because achieving similar HRTs among media types given their differing porosities resulted in substantially different loading rates that would be masked by considering the influent concentration alone (Table 1). It should be emphasized that the models are not intended to predict GHG fluxes from

other bioreactor systems, per se, but can potentially guide future assessments of bioreactor emissions.

The effect of media type, HRT, N loading, and P loading on N_2O, CH_4, and CO_2 flux was evaluated with a separate LME model for each analyte. LMEs are appropriate for longitudinal studies or repeated measures studies that would violate assumptions of independence in classical linear regression, such as this column experiment where multiple, non-independent measurements were collected from each experimental unit (media-filled column) over time. To account for this non-independence, an error term assigning a random adjustment to the intercept of each experimental unit was modeled, and a continuous first-order autoregressive correlation structure was specified to indicate greater similarity between flux measurements from an individual column closely spaced in time compared to more distant measurements. Additionally, unequal variance for the different media types was modeled to avoid violation of the assumption of homoscedastic within-group errors. These random effects, correlation, and variance structures were each determined to significantly improve model fit via the likelihood ratio test, a statistical comparison of nested models with and without the component of interest. With respect to fixed effects, the most complex model specification was constrained to two-way interactions to limit the number of modeled parameters to a level of complexity supported by the dataset, given the need to model random intercepts, correlation, and variance components. Fixed effects that were determined to be significant with the likelihood ratio test, or those main effects included in a significant interaction term, were retained in the models and the remaining terms were eliminated. Note that for testing fixed effects with the likelihood ratio test LMEs are fit by the maximum likelihood method, but for testing of random

effects, and correlation or variance structures LMEs are fit by restricted maximum likelihood method.

Model assumptions included linearity, non-collinearity, homoscedasticity, and normal distribution of residuals. To meet these assumptions, the dependent variables (N_2O, CH_4, and CO_2 flux) were transformed to linearize the relationship between flux measurements and potential explanatory variables and reduce heterogeneity of variance in the model residuals, since correlation between variability in flux measurements and flux magnitude was observed. CO_2 fluxes were transformed by taking the natural logarithm and N_2O and CH_4 fluxes were transformed by taking the cubic root and preserving the mathematic sign; since several of the N_2O and CH_4 flux measurements were negative (net transfer into the bioreactors) the more common logarithmic transformation could not be used. Acceptable levels of collinearity were achieved by centering the continuous variables N loading rate and elapsed time, and verified by examining the variance inflation factors of each fixed effect, which were found to be less than 3.5 for all models. Homoscedasticity was evaluated by examining plots of model residuals to fitted values, and boxplots of model residuals at each level of categorical variables media type and HRT (Zuur et al., 2010), which originally prompted modeling different variance according to media type. Subsequently, the Levene test the variance distribution of the residuals with respect to media type and HRT, and the null hypothesis of homogenous variance failed to be rejected at the 95% confidence level. Normality of residuals was assessed by visual examination of the normalized residuals, where normalization incorporates the modeled correlation and variance structures, compared to normal quantiles. Data transformations significantly improved model diagnostics, but residuals of the all models still demonstrated deviation from normality,

with greater of lesser heavy tailing. However, normality is considered least important assumption for LMEs, particularly for describing the relationship between dependent and explanatory variables (Gelman and Hill, p. 46, 2007), so the modeling approach was determined to be appropriate.

Statistical significance of fixed effects was evaluated with a conditional F-test and the significance of individual parameter coefficient estimates was evaluated with the Wald t-test. Back transformation was required to quantify the effect of independent variables on the original scale. Since both the cubic root and logarithmic transformations introduce nonlinearity on the original scale, the magnitude of the response to changes in the values of explanatory variables is relative to current conditions. For the natural logarithm transformation, where X_i is an explanatory variables and B_i is its corresponding coefficient, the effect of a unit increase in X_i is determined to be a percent increase in current flux equal to $(\exp^{Bi} - 1)*100$, calculated by subtracting the equation predicting flux at given value of X_i (Y_i) from flux at X_{i+1} (Y_{i+1}). For the cubic root transformation, the effect of a one unit change in X_i is equal to a change in flux of $3B_iY_i^{1/2}$, calculated by taking the derivative of the dependent variable on the original scale, $Y^{1/3}$, which is taken with respect to X_i.

3.4 Results and Discussion

Figure 1 presents all flux measurements taken from the 12 columns over nine experimental trials, totaling 1632 individual measurements, and Table 2 presents summary statistics. To assess total GHG emissions from the bed, the combined GHG emissions are also presented, reported as CO_2 equivalents (CO_2eq), an expression of the global warming potential of any GHG relative to that of CO_2 over a 100-yr timespan, calculated by multiplying N_2O and

CH_4 fluxes by factors of 298 and 25, respectively (IPCC 2007). Emissions ranged from 682 to 27.3 x 10^3 mg CO_2eq-C m^{-2} d^{-1}, and averaged 3.5 x 10^3 mg CO_2eq-C m^{-2} d^{-1}. N_2O accounted for an average of 20.9% of CO_2eq emissions, supplying at least 11.0% of the global warming potential for 75.0% of the flux measurements, but CH_4 contributions were negligible (<0.6%). CO_2 supplied 79.1% of GHG emissions on average, but as little as 15.5% when N_2O flux peaked at 77.3 mg N_2O-N m^{-2} d^{-1}, and accounted for 84.5% of CO_2eq flux. Fluxes were highly variable, N_2O, CH_4, and CO_2 having coefficients of variation (CV) of 150%, 78%, and 45%, respectively. However, LME analysis identified statistically significant relationships between flux and treatment conditions.

The relationships between dependent variables N_2O, CH_4, and CO_2 flux and potential explanatory variables media type, HRT, N loading rate, P loading rate, and elapsed time, were evaluated with LMEs as described in section 2.5. Following this methodology, the effect of P loading rate was found to be insignificant and subsequently excluded from all models. Similarly, N loading rate was found to be insignificant and excluded from the CH_4 model. Table 3 presents the results of conditional F-test for significance of fixed effects, and Table 4 presents the Wald t-test of individual parameter coefficients. Note that that coefficient estimates of explanatory variables in Table 4 predicts flux on the transformed scale. Woodchips were selected as the reference level for media type to emphasize differences between the traditional woodchip bioreactor media and the experimental biochar amendments. The HRT reference level was assigned as 6 h, corresponding to the target design HRT range 4-8 h (Christianson et al., 2011, 2013c), to emphasize the effect of HRTs above or below the recommendation.

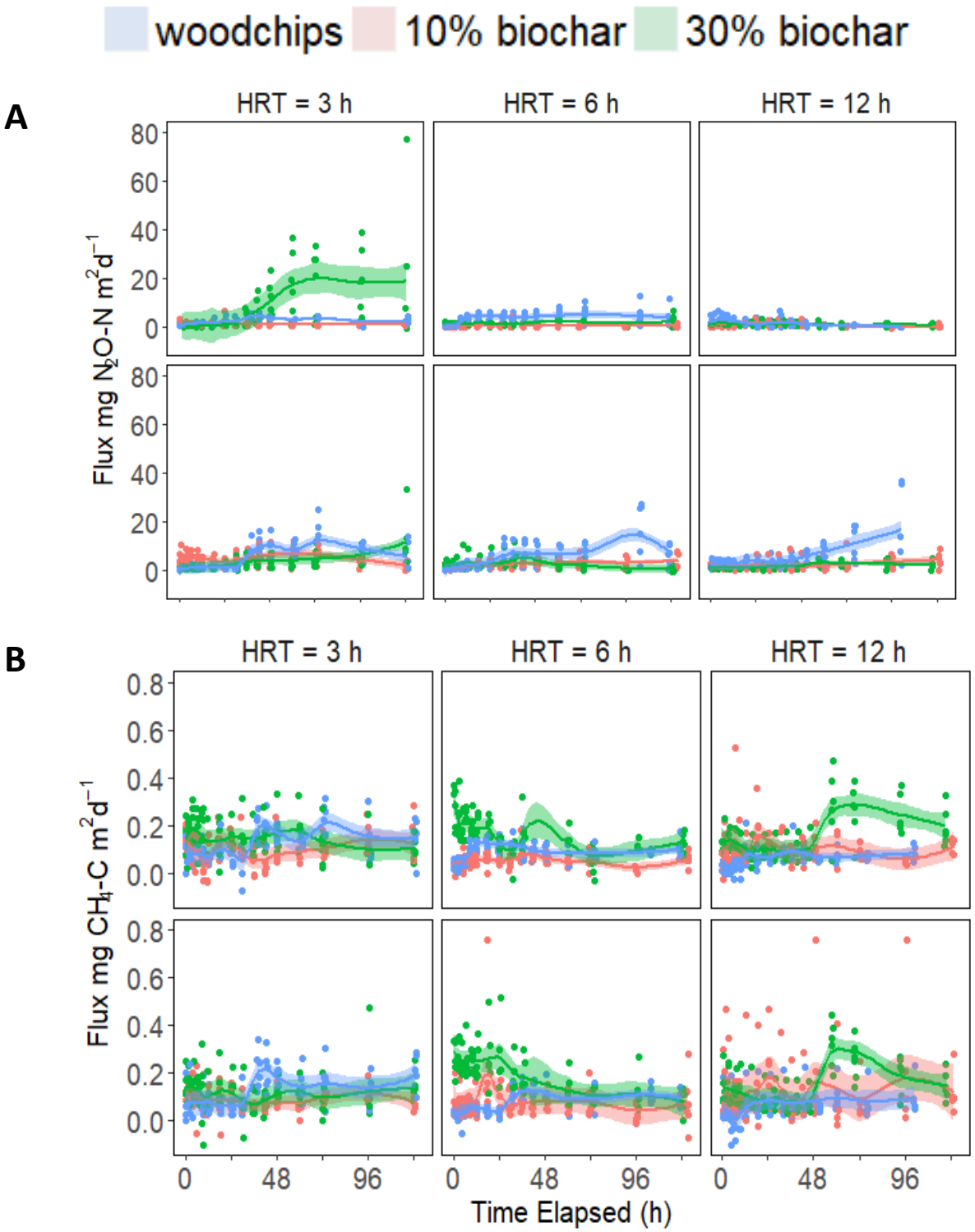
woodchips
10% biochar
30% biochar
A
HRT = 3 h
HRT = 6 h
HRT = 12 h
Flux mg N2O-N m2d−1
80
60
40
20
0
B
Flux mg CH4-C m2d−1
0.8
0.6
0.4
0.2
0.0
0
48
96
Time Elapsed (h)

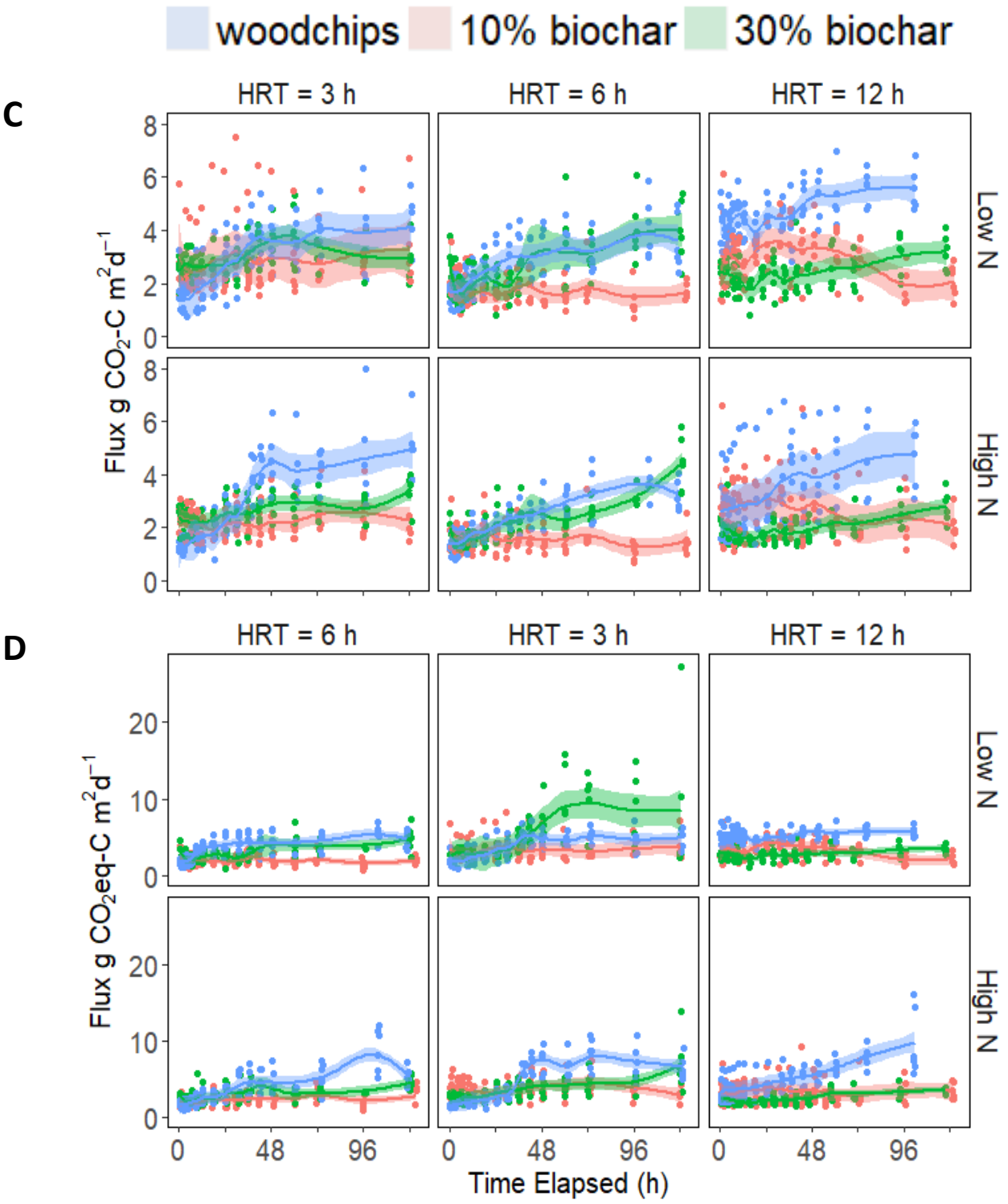

Figure 1a-d. Time series of N_2O (a), CH_4 (b), CO_2 (c), and CO_2 equivalent (d) flux measurements for 108 individual bioreactor columns, displayed separately for each combination of hydraulic residence time (HRT; 3,6, and 12 h) and influent N concentration (high 16.1 mg NO_3^--N l^{-1}, and low 4.5 mg NO_3^--N l^{-1}). Note that N_2O and CH_4 fluxes in mg m^{-2} d^{-1} while CO_2 and CO_2 equivalent fluxes are in g m^{-2} d^{-1}. Shading represents the confidence interval of the lowess regression.

Interpretation of significant interaction terms in multivariate modeling is typically guided by the principal of marginality, which dictates that the effect of independent variables on the response variable is determined by the highest level of interaction (Nelder, 1994). However, the main effects describe the flux response of the reference condition, assigned as woodchips at 6 h HRT, and are subject to valid interpretation in the presence of interaction effects. For example, when the effect of HRT, elapsed time, or N loading differs among media types, resulting in a statistically significant interaction term, the flux response for woodchips would be calculated from the coefficient estimate for the main effect of a given variable, whereas the differing response of the biochar treatments would be calculated from the sum of the coefficients of the main effect and their respective interactions effects with that same variable. Note that the continuous variables, N loading and time elapsed have been centered, so the model intercepts represent the estimate of average flux for woodchips at HRT 6 under an N loading rate of 28.7 g NO_3^--N m^{-3} d^{-1} after 37 h.

Table 2. Mean and standard deviation (sd) of N_2O, CH_4, CO_2, and CO_2-eq fluxes for each combination of media type and HRT, pooling across influent N and P concentrations.

HRT	Woodchips	10% Biochar	30% Biochar
	N_2O-N mg m^{-2} d^{-1}, mean (sd)		
3 h	3.24 (2.81)	4.94 (9.11)	3.78 (4.06)
6 h	1.46 (1.51)	1.99 (1.87)	4.16 (4.38)
12 h	1.56 (1.72)	1.52 (1.00)	3.49 (4.56)
	CH_4-C mg m^{-2} d^{-1}, mean (sd)		
3 h	0.09 (0.06)	0.13 (0.08)	0.12 (0.08)
6 h	0.07 (0.07)	0.18 (0.09)	0.08 (0.04)
12 h	0.11 (0.12)	0.14 (0.09)	0.06 (0.05)
	CO_2-C mg m^{-2} d^{-1}, mean (sd)		
3 h	2.53 (1.12) · 10^3	2.75 (0.69) · 10^3	2.95 (1.45) · 10^3
6 h	1.65 (0.55) · 10^3	2.29 (1.02) · 10^3	2.44 (0.96) · 10^3
12 h	2.84 (1.06) · 10^3	2.19 (0.65) · 10^3	4.06 (1.36) · 10^3
	CO_2eq-C mg m^{-2} d^{-1}, mean (sd)		
3 h	3.50 (1.40) · 10^3	4.24 (3.11) · 10^3	4.04 (2.31) · 10^3
6 h	2.08 (0.72) · 10^3	2.82 (1.16) · 10^3	3.62 (1.90) · 10^3
12 h	3.33 (1.37) · 10^3	2.65 (0.76) · 10^3	5.10 (1.82) · 10^3

Table 3. Fixed effects included in linear mixed effects models of N_2O, CH_4, and CO_2 flux. Note transformations of the dependent variables Effects determined to be statistically significant at the 95% confidence level are indicated by a star.

N_2O , (mg N_2O-N m^{-2} d^{-1})$^{1/3}$				
	DF_{num}	DF_{den}	F-value	p-value
Intercept	1	1511	128.915	<0.0001*
Time	1	1511	0.055	0.8139
N	1	94	8.008	0.0057*
Media	2	94	5.774	0.0043*
HRT	2	94	6.357	0.0026*
Time x N	1	1511	0.444	0.5052
Time x Media	2	1511	5.338	0.0049*
Time x HRT	2	1511	1.416	0.2430
N x Media	2	94	6.712	0.0019*
N x HRT	2	94	7.125	0.0013*
Media x HRT	4	94	4.950	0.0012*
CH_4, (mg CH_4-C m^{-2} d^{-1}) $^{1/3}$				
Intercept	1	1504	1086.276	<0.0001*
Time	1	1504	0.056	0.8128
Media	2	102	21.629	<0.0001*
HRT	1	102	0.168	0.6831
Time x Media	2	1504	27.185	<0.0001*
Time x HRT	1	1504	15.319	0.0001*
Media x HRT	2	102	5.036	0.0082*
CO_2, ln(mg CO_2-C m^{-2} d^{-1})				
Intercept	1	1491	11713.690	<0.0001*
Time	1	1491	0.054	0.8160
N	1	94	2.275	0.1348
Media	2	94	9.369	0.0002*
HRT	2	94	12.825	<0.0001*
Time x N	1	1491	8.085	0.0045*
Time x Media	2	1491	119.034	<0.0001*
Time x HRT	2	1491	7.873	0.0004*
N x Media	2	94	0.088	0.9155
N x HRT	2	94	2.399	0.0964
Media x HRT	4	94	7.958	<0.0001*

Table 4. Coefficient estimates and statistical significance (*) for parameters included in linear mixed effects models of N_2O, CH_4, and CO_2 flux. Note transformations of dependent variables.

N_2O, (mg N_2O-N m^{-2} d^{-1})$^{1/3}$					
Parameter	**Value**	**Std. Error**	**DF**	**t-value**	**p-value**
Intercept	1.17E+00	7.07E-02	1512	16.577	<0.0001*
Time	-1.48E-04	9.08E-04	1512	-0.163	0.8707
N	1.71E-02	3.77E-03	98	4.531	<0.0001*
B_{10}	1.16E-01	8.92E-02	98	1.300	0.1968
B_{30}	2.47E-01	8.96E-02	98	2.760	0.0069*
HRT	4.79E-02	2.23E-02	98	2.147	0.0343*
Time x N	1.62E-05	2.89E-05	1512	0.561	0.5746
Time x B_{10}	1.70E-03	1.37E-03	1512	1.238	0.2160
Time x B_{30}	4.56E-03	1.40E-03	1512	3.250	0.0012*
Time x HRT	-3.18E-04	1.87E-04	1512	-1.697	0.0900
N x B_{10}	-1.08E-02	4.06E-03	98	-2.648	0.0094*
N x B_{30}	-4.57E-03	4.51E-03	98	-1.014	0.3129
N x HRT	1.73E-03	7.73E-04	98	2.243	0.0272*
B10 x HRT	-5.93E-02	2.72E-02	98	-2.177	0.0319*
B30 x HRT	1.06E-02	2.76E-02	98	0.384	0.7016
CH_4, (mg CH_4-C m^{-2} d^{-1})$^{1/3}$					
Intercept	4.06E-01	1.23E-02	1504	32.959	<0.0001*
Time	-5.30E-05	2.24E-04	1504	-0.237	0.8128
B_{10}	9.92E-02	1.67E-02	102	5.942	<0.0001*
B_{30}	1.44E-02	1.68E-02	102	0.856	0.3938
HRT	1.41E-03	3.45E-03	102	0.409	0.6831
Time x B_{10}	-3.46E-04	2.80E-04	1504	-1.235	0.2171
Time x B_{30}	1.43E-03	2.88E-04	1504	4.942	<0.0001*
Time x HRT	1.13E-04	2.88E-05	1504	3.914	0.0001*
B10 x HRT	-1.99E-04	4.45E-03	102	-0.045	0.9645
B30 x HRT	-1.15E-02	4.46E-03	102	-2.570	0.0116*
CO_2 (mg CO_2-C m^{-2} d^{-1})					
Intercept	7.56E+00	5.14E-02	1517	147.060	<0.0001*
Time	-1.19E-03	4.24E-04	1517	-2.819	0.0049*
N	-8.70E-03	2.77E-03	98	-3.138	0.0022*
B_{10}	3.67E-02	6.09E-02	98	0.603	0.5477
B_{30}	2.38E-01	6.12E-02	98	3.891	0.0002*
HRT	-1.15E-02	1.68E-02	98	-0.685	0.4950
Time x N	2.02E-05	1.05E-05	1517	1.930	0.0538
Time x B_{10}	5.66E-03	5.32E-04	1517	10.639	<0.0001*
Time x B_{30}	8.62E-03	5.45E-04	1517	15.818	<0.0001*
Time x HRT	-1.68E-04	6.65E-05	1517	-2.527	0.0116*
N x B_{10}	-2.63E-03	2.93E-03	98	-0.898	0.3715
N x B_{30}	9.61E-04	3.23E-03	98	0.298	0.7667
N x HRT	-2.39E-03	5.50E-04	98	-4.344	<0.0001*
B10 x HRT	-5.32E-02	1.99E-02	98	-2.672	0.0088*
B30 x HRT	2.02E-02	2.00E-02	98	1.008	0.3160

3.4.1 Nitrous oxide

For N_2O, the two-way interaction effects of media by N loading, HRT, and elapsed time are all significant at the 95% confidence level, indicating that the flux response to changes in each of these variables differs between media types (Table 3). Additionally, the interaction between N loading and HRT is also significant, reflecting different responses to N loading among the three HRTs, as visualized in Figure 2. Although interaction terms more accurately describe the relationship between N_2O flux and the explanatory variables under specific conditions, several significant main effects reflect meaningful average predicted responses. The statistically significant positive coefficient estimates for N loading, B_{30}, and HRT suggest that, on average, N_2O flux increases as N loading rate ($p < 0.0001$) or HRT increase ($p=0.034$), and that B_{30} fluxes tend to be significantly higher than either W or B_{10} ($p=0.0069$). In addition to exhibiting the highest average flux, B_{30} is also differentiated by a significantly greater increase in N_2O flux over time ($p = 0.0012$) than W and B_{10}, which are predicted to remain relatively stable through time. For all media types, the interaction effect of N loading by HRT suggests a compounding effect of N loading at low HRTs, where a given increase in N loading results in a larger increase in N_2O flux at lower HRTs for all media types ($p = 0.0272$). For example, an increase in N loading from 20 g NO_3^--N m^{-3} d^{-1} to 40 g NO_3^--N m^{-3} d^{-1} is predicted to increase N_2O flux from woodchip columns by ~80% from 0.8 to 1.4 mg N_2O-N m^{-2} d^{-1} for a 3 h HRT, but for a 12 h HRT the same increase in N loading would be expected to increase flux by over 210%, from 1.4 to 4.3 mg N_2O-N m^{-2} d^{-1}. This explanation of the N loading by HRT interaction term requires such context due to the non-linearity of the flux response introduced by the cubic root data transformation, which means that the effect of a parameter is dependent on current conditions

(predicted flux). Thus, these nonlinear relationships are better described visually in Figure 2, which displays predicted fluxes for each HRT across three levels of N loading (10, 40, and 70 g NO_3^--N m^{-3} d^{-1}) over the trial duration (120 h).

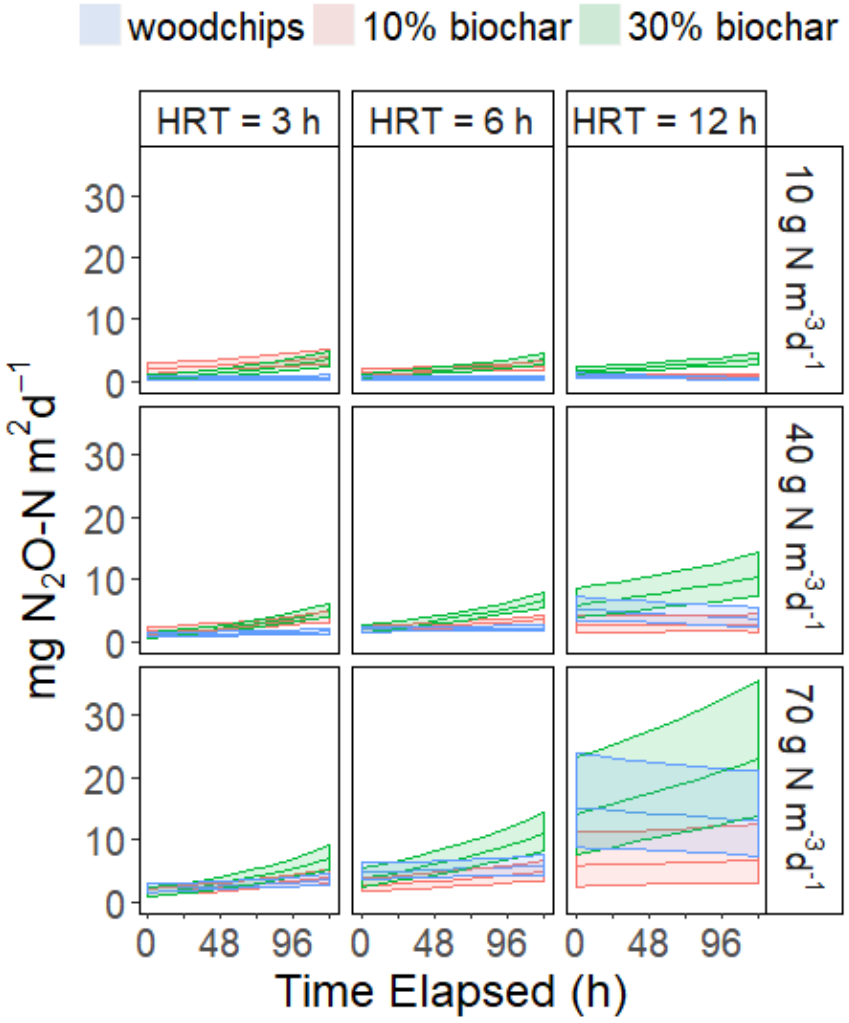

Figure 2. N_2O fluxes predicted by linear mixed effects model for each combination of representative hydraulic residence times and N loading rate. Shaded areas represent +/- one standard error of the predicted flux.

Unexpectedly high fluxes were observed in B_{10} columns under low N loading at HRT_3 (Figure 1a), the highest N_2O fluxes measured during the experiment (up to 77.3 mg N_2O-N m^{-2} d^{-1}), in comparison to all other combinations of HRT and N loading where B_{30} columns exhibited

the highest average N_2O flux (Table 2). As a result, the fitted model included significant interaction terms predicting higher fluxes for B_{10} at lower HRTs ($p = 0.0319$) and, more problematically, prescribed an inverse relationship between B_{10} and N loading ($p = 0.0094$). Subsequently, the model was refit excluding flux measurements from the twelve bioreactor columns with experimental treatment combination B_{10} and 3 h HRT data to determine how these data points affected coefficient estimation of the fixed effects. The determinations of significance at the 95% confidence level for each term shared by the models were in agreement except for the B_{10} by HRT interaction term, which became non-significant in the partial model (data not shown). All coefficient estimates shared the same mathematic sign and differed by less than two times the standard error except for B_{10}, which decreased from 0.116 to -0.081, and in contrast with the full model indicating predicted lower average N_2O fluxes from B_{10} compared to W. However, the effect of B_{10} was not significant in either the partial ($p=0.3678$) or full ($p=0.1968$) models. Nonetheless, some of the highest N_2O emission factors were observed for B_{10} at HRT 3 under low influent concentration, up to 5.1% of NO_3^--N removed, exceeded only by B_{30} at HRT 12 under high N in influent (Figure 3) when N_2O accounted from 9.5% of NO_3^--N removed, and without cause to doubt validity of these data, uncertainty in treatment effects persists due to substantial variability in flux measurements.

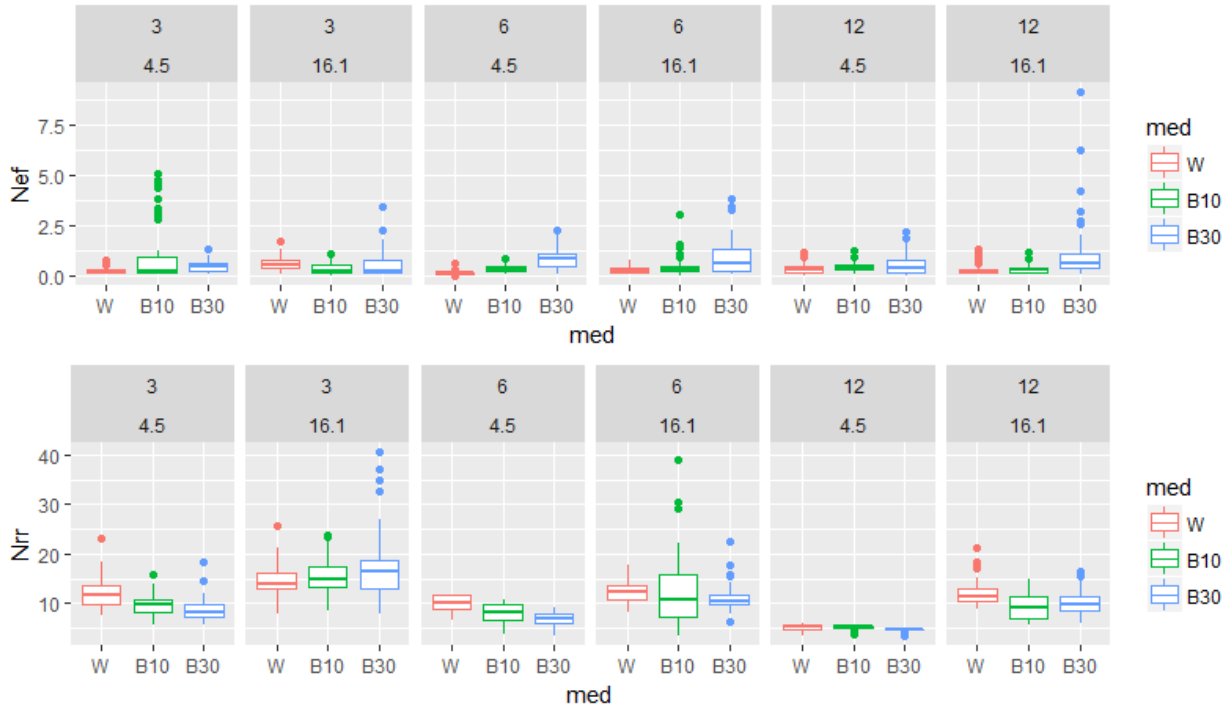

Figure 3. N_2O emission factors (Nef, top) and NO_3^--N removal rates (Nrr, bottom) of each media type, woodchips (W), 10% biochar (B_{10}), and 30% biochar (B_{30}, for each combination of tested hydraulic residence time (HRT) and NO_3^--N loading rate.

3.4.2 Methane

Although media type, HRT, and elapsed time significantly affected CH_4 flux as determined by the LME model (Tables 3 and 4), CH_4 contributed negligibly to total GHG emissions evaluated in terms of CO_2eq. With such insignificant fluxes, less than 1% of the CO_2eq from N_2O, evaluation of the effect of the explanatory variables on CH_4 flux is of limited value. However, notable effects include W producing the lowest average flux across HRT and time (>0.1 mg CH_4-C m^{-2} d^{-1}), with B_{30} averaging twice the W flux, and a significant increase in B_{30} flux over time across HRTs (directionality of trend over time changes for W and B_{10} across HRTs). These results indicate that the highest potential for CH_4 emissions, like N_2O emissions, occurs in

the B_{30} columns, albeit the differences in CH_4 flux among media types and treatment conditions are not of environmental significance.

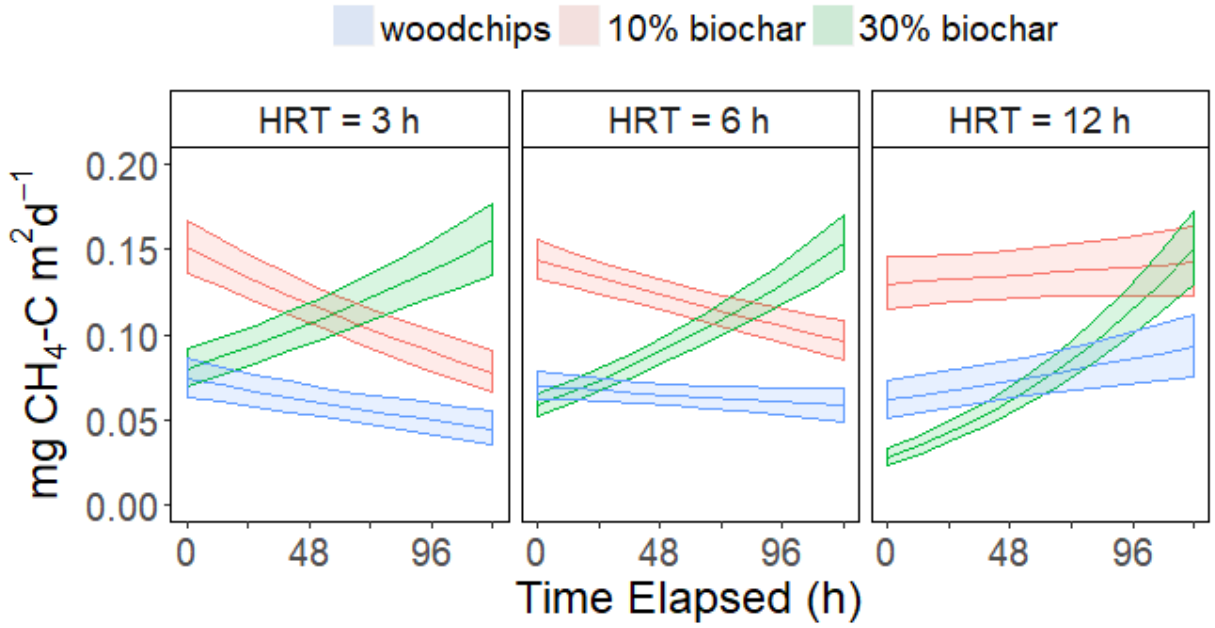

Figure 4. CH_4 flux predicted by linear mixed effects model for each media type for the three tested hydraulic residence times. Shaded areas represent +/- one standard error of the predicted flux.

3.4.3 Carbon Dioxide

For CO_2, all two-way interaction effects with time were significant, as was the interaction between HRT and media type (Table 2), and these relationships are displayed in Figure 5. The media by time effect reflects that B_{10} and B_{30} CO_2 flux is predicted to increase over time at rates of 9.3-13.5% and 16.8-21.7% per day, respectively, under average N loading (~30 g N m^{-3} d^{-1}), whereas the W flux slightly decreases over time (1.1-4.6% per day). Ranges for the effect of the time by media interaction are reported because the time by HRT interaction is also significant (Table 2, p=0.0004), and the reported flux response represents the combined predictions for HRTs of 3, 6, and 12 hours. The N loading rate is also provided as context for the

estimated effect due to significance of the time by loading interaction (Table 2, p =0.0045), although the parameter coefficient is only marginally significant and the coefficient estimate is small (Table 3, p=0.0538). Additionally, HRT interacts significantly with media, as can been seen in Figure 5 where B_{30} fluxes increase with HRT (p<0.001), B_{10} fluxes decrease with increasing HRT (p<0.0001), and W fluxes are not significantly correlated with HRT (p=0.4950). Overall, across N loading rates and HRTs, W fluxes are the lowest while B_{30} fluxes are the highest and increase the most over time.

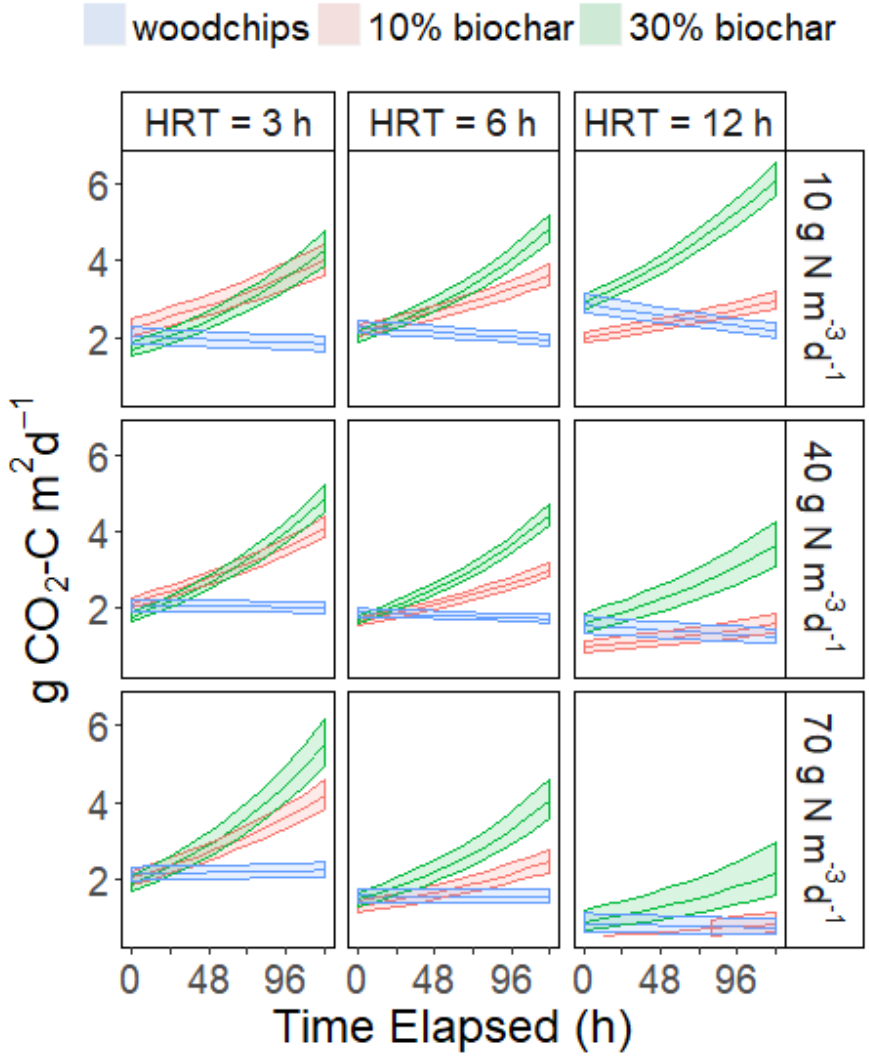

Figure 5. CO_2 fluxes predicted by linear mixed effects model for each combination of representative hydraulic residence times and N loading rates. Note that flux units are g m^{-2} d^{-1}. Shaded areas represent +/- one standard error of the predicted flux.

3.4.4 Greenhouse gas emissions in context

Woodchips generally produced the lowest GHG emissions among the media types across a range of HRTs and N loading rates, and were less likely to increase in flux over time. However, the LME predictions rely on the assumption of a linear relationship between independent and predictive variables, which is unlikely to capture GHG flux dynamics over time, and not fully justified as Figure 1 suggests nonlinear relationships. Close examination of flux time series shows a variety of responses over time including stability, peaks followed by a return to baseline, and increases with or without a plateaus (Figure 1). Previous bioreactor column studies in closed system batch experiments, in contrast to this flow-through system with free exchange of headspace with the atmosphere, have shown both constant headspace concentrations and peaks within similar timespans (Bock et al., 2015; Easton et al., 2015). While headspace GHG concentrations in gastight columns are likely poor predictors of GHG fluxes in open systems, steady increases observed here could be the rising limb of flux peaks. Consequently, constraining interpretation of predicted increases in flux over time as indicative of higher average fluxes may be more appropriate although elapsed time had a statistically significant effect in all models. Fluxes also tended to increase with HRT, suggesting that lower flows resulting in higher HRTs may increase GHG emissions as N_2O and CO_2 even in the absence excessively reducing conditions that would support methanogenesis; lengthy HRTs resulting in

highly reduced environments which would be expected to yield significant CH_4 fluxes. Christianson et al. (2011) also observed a correlation between N_2O emissions and HRT in woodchip and biochar-amending laboratory columns. In addition, GHG fluxes increased as N loading increased, with a potentially important interaction exacerbating the effect of HRT, resulting in the highest observed N_2O fluxes and emission factors, the proportion of removed NO_3^--N converted to N_2O. Nitrous oxide emissions averaged only 0.47% of NO_3^--N removed but ranged from -0.07% to 9.5% (Figure 3), with negative fluxes, net transfer of N_2O into the columns in <2% of measurements.

Woli et al. (2010) measured N_2O fluxes similar to the mean treatment fluxes reported in Table 1 (1.46-4.94 mg m^{-2} d^{-1}) from a denitrifying bioreactor receiving tile drainage and operating with removal rates of 6.4 g NO_3^--N m^{-3} d^{-1}, which ranged 0.24-3.12 mg N_2O-N m^{-2} d^{-1} and were considered by the authors to be negligible. Column fluxes less than the maximum flux reported by Woli et al. (2010) accounted for over 73% of the measurements, but the top 5% ranged 9.8-77.3 mg N_2O-N m^{-2} $d^{-1}$and occurred almost exclusively in the B_{10} columns with 3 h HRTs; fluxes were highly variable and variability was correlated with flux magnitude, the second highest of N_2O flux only 39.2 mg N_2O-N m^{-2} d^{-1}, significantly larger N_2O fluxes than even the highest encountered in this experiment were observed by Warneke et al. (2011) from a woodchip bioreactor receiving very high N influent from a greenhouse (>100 mg NO_3^--N l^{-1}), which ranged 61.6-158.8 mg N_2O-N m^{-2} $d^{-1}$and averaged 113 mg N_2O-N m^{-2} d^{-1}; CH_4 and CO_2 emissions were similar to those measured in the columns, ranging 0.03-0.73 mg CH_4-C m^{-2} d^{-1} and 7.9-37.2 g CO_2-C m^{-2} d^{-1}, respectively, although average the fluxes were about twice the magnitude of those in the columns. Warneke et al. (2011) also reported simultaneous

measurements of dissolved GHGs, and found that while 1% of NO_3^--N removed was emitted from the bed surface at N_2O an additional 3.3% was exported as dissolved N_2O, and considered the total 4.3% conversion of NO_3^--N to N_2O a significant adverse effect. Thus, measurements of surface emissions alone may underestimate the total GHG produced by the bioreactor columns, when significant quantities of GHGs are exported dissolved in the effluent. However, Elgood et al. (2010) and Moorman et al. (2010) observed much smaller losses of dissolved N_2O, averaging only about 0.6% of NO_3^--N removed in both cases, in applications more representative of bioreactor applications in agroecosystems, a streambed and tile-drain-fed bioreactor, respectively. Elgood et al. (2010) also presented export of dissolved N_2O as an area-normalized flux, 5.4-14.6, which corresponds to approximately the 85th to 98th percentile of measured column fluxes, suggesting that a similar partitioning of N_2O export between gaseous and dissolved fluxes similar to that reported by Warneke et al. (2010), where dissolved export exceeds gaseous flux by a factor of three. In contrast, Moorman et al. (2010) observed no differences in dissolved N_2O concentrations between bioreactor effluent and tile drainage in untreated control plots, and concluded that the bioreactor did not increase indirect losses of N_2O. Given the technical demands of simultaneously quantifying dissolved and gaseous greenhouse gas flux, it is unsurprising that Warneke et al. (2010) remains the only bioreactor study to measure both loss pathways, but elucidating controls on GHG production in bioreactors will require experiments providing a more complete mass balance, ideally in the field setting.

3.5 Conclusions

Amendment of laboratory-scale woodchip bioreactors with a hardwood feedstock biochar induced higher GHG fluxes. While biochar may increase N removal rates (Bock et al., 2016; Pleur et al., 2016), at least temporarily, the added water quality benefits may not be worth the additional cost of GHG emissions, particularly since biochar has not proved to be an effective P sorbent as had previously been hypothesized (Christianson et al., 2011; Pluer et al., 2016). Overall, the woodchip bioreactor emitted the smallest quantities of GHGs among for a range of influent NO_3^--N concentrations and HRTs, often maintaining relatively low and stable fluxes throughout the trials. However, this experiment did not address potential losses of GHGs dissolved in the bioreactor effluent, which can be contribute substantially to total GHG export. As more comprehensive approaches are taken with respect to evaluating the environmental impact of denitrifying bioreactors, more work must be done to determine the variables controlling unwanted effects like GHG emissions.

3.6 References

Addy, K., Gold, A.J., Christianson, L.E., David, M.B., Schipper, L.A., Ratigan, N.A., 2016. Denitrifying bioreactors for nitrate removal: a meta-analysis. J. Environ. Qual. 45(3):873–881. doi:10.2134/jeq2015.07.0399

Beck, D., Johnson, G., Spolek, G., 2011. Amending greenroof soil with biochar to affect runoff water quantity and quality. Environ. Pollut. 159(8-9):2111-2118. doi: 10.1016/j.envpol. 2011.01.022

Bock, E., Smith, N., Rogers, M., Coleman, B., Reiter, M., Benham, B., Easton, Z.M., 2015. Enhanced nitrate and phosphate removal in a denitrifying bioreactor with biochar. J. Environ. Qual. 44(2):605-613. doi:10.2134/jeq2014.03.0111

Bock, E.M., Coleman, B., Easton, Z.M., 2016. Effect of biochar on nitrate removal in a pilot-scale denitrifying bioreactor. J. Environ. Qual. 45(3):762-771. doi:10.2134/jeq2015.04.0179

Bruun, E.W., Müller-Stöver, D., Ambus, P., Hauggaard-Nielsen, H., 2011. Application of biochar

to soil and N_2O emissions: potential effects of blending fast-pyrolysis biochar with anaerobically digested slurry. Eur. J. Soil Sci. 62(4):581–589. doi:10.1111/j.1365-2389.2011.01377.x

Case, S.D.C., McNamara, N.P., Reay, D.S., Stott, A.W., Grant, H.K., Whitaker, J., 2015. Biochar suppresses N_2O emissions while maintaining N availability in a sandy loam soil. Soil Biol. Biochem. 81:178-185. doi:10.1016/j.soilbio.2014.11.012

Christianson, L.E., Bhandari, A., Helmers, M.J., 2011. Pilot-scale evaluation of denitrification drainage bioreactors: reactor geometry and performance. J. Environ. Eng. 137(4):213–220. doi:10.1061/(ASCE)EE.1943-7870.0000316

Christianson, L.E., Bhandari, A., Helmers, M.J., 2011b. Potential design methodology for agricultural drainage denitrification bioreactors. World Environmental and Water Resources Congress 2011. American Society of Civil Engineers, Reston, VA, pp. 2740–2748. doi:10.1061/41173(414)285

Christianson, L.E., Hedley, M., Camps, M., Free, H., Saggar, S., 2011c. Influence of biochar amendements on denitrificaiton bioreactor performance. Report. Massey University.

Christianson, L.E., Christianson, R., Helmers, M., Pederson, C., Bhandari, A., 2013a. Modeling and calibration of drainage denitrification bioreactor design criteria. J. Irrig. Drain. Eng. 139(9): 699–709. doi:10.1061/(ASCE)IR.1943-4774.0000622

Christianson, L.E., Helmers, M., Bhandari, A., Moorman, T., 2013b. Internal hydraulics of an agricultural drainage denitrification bioreactor. Ecol. Eng. 52:298–307. doi:10.1016/j.ecoleng.2012.11.001

Christianson, L.E., Lepine, C., Sharrer, K.L., Summerfelt, S.T., 2016. Denitrifying bioreactor clogging potential during wastewater treatment. Water Res. 105:147-156. doi:10.1016/j.watres.2016.08.067

Christianson, L.E., Schipper, L.A., 2016. Moving denitrifying bioreactors beyond proof of concept: introduction to the special section. J. Environ. Qual. 45(3):757-761. doi:10.2134/jeq2016.01.0013

Christianson, L.E., Lepine, C., Sibrell, P.L., Penn, C., Summerfelt, S.T. 2017. Denitrifying woodchip bioreactor and phosphorus filter pairing to minimize pollution swapping. Water Res. 121, 129–139. doi:10.1016/J.WATRES.2017.05.026

Chun, J.A., Cooke, R.A., Eheart, J.W., Kang, M.S., 2009. Estimation of flow and transport parameters for woodchip-based bioreactors: I. laboratory-scale bioreactor. Biosyst. Eng. 104(3):384–395. doi:10.1016/j.biosystemseng.2009.06.021

Clough, T.J., Condron, L.M., 2010. Biochar and the nitrogen cycle: introduction. J. Environ. Qual. 39(4):1218-1223. doi:10.2134/jeq2010.0204

Coleman, B.S.L., 2017. Impact of retention time and influent concentration on N and P removal in horizontal flow through bioreactors. Master's thesis, Virginia Polytechnic and State

University.

Collier, S.M., Ruark, M.D., Oates, L.G., Jokela, W.E., Dell, C.J., 2014. Measurement of greenhouse gas flux from agricultural soils using static chambers. J. Vis. Exp. 90:e52110. doi:10.3791/52110

DeBoe, G., Bock, E., Stephenson, K., Easton, Z., 2017. Nutrient biofilters in the Virginia Coastal Plain: nitrogen removal, cost, and potential adoption pathways. J. Soil Water Conserv. 72(2): 139–149. doi:10.2489/jswc.72.2.139

De Klein, C.A.M., Harvey, M.J., 2012. Nitrous oxide Chamber Methodology Guidelines--Version 1.1. Global Reserch Alliance on Agricultural Greenhouse Gases. Available: <https://globalresearchalliance.org/wp-content/uploads/2015/11/Chamber_Methodology_Guidelines_Final-V1.1-2015.pdf> (accessed December 10, 2017)

Delwiche, C.C., Steyn, P.L., 1970. Nitrogen isotope fractionation in soils and microbial reactions. Environ. Sci. Technol. 4(11):929-935. doi: 10.1021/es60046a004

Dinnes, D.L., Karlen, D.L., Jaynes, D.B., Kaspar, T.C., Hatfield, J.L., Colvin, T.S., Cambardella, C.A., 2002. Nitrogen management strategies to reduce nitrate leaching in tile-drained Midwestern soils. Agron. J. 94:153–171.

Easton, Z.M., Rogers, M., Davis, M., Wade, J., Eick, M., Bock, E., 2015. Mitigation of sulfate reduction and nitrous oxide emission in denitrifying environments with amorphous iron oxide and biochar. Ecol. Eng. 82:605-613. doi:10.1016/j.ecoleng.2015.05.008

Elgood, Z., Robertson, W.D., Schiff, S.L., Elgood, R., 2010. Nitrate removal and greenhouse gas production in a stream-bed denitrifying bioreactor. Ecol. Eng. 36:1575–1580. doi: 10.1016/j.ecoleng.2010.03.011

Erisman, J.W., 2004. The Nanjing declaration on management of reactive nitrogen. BioSci. 54(4):286-287.

Florinsky, I. V, McMahon, S., Burton, D.L., 2004. Topographic control of soil microbial activity: a case study of denitrifiers. Geoderma 119(1):33–53. doi:10.1016/s0016-7061(03)00224-6

Fruth, D., Ponzi, J., 2010. Adjusting carbon management policies to encourage renewable, net-negative projects such as biochar sequestration. William Mitch Law Rev. 36(3):992-1013

Galloway, J., Schlesinger, W., Levy, H., Michaels, A., Schnoor, J., 1995. Global Biogeochem. Cy. 9(2):235-252. doi: 10.1029/95GB00158

Galloway, J., Aber, J., Erisman, J., Seitzinger, S., Howarth, R., Cowling, E., Cosby, B. 2003. The nitrogen cascade. BioSci. 53(4):341-356. doi: 10.1641/0006-3568(2003)053[0341:TNC]2.0.CO;2

Gelmen, A., Hill, J., 2007. Data Analysis Using Regression and Multilevel/Hierarchical Models. Cambridge University Press, New York, NY. p 46.

Hartz, T., Smith, R., Cahn, M., Bottoms, T., Bustamante, S.C., Tourte, L., Johnson, K., Coletti, L.,

2017. Wood chip denitrification bioreactors can reduce nitrate in tile drainage. Calif. Agric. 71(1):41–47. doi:10.3733/ca.2017a0007

Healy, M.G., Ibrahim, T.G., Lanigan, G.J., Serrenho, A.J., Fenton, O., 2012. Nitrate removal rate, efficiency and pollution swapping potential of different organic carbon media in laboratory denitrification bioreactors. Ecol. Eng. 40:198–209. doi:10.1016/j.ecoleng.2011.12.010

Healy, M.G., Barrett, M., Lanigan, G.J., João Serrenho, A., Ibrahim, T.G., Thornton, S.F., Rolfe, S.A., Huang, W.E., Fenton, O., 2015. Optimizing nitrate removal and evaluating pollution swapping trade-offs from laboratory denitrification bioreactors. Ecol. Eng. 74:290–301. doi:10.1016/j.ecoleng.2014.10.005

Hua, G., Salo, M.W., Schmit, C.G., Hay, C.H., 2016. Nitrate and phosphate removal from agricultural subsurface drainage using laboratory woodchip bioreactors and recycled steel byproduct filters. Water Res. 102:180-189. doi:10.1016/j.watres.2016.06.022

IPCC, 2007. Contribution of Working Groups I, II, and III to the Fourth Assessment Report of the Intergovernmental Panel on Climate Change. Core Writinng Team, Pachauri, R.K. and Reisinger, A. (Eds.)

IPCC, Geneva, Switzerland.

Kookana, R.S., Sarmah, A.K., Van Zwieten, L., Krull, E., Singh, B., Donald L. Sparks, 2011. Chapter three - Biochar Application to Soil: Agronomic and Environmental Benefits and Unintended Consequences. pp. 103–143. Elsevier Academic Press Inc. San Diego, CA.

Lehmann, J., Rillig, M., Thies, J., Masiello, C., Hockaday, W., Crowley, D., 2011. Soil Biol. Biochem. 43(9):1812-1836. doi: 10.1016/j.soilbio.2011.04.022

Mathieu, O., Lévêque, J., Hénault, C., Milloux, M.-J., Bizouard, F., Andreux, F., 2006. Emissions and spatial variability of N_2O, N_2 and nitrous oxide mole fraction at the field scale, revealed with ^{15}N isotopic techniques. Soil Biol. Biochem. 38(5):941–951. doi:10.1016/j.soilbio.2005.08.010

McLaughlin, H., Anderson, P., Shields, F., Reed, T., 2009. All biochars are not created equal and how to tell them apart. North Amer. Biochar. 2:1-36.

Moorman, T.B., Parkin, T.B., Kaspar, T.C., Jaynes, D.B., 2010. Denitrification activity, wood loss, and N_2O emissions over 9 years from a wood chip bioreactor. Ecol. Eng. 36:1567–1574. doi: 10.1016/j.ecoleng.2010.03.012

Nelder, J.A., 1994. The statistics of linear models: back to basics. Stat. Comput. 4(4):221–234. doi:10.1007/BF00156745

Oertel, C., Matschullat, J., Zurba, K., Zimmermann, F., Erasmi, S., 2016. Greenhouse gas emissions from soils—a review. Chemie der Erde - Geochemistry 76(3):327–352.

Pluer, W.T., Geohring, L.D., Steenhuis, T.S., Walter, M.T., 2016. Controls influencing the treatment of excess agricultural nitrate with denitrifying Bioreactors. J. Environ. Qual. 45(3):772-778. doi:10.2134/jeq2015.06.0271

Robertson, W.D., 2010. Nitrate removal rates in woodchip media of varying age. Ecol. Eng. 36, 1581–1587. doi:10.1016/j.ecoleng.2010.01.008

Robertson, W.D., Blowes, D.W., Ptacek, C.J., Cherry, J.A., 2000. Long-term performance of in situ reactive barriers for nitrate remediation. Ground Water 38(5):689–695. doi:10.1111/j.1745-6584.2000.tb02704.x

Saarnio, S., Heimonen, K., Kettunen, R., 2013. Biochar addition indirectly affects N_2O emissions via soil moisture and plant N uptake. Soil Biol. Biochem. 58:99-106. doi:10.1016/j.soilbio.2012.10.035

Saliling, W., Westerman, P., Losordo, T., 2007. Wood chips and wheat straw as alternative biofilter media for denitrification reactors treating aquaculture and other wastewaters with high nitrate concentrations. Aquac. Eng. 37(3):222-233. doi: 10.1016/j.aquaeng. 2007.06.003

Schipper, L.A., Gold, A.J., Davidson, E.A., 2010a. Managing denitrification in human-dominated landscapes. Ecol. Eng. 36:1503–1506. doi:10.1016/j.ecoleng.2010.07.027

Schipper, L.A., Robertson, W.D., Gold, A.J., Jaynes, D.B., Cameron, S.C., 2010b. Denitrifying bioreactors—An approach for reducing nitrate loads to receiving waters. Ecol. Eng. 36:1532–1543. doi:10.1016/j.ecoleng.2010.04.008

Sharrer, K.L., Christianson, L.E., Lepine, C., Summerfelt, S.T., 2016. Modeling and mitigation of denitrification “woodchip” bioreactor phosphorus releases during treatment of aquaculture wastewater. Ecol. Eng. 93:135-143. doi:10.1016/j.ecoleng.2016.05.019

Sohi, S., Krull, E., Lopez-Capel, E., Bol, R., 2010. A review of biochar and its use and function in soil. Adv. Agron. 105:47-82. doi:10.1016/S0065-2113(10)05002-9

Warneke, S., Schipper, L.A., Bruesewitz, D.A., McDonald, I., Cameron, S., 2011a. Rates, controls and potential adverse effects of nitrate removal in a denitrification bed. Ecol. Eng. 37:511–522. doi:10.1016/j.ecoleng.2010.12.006

Warneke, S., Schipper, L.A., Matiasek, M.G., Scow, K.M., Stewart Cameron, Bruesewitz, D.A., McDonald, I.R., 2011b. Nitrate removal, communities of denitrifiers and adverse effects in different carbon substrates for use in denitrification beds. Water Res. 45(17):5463–5475. doi:doi: 10.1016/j.watres.2011.08.007

Woli, K.P., David, M.B., Cooke, R.A., McIsaac, G.F., Mitchell, C.A., 2010. Nitrogen balance in and export from agricultural fields associated with controlled drainage systems and denitrifying bioreactors. Ecol. Eng. 36:1558–1566. doi:10.1016/j.ecoleng.2010.04.024

Yanai, Y., Toyota, K., Okazaki, M., 2007. Effects of charcoal addition on N_2O emissions from soil resulting from rewetting air-dried soil in short-term laboratory experiments. Soil Sci. Plant Nutr. 53(2):181–188. doi:10.1111/j.1747-0765.2007.00123.x

Zuur, A.F., Leno, E.N., Elphick, C.S., 2010. A protocol for data exploration to avoid common statistical problems. Methods Ecol. Evol. 1(1):3-14. doi: 10.1111/j.2041-210X.2009.00001.x

4. NUTRIENT REMOVAL AND GREENHOUSE GAS EMISSIONS IN AN UNDER-LOADING DENITRIFYING BIOREACTOR IN THE VIRGINIA COASTAL PLAIN

4.1 Abstract

Nutrient removal and greenhouse gas emissions were quantified in a 36.6 m^3 woodchip denitrifying bed with a 17% volumetric addition of biochar interfaced with a 6.5 ha subsurface drainage system located in the Virginia Coastal Plain during the second year of operation. Exceptionally low nitrogen (N) loading to the bed resulted in low mass removal rates averaging 0.41 g NO^{3-}-N m^{-3} d^{-1}. No P removal was observed. Temperature, hydraulic residence time (HRT), and influent NO^{3-}-N concentration were all found to be significant controls on N removal rates. Closed dynamic soil flux chamber methodology was used to quantify fluxes of nitrous oxide (N_2O), methane (CH_4), and carbon dioxide (CO_2) form the bed surface. Nitrous oxide emission factors, proportion of NO_3^--N removed lost as N_2O ranged -6.5-8.1%, indicating that the bioreactor could serve both as a source and sink for N_2O. On the basis of CO_2 equivalents, N_2O flux accounted for an average of 6.0% of GHG emission from the bed, with a maximum of 44%; CH_4 averaged 3.6% of GHG emissions and reached a maximum of 15%. Understanding the effect of in-bed conditions that limit N removal and increase GHG production and how they are derived from field conditions will help adapt bioreactor designs to a wider range of agricultural systems and geographic regions.

4.2 Introduction

Artificial drainage of agricultural land increases productivity and promotes soil conservation, but elevated concentrations of nitrogen (N) and phosphorus (P) are often detected in drainage waters, and a large body of research links agricultural drainage to

increased N and P export to water bodies, resulting in water quality degradation (e.g., David et al., 2015; Dinnes et al., 2002; Ikenberry et al., 2014; Kladivko et al., 1991). Nutrient losses are exacerbated by the accelerated removal of water from the soil profile, the object of drainage, through both surface (ditches) and subsurface (tile) drainage, which short circuits interaction of nutrient laden waters with the soil and reduces opportunity for natural uptake and nutrient cycling to occur. With over 36.8 million hectares of tile drained cropland in the US according to the 2012 census of agriculture (USDA NASS, 2012), various best management practices (BMPs) to reduce the water quality impact have been developed, including incorporation of level control structures to adjust in-field water table height, riparian buffers, and denitrifying bioreactors.

Denitrifying bioreactors are structural best management practices that mitigate excess N by intercepting N-enriched drainage water and supporting naturally occurring soil microorganisms that convert nitrate (NO_3^-) into inert dinitrogen gas (N_2), thereby removing it before it enters a water body. This process of heterotrophic denitrification occurs in the presence of sufficient N as an electron acceptor, organic carbon as an electron donor, and under anaerobic conditions where oxygen is not available to serve as the thermodynamically preferred electron acceptor. Denitrifying bioreactors are becoming accepted management practices used in conjunction with subsurface drainage in the Midwest, as evidenced by their incorporation into state-level nutrient reduction strategies in the Upper Mississippi River Basin (IA EPA, 2015; IDALS, 2014; MN PCA, 2014) and the development of a conservation practice standard by the USDA Natural Resources Conservation Service (USDA-NRCS, 2015). However, less work has been done outside of the Corn Belt to evaluate the utility of bioreactors in

meeting water quality goals in other agriculturally significant areas of the United States. This work contributes to early efforts to adapt denitrifying bioreactors to agricultural systems in the Mid-Atlantic to meet Chesapeake Bay water quality improvement goals.

Building on previous laboratory (Bock et al., 2015a, Easton et al., 2015) and pilot-scale experiments (Bock et al., 2016) on biochar-amended woodchip bioreactors, a field-scale woodchip bioreactor amended with 10% biochar by volume was installed in August 2014 in a field with subsurface drainage in a nutrient management target area identified by the Chesapeake Bay TMDL. The bioreactor was monitored from March 2015 to December 2016 to quantify N removal, P removal, and emissions of the greenhouse gases (GHGs) carbon dioxide (CO_2), methane (CH_4), and nitrous oxide (N_2O). Nutrient removal was calculated as the difference in influent and effluent loads, determined from measurements of outlet flow and nutrient concentrations in aqueous samples. GHG flux was measured in the field using a non-steady-state flow-through chamber method with Picarro GHG analyzer. This system provides a useful case study of bioreactor performance at the lower limits of N loading and pH reported in the literature, providing an information pertinent to the adaptation of bioreactor designs to the US Mid-Atlantic.

4.3 Materials and Methods

4.3.1 Site description and bioreactor design

A denitrifying bioreactor was installed in August 2014 to treat subsurface drainage from a 6.5 ha area on a farm located in the tidal portion of the Rappahannock River in Middlesex County, VA, in the Coastal Plain physiographic region. The field was planted in soy 2014-2016, no fertilizer was applied per agronomic recommendations. The dominant soils comprising

approximately 60% of the drainage area are poorly drained, including the Myatt loam (30%) and an equal mixture of Bertha and Daleville soils (30%); (Soil Survey Staff, accessed 4/6/2017). The remaining 40% of the soils are moderately well drained (20% Slagle silt loam, 15% Nansemond loamy fine sand, and 5% other soil types); (Soil Survey Staff, accessed 4/6/2017). All of these soil types are characterized by a low pH, measured in a 1:1 soil/water slurry, their average values ranging 4.6-5.1.

The bioreactor is 36.6 m^3, 5.79 m long by 5.33 m wide by an average 0.82 m deep (after woodchip settling), and intercepts a 15.24 cm (6 in) terra cotta tile drain serving as the outlet to a 6.5 ha drainage area. The sides and bottom of the bed are lined with impermeable polyethylene and the top is covered with permeable landscaping fabric. The bed was not covered with a layer of soil, as is typical, to maximize the potential for greenhouse gas emissions to reduce the chance of underestimating fluxes based on a limited number of measurements. The bioreactor connects to the tile drain with a water-level control structure (AgriDrain Corp., Adair, IA), and an identical control structure with removable stoplogs serves as the outlet. The water-control structures can govern the inflow and outflow by adjusting the stage by adding or removing stoplogs. An inlet manifold, consisting of two lengths of 15.24 cm (6 in) PVC pipe with many 0.6 cm (0.25 in) drilled holes, connects to the inlet control structure with a T and runs width of the bioreactor to promote uniform residence times by distributing the flow to increase mixing and minimize bypass flow. During installation, the bed was filled with 55 m^3 mixed hardwood woodchips and 6.1 m^3 of biochar, which was mixed into the woodchips as they were added. The additional woodchips were mounded to compensate for settling, which ultimately resulted in the 36.6 m^3 measured bed volume with a biochar

amendment rate of about 17% by volume, which was increased to nearly 19% when an additional 0.76 m^3 was incorporated in March 2016 in an effort to raise bed pH. Biochar was selected as a supplemental source of organic carbon based on laboratory-scale evidence from batch experiments that biochar amendment reduces N_2O production and increases N and P removal relative to woodchip bioreactors (Bock et al., 2015; Easton et al., 2015). A pilot-scale experiment on a paired woodchip only and biochar-amended bioreactor system provided limited evidence that biochar may increase N removal with moderate to high influent NO_x-N concentrations (>10 mg l^{-1}), but field-scale evidence of biochar's enhancement of bioreactor performance remains lacking (Bock et al., 2016). The biochar was purchased from Biochar Solutions Inc. (Carbondale, CO), produced from a pine feedstock via a two-stage pyrolysis process. Briefly, the feedstock is held for <1 min at 500-700°C under low oxygen conditions, and then the temperature is reduced to 300 to 550°C and held for up to 14 min. Two size fractions are produced by passing the biochar through an auger, yielding a biochar consisting of about 80% pieces approximately 1.5 cm long by 1 cm wide by 0.5 cm and 20% as a fine dust fraction on the order of 10-100 μm.

4.3.2 Data collection

4.3.2.1 Water chemistry monitoring and sampling

Retrieval of aqueous samples, greenhouse gas flux measurement (described in 4.3.2.2), and equipment maintenance occurred approximately every two to four weeks between December 2014 and November 2016. Aqueous grab samples were collected in triplicate from the inlet and outlet control structures, as well as a peizometer within the bed, on 31 occasions (on 8 others the bed was dry). An automated monitoring and sampling system installed April

2015 provided more inlet and outlet water samples, and recorded rainfall, bed outflow, and water chemistry. The automated system consisted of two 24-bottle Isco autosamplers (Teledyne Isco, Lincoln, NE); a rain gauge (Isco module 674); pressure transducer (Isco submerged flow module 720) installed in the outlet control structure, along with a 45˚ v-notch weir, to calculate flow rate; a multiparameter sonde (TROLL 9500, In-Situ, Inc.) fitted with sensors to measure dissolved oxygen (DO), pH/ORP (combined sensor for pH and oxidation reduction potential), temperature, and barometric pressure; and a power source, two deep cycle marine batteries in parallel, recharged by a 110 watt solar panel. Additionally, two capacitance probes (WT-HR Data Logger, TruTrack, Intech Instruments LTD, NZ) recorded water levels in the inlet and outlet control structures at 15- to 30-min intervals.

Recorded flow triggered nearly simultaneous sample collection at the inlet and outlet, one 200 ml sample for every 5 m^3 of effluent, with four 200 ml samples per 1000 ml bottle. Beginning in May 2015, fresh sample bottles were prepared with 5 ml of 10% concentrated sulfuric acid (H_2SO_4) to prevent sample degradation at ambient temperature, following the method of Burke et al. (2002), who demonstrated that H_2SO_4 preservation maintained stable NO_3^- and TP concentrations in groundwater samples for up to seven days in the field at temperatures exceeding those observed at the bioreactor site. Testing of field spikes and comparison of refrigerated and unrefrigerated acid-preserved samples showed that this approach was adequate for ensuring stability of NO_3^- and TP sample concentrations for up to two weeks in the field (data not shown).

Grab samples were field-filtered with 0.45 m nylon filters and stored on ice for transport from the field site to the lab, and subsequently stored at 4˚C until analyzed, typically within 48

h. Acid-preserved autosampler-collected samples were transported and stored at ambient temperature until pH-adjusted to neutral with 0.5 M sodium hydroxide solution using an autotitrator (Easy pH Titrator System, Mettler Toledo), after which they were filtered and analyzed or stored at 4˚C until further analysis. Filtered samples collected between January 2015 and March 2015 were analyzed colorimetrically by spectrophotometer (Thermo Scientific Orion AquaMate 7000 Vis Spectrophotometer) to measure NO_3^--N (chromotropic acid method, Orion AQUAFast method ACR007) and either PO_4^{3-} (ascorbic acid method, ACR095) or TP (ascorbic acid/persulfate digestion method, ACD095). Note that because all samples were filtered prior to analysis, TP more precisely refers to total filterable phosphorus. Early grab samples were analyzed for ammonium (salicylate method, ACR012), but all results were below the method detection limit 0.02 NH_4^+-N mg l^{-1}; autosampler-collected samples were not analyzed for NH_4^+-N, because the measurement would be invalid due to the instability of the analyte under field conditions. Beginning April 2016, samples were analyzed by flow injection analysis system (QuikChem® 8500, Lachat Instruments, Loveland, CO), using the cadmium reduction method for NO_x (NO_3^-+NO_2^-, Lachat method 10-107-04-1-A); the sodium salicylate gas diffusion method for NH_4^+ (10-107-06-5-J); and the ascorbic acid method for PO_4^{3-} (DRP) and TP, using undigested and persulfate digested samples, respectively (10-115-01-4-C). Grab sample concentrations of NH_4^+ continued to be below the new method detection limit, 0.1 NH_4^+-N mg l^{-1}, so analysis was discontinued. Note that in subsequent discussion NO_x will be referred to as NO_3^-, because NO_2^- is relatively unstable and NO_3^- is the dominant form of dissolved N observed in tile drainage waters (Williams et al., 2015). Likewise, NH_4^+ is discussed although the precise

proportion of un-ionized NH_3 to ionized NH_4 is unknown, NH_4^+ is the dominant dissolved form in the acidic bioreactor environment.

4.3.2.2 Greenhouse gas flux measurement

Three soil collars were installed December 2015, deployed in a row perpendicular to the direction of flow 1.9 m upstream from the outlet water control structure, centered along the width of the bioreactor. Collars were constructed from 0.5 m sections of 25.4 cm (10 in) inner diameter (i.d.) schedule 40 PVC with beveled bottom ends. Each collar was installed to a depth of approximately 30 cm to isolate vertical gas transport and prevent exchange between the atmosphere and air within the bioreactor media through the large voids between the woodchips, leaving a 20 cm section above the bed surface. Collars were refilled with the mixture of woodchips and soil removed during excavation to a height within the collar level to the bed surface. Collar placement aimed to provide replicate measurements of GHG flux by minimizing the effect of position rather than capture longitudinal variation in flux that might be expected as NO_3^- and DO concentrations, known to affect N_2O vary along the direction of flow (Elgood et al., 2010).

GHG fluxes from the bioreactor were measured in each of the three collars on 15 occasions between January and October 2016 using the non-steady-state flow-through method (Duran and Kucharik, 2013); the first measurements occurred four weeks after collar installation, to minimize the effect of disturbance the resultant disturbance. The non-steady-state flow-through method uses an inline instrument that recirculates air between the soil collar headspace and instrument's detector and records the changing trace gas concentration, from which flux is calculated using regression techniques to estimate the rate of change of gas

concentration (Duran and Kucharik, 2013). A portable cavity ring-down spectroscopy (CRDS) analyzer (Picarro G2508, Santa Clara, CA) measured real time CO_2, CH_4, and N_2O concentrations, pumping headspace from the top of the collar through the inlet line to the analyzer and returning through the exhaust line to the collar and discharged from an L-connector midway between the soil surface and inlet sampling port (~10 cm from the soil surface) toward the side of the collar to prevent short circuiting the flow. Two 15.24 m lengths of 3.2 mm i.d. inert, polyethylene-lined tubing with an ethyl vinyl acetate shell were used for the inlet and exhaust lines, attached to the PVC collar cap with compression fittings, and affixed to the collar cap with bulkhead unions inserted through holes in the PVC cap paired with rubber gaskets to prevent leakage around connections. Each collar was capped for two minutes during which the instrument recorded CO_2, CH_4, and N_2O concentrations and water content, needed to calculate the dry molar fraction of the analytes. The collar was vented, per the recommendations of de Klein and Harvey (2012), by disconnecting the inlet line from the cap during capping to prevent changes to the pressure inside the collar and disruption of the gas concentration gradient driving diffusive gas flux. Before reconnecting the inlet line, a wide elastic band was secured around the overlap of the collar and cap to create a gastight seal. Ambient air was pumped through the instrument between measurements for five minutes to allow a complete return to atmospheric concentration prior to measuring flux from the next collar. Air temperature and barometric pressure were recorded during flux measurements using a calibrated digital thermometer with an accuracy +/- 0.2 ˚C and barometer accuracy of +/-0.8 kPa, for calculation of analyte mass concentration from dry molar fraction using the ideal gas law. Flux measurements were conducted consistently at midday, approximately 12:00 to 14:00, to

minimize variation due to diurnal patterns in GHG flux, recognizing that this window likely captures fluxes slightly greater than the daily average expected 10:00 to 12:00 (de Klein and Harvey, 2012).

4.3.3 Data processing and calculations

All calculations were performed using the R language and environment for statistical computing (R development core team, 2017).

4.3.3.1 Nutrient loading and removal

Nutrient loading and removal were assessed for over a one-year period beginning approximately one year after bioreactor installation, September 30, 2015 to September 29, 2017. Daily average concentrations were used for calculations when multiple concentration measurements are available for a given day. Nutrient concentrations determined with different analytical methods (e.g., spectrophotometer and FIA) were treated as equivalent based on testing a subset of samples analyzed with both methods. Samples below the method detection limit were assigned as half of that concentration, 0.01 for TP quantified by FIA, 0.06 for TP quantified by spectrophotometer; NO_3-N concentrations of all samples exceeded the detection limit. At least one sample was collected from the inlet and outlet to measure nutrient concentration on 42% and 46% of the days in the observation period for N and P, respectively. Flow rates were calculated from a continuous record of nappe height using an equation calibrated specifically for the AgriDrain 45˚ degree v-notch weir:

$$Q = 1.7406\ H^{1.953} \quad (1)$$

where Q is the flow (l min^{-1}) and H is the nappe over the v-notch (cm), which is valid for flows 5-153 l min^{-1} (Partheeban et al., 2014). Non-zero daily flow averages were below the calibration

range only 3% of the time. The daily drainage volume passing through the bed (V_{flow}), used to calculate the mass of N and P into and out of the bed, is the sum of measured flow rates multiplied by the time elapsed between measurements (15-30 min).

For consistency with the body of bioreactor research, average removal (or export) rates are reported as g m^{-3} d^{-1} on the basis of total bed volume (36.6 m^3), calculated as:

$$\sum(C_{in} - C_{out})*Q_d/V_{bed} \quad (2)$$

where C_{in} and C_{out} are the bed inlet and outlet concentrations of the analyte, Q_d is the measured flow rate for a given day, and V_{bed} the total bed volume. For evaluation of the relationship between removal rates and bed conditions, actual daily removal rates were estimated on the basis of saturated bed volume (V_{sat}); V_{sat} is the product of bed surface area and the average daily water depth, as measured by the capacitance probes in the inlet and outlet drainage control structures.

4.3.3.2 Greenhouse gas flux estimates

GHG fluxes were calculated from chamber headspace concentration measurements over time using two methods, linear regression (LR) and a physically-based, non-steady-state diffusive flux estimator (NDFE) developed by Livingston et al. (2006). The NDFE method estimates pre-deployment flux by applying Fick's Law (stating gas diffusion is proportional the concentration gradient) and assuming gas transport only occurs in the vertical direction, matrix homogeneity, and a trace gas source supplying a constant, positive flux under undisturbed conditions. The 30 cm depth to which the soil collars were installed, preventing horizontal gas movement, and the relative uniformity of the woodchip mixture were deemed to meet these assumptions adequately. Ultimately, the fluxes calculated with NDFE method were used for

subsequent analysis unless LR flux estimates were negative (bed acting as GHG sink), in which case the NDFE equation is invalid, or the LR better fit the data, as described below.

Prior to applying the regression equation estimates, concentration data were processed by visually examining the data and adjusting the two-minute recording interval to remove measurements of ambient GHG concentrations prior to curve fitting. The dry molar fraction GHG gas concentrations recorded by the GHG analyzer were converted from volumetric (ppmv) to mass (mg m^{-3}) using ideal gas law, molecular weight of the element of interest in analyte (C in CO_2 and CH_4, N in N_2O), and ambient temperature and pressure recorded during flux measurement (Collier et al., 2014). First, fluxes were calculated by LR as:

$$F = S \cdot V \cdot A^{-1} \quad (3)$$

where F is flux, S is the slope of the analyte concentration regressed over time, V is total volume of the recirculating system, and A is the surface area contained in the soil collar for which flux is measured (Duran and Kucharik, 2013). Volumes were measured for the right, middle, and left collars as 8181, 9198, and 9774 cm^3, respectively, including the internal volume of the analyzer and connecting tubing, and surface area contained within each collar was defined as 504.3 cm^2. Next, the NDFE method was used to calculate flux for all measurements of positive flux as determined by LR, which was 26 of 45 for N_2O, and 37 of 45 of the CH_4 measurements, and all of the CO_2 flux measurements. GHG concentration curves were fit to the NDFE equation (Eq. 4) with a Levenberg-Marquardt modification to the least-squares algorithm:

$$C_t = C_0 + f_0 \tau \left(\frac{A}{V}\right) \left[\frac{2}{\sqrt{\pi}} \sqrt{t/\tau} + \exp(t/\tau)\, \mathrm{erfc}(\sqrt{t/\tau}) - 1\right] \quad (4)$$

where C_t is headspace concentration at a given time, t, f_0 is pre-deployment flux, C_0 is ambient trace gas concentration, τ is an experimental constant representing the time until the concentration gradient in the chamber decreases to zero for a specific collar design, soil, and gas species as gases accumulate in the headspace, and *erfc* is the complimentary error function. Starting values of f_0 are assigned as the LR flux calculation, and τ is set to $(V/A)^2/D$, where V is the total internal volume and A is the soil surface area contained within the collar, and D is the diffusivity of the trace gas in air.

Given the many reports that LR substantially and systematically underestimates trace gas flux in closed soil flux chambers, even with the short deployment times associated with flow-through chambers meant to avoid deviations from linearity (Duran and Kucharik, 2013; Kutzbach et al., 2007; Livingston et al., 2006), NDFE was preferred when selecting between the two calculations. Livingston et al. (2006) demonstrated that NDFE was significantly more accurate than LR for CO_2 flux at a rate of 50 μg CO_2-C m^{-2} s^{-1} or less, which was lower than the majority of the observed CO_2 fluxes from the bioreactor, so the NDFE calculation of CO_2 fluxes was used for all subsequent analyses. Graphical assessment of the goodness-of-fit for the CO_2 data supported the use of the NDFE model. For the CH_4 flux estimates, NDFE was used for all except the five negative LR fluxes, which could not be calculated by NDFE. Agreement between LR and NDFE for the low magnitude CH_4 fluxes provided confidence in the accuracy of the LR calculations of the small negative fluxes; the ten lowest positive fluxes (all greater in absolute value than the negative fluxes) differed by less than 7.2%. The differences in fluxes calculated with the two methods increased as fluxes approached the 50 μg C m^{-2} s^{-1} rate at which Livingston et al. (2006) demonstrated significant nonlinearity. N_2O fluxes, however, were

several orders of magnitude smaller than the CO_2 and CH_4 fluxes that produced nonlinear soil collar headspace concentration curves, approximately -0.01 to 0.4 μg N_2O-N m^{-2} s^{-1}. Graphical assessment did not show significant deviations form linearity despite low LR r^2 values, which appear to be driven by the high signal to noise ratio of the headspace concentration data. Given that over 40% of the N_2O flux measurements were negative and could only be calculated with LR, and the relatively low robustness of the LR flux calculation method to measurement error compared to NDFE (de Klein and Harvey, 2012), LR calculations were used for all except the two highest N_2O fluxes, where nonlinearity was visually apparent and which were better fit by the NDFE equation. Diffusion theory supports the observation of a transition from a linear to nonlinear increase in headspace trace gas concentrations for larger fluxes due to depression of the soil-headspace concentration gradient driving diffusive flux as gas accumulates in the closed system, as has been well established in chamber-based flux measurement applications (de Klein and Harvey, 2012). However, for sufficiently sized chambers with small increases in headspace trace gas concentration enabled by short measurement windows, LR can be an appropriate method of flux calculation, as was determined to be the case for these N_2O flux measurements (de Klein and Harvey, 2012; Healy et al., 1996). To estimate the proportion of NO_3-N removed by the bed that was completely reduced to N_2 as opposed to in complete denitrification resulting in release of N_2O, the daily mass of N_2O emitted from the bed was calculated by extrapolating the average flux of the three collars to the entire bed surface area (30.9 m^2), assuming the measured flux to represent average flux over a 24 h period.

4.3.4 Statistical Analysis

4.3.4.1 Nutrient Removal

The average removal rates of N and P and their statistical significance were calculated from the irregularly spaced time series of flow and nutrient concentration measurements collected during the second year of operation (mo 13-26) using one-sample t-tests adjusted for serial correlation. To compensate for the pseudoreplication present in the time series of calculated removal rates, the procedure descried by Ghane et al. (2016) was followed, whereby anticonservative p-values are corrected adjusting the standard error for autocorrelated data. Removal rates during the growing (4/10/16-9/29/16) and non-growing (9/30/15-4/9/16) seasons were also evaluated separately, and the mean difference was determined with an unpaired two-sample t-test. The t-test assumption that sample means are normally distributed within the population was verified by graphical examination of the distribution of bootstrapped mean removal rates (calculated from 10,000 sample subsets (n=10) with replacement), validating the assumption of normality by the central limit theorem. The anticipated serial correlation of the measured removal rates of N and P was confirmed with the Durbin-Watson test for autocorrelation of errors at the p=0.1 significance level (N p<0.0001; P p=0.0867). To account for this serial correlation, we adjusted the standard error term after Ghane et al. (2016) as:

$$SE = \sqrt{\frac{1+r_1}{1-r_1}}\frac{s}{\sqrt{n}} \quad (5)$$

where *s* is the standard deviation of the measured removal rates, *n* is the sample size, and r_1 is the correlation coefficient at lag=1 of a first order autoregressive model (AR1). N and P removal

rates were determined to be appropriately represented by an AR1 model because partial autocorrelation function was below the 0.05 significance level after the first lag. One year of data was insufficient to assess the stationarity of the nutrient removal time processes.

The effects of influent N concentration, HRT, and temperature on nutrient removal rates were examined using a linear model fit by generalized least squares (GLS). GLS relaxes the assumption of independence of errors required for ordinary least squares, and a continuous AR1 correlation structure was included in the model to account for non-independence and serial correlation errors over time. Model parameters were selected by comparing nested models with the log likelihood ratio test, beginning with maximal model including all interactions in addition to the main effects and iteratively removing terms. The significance of individual predictors in the final model was determined by analysis of variance (ANOVA), specifying the test type as marginal (equivalent to type II sum of squares). The model was fit using 118 days of data collected during a subset of the monitoring period (1/16/16-10/4/16, mo 17-26) for which measurements of influent and effluent nutrient concentration, flowrate, and saturated volume were recorded. Validity of model assumptions were evaluated by visual examination of the normalized residuals compared to normal quantiles and fitted values, the Shaprio test of normality, the Breusch-Pagan test of heteroskedasticity, the autocorrelation function to assess error independence, and the variance inflation factor to assess collinearity. Note that normalized residuals were used for these assessments, which incorporate the modeled error correlation structure. All model assumptions were met except for normality of residuals, which is the least important assumption for linear models, especially for describing

relationships between the explanatory and dependent variables as opposed to predicting responses under specific conditions (Gelman and Hill, p. 46, 2007).

4.3.4.2 Greenhouse gas flux models

To characterize the relationship between bioreactor conditions and GHG emissions from the bed surface, N_2O, CO_2, and CH_4 flux measurements were each regressed by potential predictive variables influent N concentration, HRT, temperature, and collar position (left, right, and center along a transect perpendicular to flow) by generalized least squares. To fit the model, measurements were excluded for 3 of the 15 measurement dates (June 29, Aug. 24, and Sept. 21) during periods of no flow through the bioreactor, and an additional single measurement from June 15 was excluded from the CH_4 dataset due to poor data quality. Interaction effects were not evaluated due to the small size of the dataset (N_2O and CO_2 n=36, CH_4 n=35). GLS was, again, used to estimate linear regression parameters and account for temporal correlation of fluxes. All explanatory variables were centered by subtracting their mean value. Model assumptions were evaluated as described in 2.4.1, with the addition of the Levene test of equality of variance between collars. To meet assumptions of homoscedasticity and normality of errors, each of the dependent variables (N_2O, CO_2, and CH_4 flux measurements) was transformed. A cubic root transformation was applied to N_2O and CH_4 flux measurements, which included negative values (net transfer into bed) that precluded the logarithmic transformation for positive skew. The natural log transformation was applied to CO_2, for which all flux measurements were positive.

Transformed dependent variables necessitate back transformation to describe the relationship between explanatory variables and flux on the original scale. Since both the cubic

root and logarithmic transformation introduce nonlinearity on the original scale, the effect of a change in temperature, HRT, or influent concentration is dependent on the current conditions (current predicted flux) to which this change is applied. The approach to interpreting a liner model where the dependent variable is a natural logarithm is, where X_i is one of the explanatory variables and B_i is its corresponding coefficient, subtracting the equation for flux at given value of X_i (Y_{xi}) from flux at X_i +1 (Y_{xi+1}) and algebraically rearranging to determine that the effect of a unit increase in Xi is a percent increase in flux equal to $(\exp^{Bi} - 1)*100$. The approach to interpretation with a cubic root transformed dependent variable is to take the derivative of the dependent variable on the original scale, $Y^{1/3}$, with respect to X_i, which by applying the chain rule is equal to $3B_iY^2$; that is, the effect of a one unit change in X_i is equal to three times the coefficient of X_i (B_i) multiplied by the square of the current flux.

4.4 Results

4.4.1 Nutrient loading and removal

Nutrient loading to the bioreactor represented export from the 6.5 ha drainage area at an average rate of approximately 10.0 kg NO_3^--N ha^{-1} yr^{-1} without fertilizer application. Average nutrient loading, removal, and influent and effluent concentrations for the period September 2015 to September 2016 and separates the growing (April 10 to September 29 2016) and non-growing (September 30, 2015 to April 9, 2016) seasons are shown in Table 1. Mean values were calculated from direct observations (Figure 1a-c) and their 95% confidence intervals were calculated using t-tests with standard error adjustment for autocorrelation as described in section 2.5.1. Figures 1a and 1b show the seasonal trends of flow and temperature; with the exception of storm response, flows were inversely correlated with temperature. Figures 1b and

1c show a seasonal trend in influent nutrient concentrations, with higher N and P

concentrations occurring during the non-growing season.

Table 1. Mean nutrient loading rate, bed-normalized removal rate, and flow-weighted influent and effluent concentrations calculated from observed data are presented; 95% confidence interval of the mean loading and removal rates are determined by one-sample t-test with standard error adjustment for serial correlation. Total phosphorus removal is not reported because it is not statistically significant.

Nitrogen as Nitrate		**Annual**	**Growing**	**Non-grow**
		mean (95% confidence interval)		
Loading	**kg ha^{-1} yr^{-1}**	10.0 (6.9-13.1)	4.0 (2.7-5.4)	14.2 (7.0-21.3)
	g m^{-3} d^{-1}	4.86 (3.34-6.37)	1.96 (1.31-2.61)	6.89 (3.40-10.36)
Removal	**g m^{-3} d^{-1}**	0.41 (0.32-0.51)	0.40 (0.17-0.63)	0.40 (0.32-0.49)
	mean %	8.4	20.4	5.8
Conc.	**inlet mg l^{-1}**	4.37	3.07	5.06
	outlet mg l^{-1}	4.04	2.45	4.77
Total Phosphorus		**Annual**	**Growing**	**Non-grow**
		mean (95% confidence interval)		
Loading	**kg ha^{-1} yr^{-1}**	0.27 (0.11-0.43)	0.04 (0.01-0.07)	0.48 (0.30-0.65)
	g m^{-3} d^{-1}	0.13 (0.06-0.21)	0.02 (0.00-0.03)	0.23 (0.15-0.32)
Conc.	**inlet mg l^{-1}**	0.139	0.187	0.029
	outlet mg l^{-1}	0.127	0.170	0.025

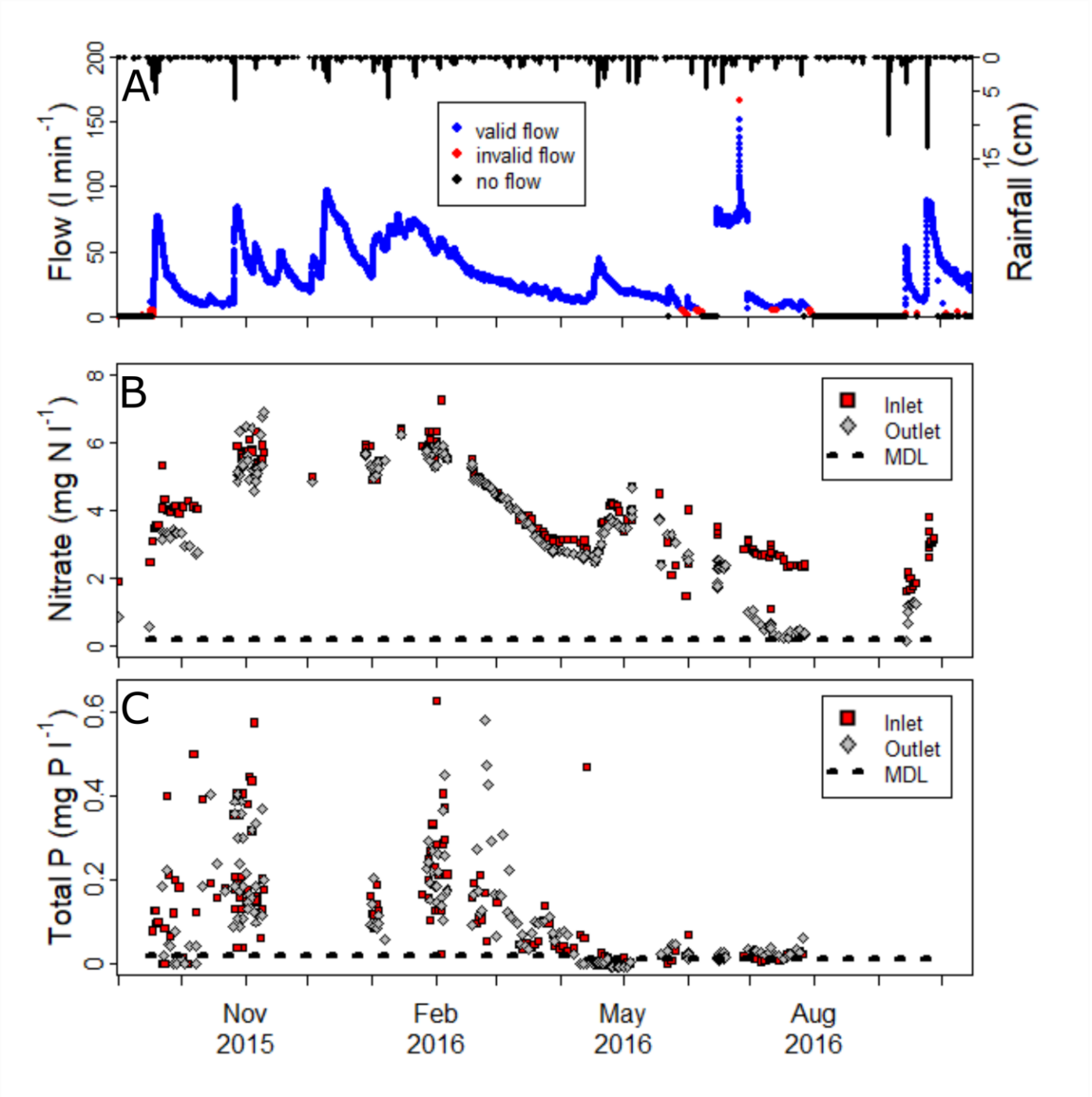

Figure 1a-c. Measured flowrate of water leaving the bioreactor and daily rainfall (a); concentrations of nitrate as nitrogen (b) and total phosphorus (c) in bed influent and effluent water samples. Dashed lines represent method detection limits (MDL).

The bioreactor removed approximately 8.4% of the influent NO_3^--N at an average bed-normalized rate of 0.41 g m^{-3} d^{-1}, but significant TP removal was not observed. Note that NO_3^--N reported rates in Table 1 are calculated on the basis of total bed volume for consistency with the literature and to facilitate comparison between studies. Actual rates of denitrification within the bed on the basis of saturated volume would be higher since the median measured saturated volume (from inlet and outlet water height) was just below 50% and ranged ~13-60%. Indeed, the bed-normalized removal rate is estimated to be only about 47% of the actual removal rate by simple GLS linear regression including a correlation structure for non-independence or errors over time. Bed normalized removal rates ranged -0.93-1.58 g NO_3^--N m^{-3} d^{-1} while actual removal rates ranged -1.76-5.23 g NO_3^--N m^{-3} d^{-1}, negative rates represent net export of NO_3^--N from the bed. Flow through the bed was continuous through the non-growing season, but flow ceased for 49 days (~28%) of the growing season, 6/24/16-6/29/16 and 8/17/16-9/28/16.

Mean NO_3^--N removal was statistically significant during the observation period (t-statistic=9.57, $p<0.001$), and the 95% confidence interval (CI) of the mean removal rate, estimated as 0.41 g NO_3^--N m^{-3} d^{-1}, was 0.32-0.51 g NO_3^--N m^{-3} d^{-1} (Table 1). Removal rates were not statistically different between the growing and non-growing season (t-statistic=0.0171, $p=0.9863$). However, NO_3^--N loading differed seasonally (t-statistic=-4.365, $p<0.001$), with growing season NO_3^--N loading averaging a very low 1.96 g m^{-3} d^{-1} (95% CI 1.32-2.61 g m^{-3} d^{-1}, Table 1) compared to 6.89 g m^{-3} d^{-1} (95% CI 3.40-10.36, Table 2) during the non-growing season. Both greater influent NO_3^--N concentrations (Table 1) and drainage volumes (Table 2) during the non-growing season drove seasonal differences in loading, and the flow-weighted influent

concentration was 60% higher than during the growing season. From the field perspective, the rate of NO_3^--N export via tile drainage was more than three times greater in the non-growing season (14.2 kg ha^{-1} yr^{-1}) than the growing season (4.0 kg ha^{-1} yr^{-1}).

Mean TP removal was not significantly different from zero during the observation period (t-statistic=1.261, p=0.2082) or for either the growing (t-statistic=0.2012, p=0.8003) or non-growing season (t=2.008, p=0.2354). TP loading to the bioreactor was about 6.5 times greater during the non-growing season, which was a statistically significant difference (t-statistic=-3.654, p=0.0003). Given that TP concentrations were below the limit of quantification at 0.01 mg P l^{-1} in approximately 30% and 22% of the influent and effluent samples, respectively, it is unsurprising that no statistical difference was found between inlet and outlet concentrations despite the flow-weighted average concentrations being slightly lower at the outlet (Table 1).

Table 2. Cumulative rainfall and drainage volume flowing through the bioreactor as well as average temperature and flow rate on an annual basis and separated by growing and non-growing season.

		Annual	**Growing**	**Non-growing**
Total	**drainage (cm)**	22.8	6.0	16.8
	rainfall (cm)	151.9	77.4	74.5
Mean	**temp (˚C)**	17.9	21.7	12.5
	flow (l s^{-1})	28.1	15.5	39.3
	pH	5.3	5.2	5.5

4.4.2 Variables influencing N removal

N removal rate was found to be significantly correlated with influent N concentration, HRT, and temperature as determined by GLS regression. The interaction effects of influent concentration by HRT and temperature by HRT were significant at the 95% confidence level, as were the main effects of influent concentration and temperature (Table 3). Significant

interactions with HRT indicate that the relationship between either influent concentration and removal rate or temperature and removal rate is dependent on HRT. The interaction effect between influent concentration and temperature was not significant, meaning that at a given HRT that the effect of influent concentration on N removal is constant across temperatures and the effect of temperature on N removal is constant across influent concentrations; this non-significant interaction term was removed from the model. Note that modeled removal rates were normalized to saturated volume rather than bed volume to avoid the confounding effect of adjustment of stop log position in the drainage control structures, and thus not equivalent to bed normalized removal rates reported in Table 1.

The N removal rate generally increases as influent concentration increases, reflecting a first-order kinetic relationship (Figure 2a). However, the standard error band for the regression of removal rate by influent concentration for the 20 h HRT encompasses a zero slope, uncertainty in removal rates increasing as the difference between influent and effluent concentrations decreases, indicating that influent concentration may not be directly related to removal rate after a threshold HRT is exceeded. Below this threshold, a difference in influent concentration will have a larger effect on removal rate for lower concentrations. For example, if influent concentration increases from 3 mg N l^{-1} to 4 mg N l^{-1} when HRT is 12 h, N removal rate is predicted to increase by an average of 1.2 g N m^{-3} d^{-1}, but the increase in removal rate is approximately doubled for the 1 mg N l^{-1} increase in influent concentration, 2.5 g N m^{-3} d^{-1}. Figure 2b shows that N removal rate increases as temperature increases, as would be expected for a biochemical reaction like denitrification. As with influent concentration, differences in temperature have a larger effect on N removal rate as HRT decreases; an increase of 5°C

increases removal rate by 3.81 g N m^{-3} d^{-1} when HRT is 12 hours, but by only 2.55 g N m^{-3} d^{-1} when HRT is 6 hours. Relative to the range of observed bed conditions (influent concentration 1.77-6.32 mg NO_3-N l^{-1} and temperature 8.1-25.3°C), changes in influent concentration were associate with larger differences N removal rate than changes in temperature. While N removal rates up to 8.3 g N m^{-3} d^{-1} were predicted for higher influent concentrations and temperatures (values approximately in the upper 50% of observed influent concentrations and temperatures), N export was predicted for lower influent concentrations and temperatures (Figure 2a, b); the rates of both removal and export were intensified at lower HRTs. N export occurred during 16% of the observations (19 d) used to fit the model, 15 of which were attributable to differences between influent and effluent concentration of <0.25 mg N l^{-1} resulting in low magnitude export, up to -0.28 (-0.15 bed-normalized) g N m^{-3} d^{-1}. More substantial export was observed during four consecutive days in June 2016, up to -1.76 (bed-normalized -0.93 g N m^{-3} d^{-1}). Note that predicted export and removal rates displayed in Figures 2a and 2b across representative bed conditions exceed the range of observed values (-1.76-5.28 g N m^{-3} d^{-1}) and must be interpreted with caution.

Table 3. Summary of a generalized least squares linear model of N removal rate (g N m-3 d-1), fit by restricted maximum likelihood, with influent N concentration, HRT, bed temperature, and their two-way interactions as independent variables. Note that removal rates are calculated on the basis of saturated volume, not total bed volume. Starred p-values denote statistical significance at the 95% confidence level.

Explanatory Variable	N Removal Rate			
	coefficient	standard error	t-value	p-value
Intercept	0.422	0.575	0.734	0.4643
[N_{in}]	1.248	0.179	6.981	<0.0001*
HRT	-0.053	0.031	-1.699	0.0920
Temp	0.521	0.083	6.245	<0.0001*
[N_{in}] : HRT	-0.162	0.028	-5.859	<0.0001*
HRT : Temp	-0.031	0.005	-5.809	<0.0001*

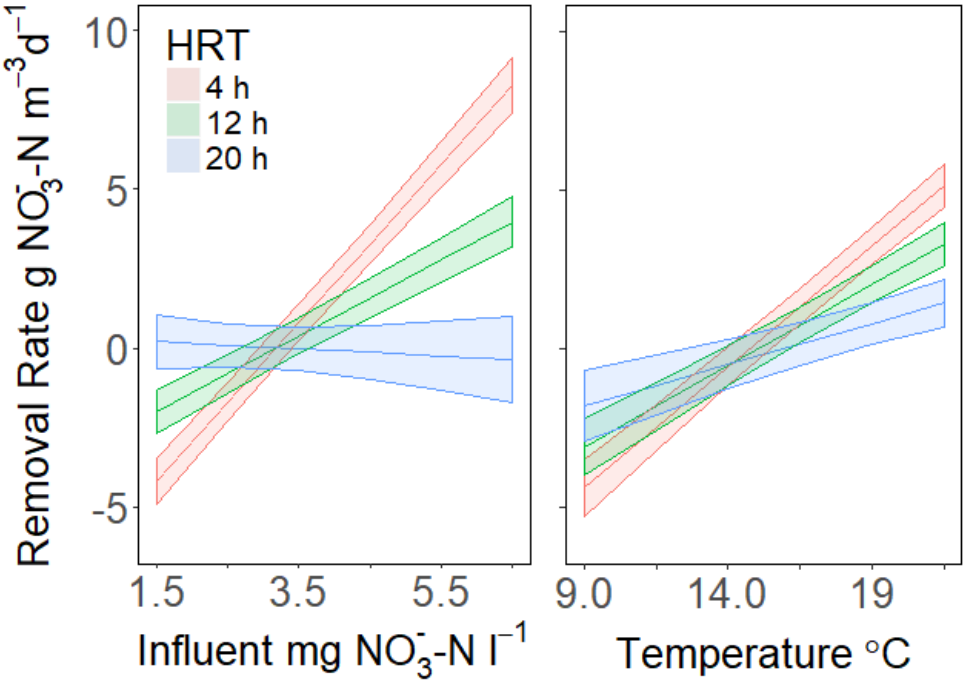

Figure 2. Modeled interaction effects of influent N by HRT (left) and temperature by HRT (right) from GLS model of N removal rate with prediction bands indicating +/- the standard error. The interaction of influent N by HRT is presented at median temperature (15.8 °C), and the interaction of temperature by HRT is presented at median influent concentration (3.5 mg N l-1). Limits of the x axes correspond to the range of respective variables observed in the bioreactor.

4.4.3 Greenhouse gas flux

Measured GHG flux from the surface of the denitrifying bioreactor exhibited high variability both spatially, between soil collars and temporally, between measurement dates January to October 2016 (Figure 3a-d). During periods of active flow through the bioreactor, N_2O had the greatest variability with a 310% coefficient of variation (CV) and measured fluxes ranging -0.60-19.7 mg N_2O-N m^{-2} d^{-1}, followed by CH_4 ranging -0.03-308 mg CH_4-C m^{-2} d^{-1} with 260% CV, and CO_2 ranging 540-82,250 mg CO_2-C m^{-2} d^{-1} with 160% CV. Median fluxes were 0.08 mg N_2O-N m^{-2} d^{-1}, 1.66 mg CH_4-C m^{-2} d^{-1}, and 4,580 mg CO_2-C m^{-2} d^{-1}. Variability generally increased as the mean flux from the soil collars increased, as indicated by the error bars in Figure 3a-d. To assess total GHG emissions from the bed, the combined GHG flux is reported as CO2 equivalents (CO_2-eq), whereby N_2O and CH_4 fluxes are multiplied by their global warming potential over a 100-yr timespan, factors of 25 and 298, respectively (IPCC 2007). From this perspective, both N_2O and CH_4 contributed substantial portions of total warming potential of GHGs emitted from the bed at certain times. Up to 44% of total CO_2-eq flux of was supplied by N_2O, although the average contribution was just over 6%, and CH_4 accounted for up to 15% of CO2-eq, but averaged only 3.6%. Calculated CO_2-eq ranged 1.3-166.6 g CO_2-eq m^{-2} d^{-1}, over 90% of which was emitted as CO_2 on average. The N_2O emission factor, percentage of removed NO_3^--N emitted as N_2O-N, ranged -1.9-7.0%.

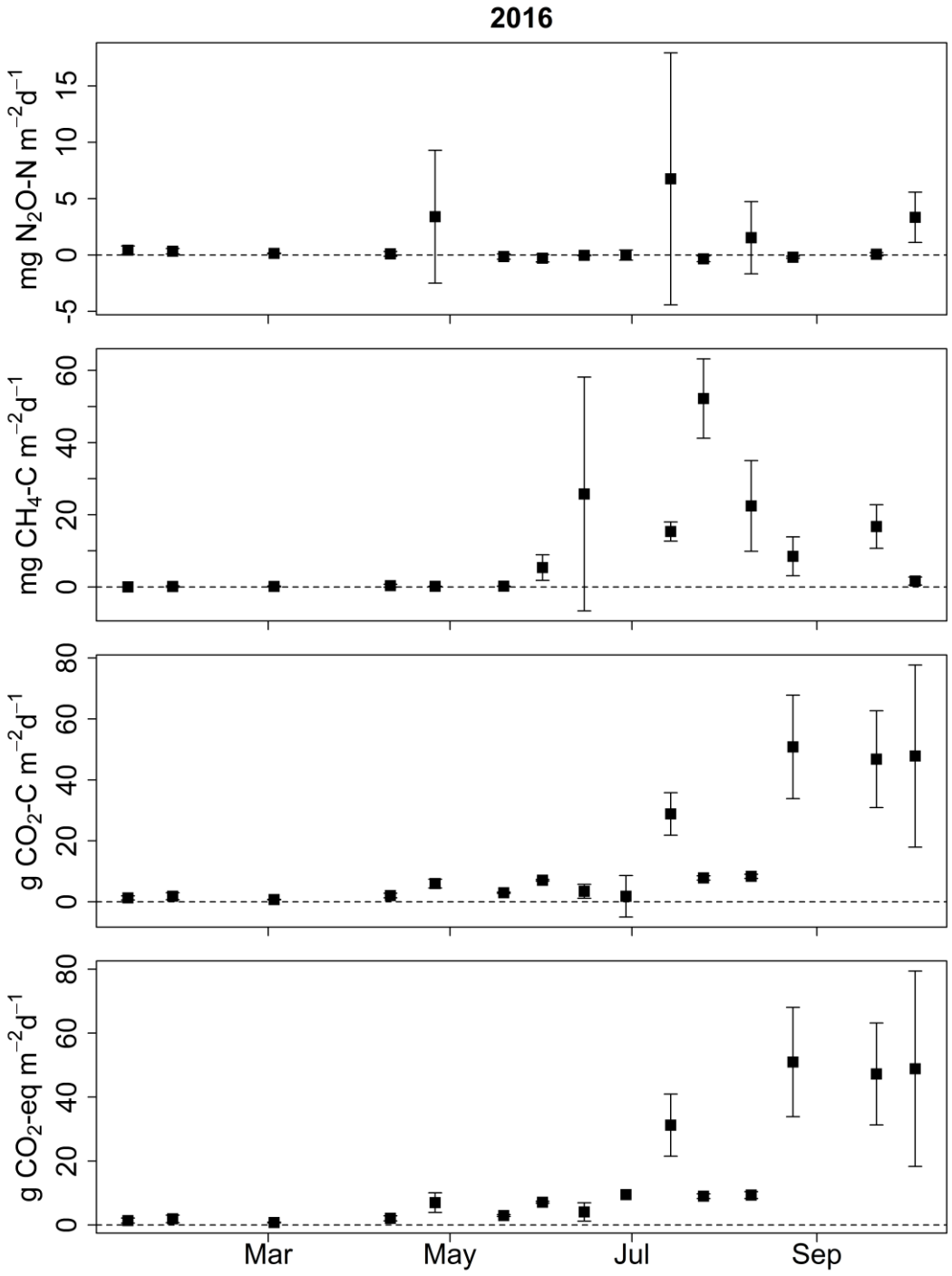

Figure 3a-d. Average flux measurements of N_2O (a), CH_4 (b), CO_2 (c), and the combined warming potential of the three gases as CO_2 equivalents (d) from three soil collars installed in a denitrifying bioreactor. Error bars represent +/- one standard deviation, and the dashed line is positioned at zero net flux. Note y axes are different scales and units differ between 3a-b (mg m^{-2} d^{-1}) and 3c-d (g m^{-2} d^{-1}).

Table 4 presents the GLS linear models of the N_2O, CH_4, and CO_2 flux. As described in section 2.4.2, the dependent variables (flux measurements) were transformed to ensure homogeneity of variance and linearize the relationships between flux measurements and potential explanatory variables; a cubic root transformation was applied to N_2O and CH_4 measurements, and the natural log transformation was applied to CO_2. The coefficients of explanatory variables and their standard errors are presented on the transformed scale, and back transformation was performed as described in section 2.4.2.

The model predicts N_2O flux at average temperature (17.6°C), HRT (13.4 h), and influent concentration (3.5 mg NO_3-N l^{-1}) as 0.029 mg N_2O-N m^{-2} d^{-1}, and the 95% confidence interval (>0.001-0.150 mg N_2O-N m^{-2} d^{-1}) encompassed the median observed value, 0.08 mg N_2O-N m^{-2} d^{-1}. HRT was the only variable with a statistically significant correlation with N_2O flux ($p = 0.0017$). Although the predicted fluxes were not significantly different between the three collars, the collar variable was retained in the model because it improved model residuals; only the average effect of HRT on flux is of interest. Flux was predicted to decrease as HRT increased, a 1 h increase from the mean HRT predicted to eliminate N_2O flux (a decrease of 0.029 mg N_2O-N m^{-2} d^{-1}, 95% 0.012-0.046). The high variability in N_2O flux was not explained by the variation in temperature, HRT, or influent concentration.

Average predicted CH_4 flux was 2.48 mg m^{-2} d^{-1} (95% CI 0.94-5.15) and both temperature and HRT were found to have a significant, positive exponential correlation with CH_4 flux. An increase in temperature from the mean of 17.6 to 18.6°C increases the flux by 1.05 mg m^{-2} d^{-1} (95% CI 0.69-1.42), and a further increase to 19.6°C adds another 1.26 mg m^{-2} d^{-1} (95% CI 0.82-1.69), while a decrease to 15.6°C is predicted to eliminate CH_4 flux. A 1 h increase

in the mean HRT (13.4) to 14.4 h is predicted to increase CH_4 emissions by only 0.32 mg m^{-2} d^{-1} (95% CI 0.16-0.49), and a further 1 h increase adds an additional 0.34 mg m^{-2} d^{-1} (0.17-0.52). The model suggests that when HRT decreases to about 8 h CH_4 emissions cease. Uncertainty in predicted fluxes increases exponentially as the absolute difference from mean temperature and HRT increases.

Average predicted CO_2 flux is 4510 mg m^{-2} d^{-1} (95% CI 4120-4950). All tested variables displayed significant correlation with CO_2 flux, with flux increasing as temperature increased, but decreasing as HRT and influent concentration increased. On the original scale, an increase of 1 °C from the mean results in a 9.5% increase in flux (95% CI 4.3-14.9%), an increase in the HRT by one hour results in an 8.7% decrease (95% CI 6.2 to 11.2%), but influent concentration was most influential, with a 1 mg l^{-1} increase from the average influent concentration (3.5 mg l^{-1}), reduced emissions by 51% (95% CI 39-61%).

Table 4. Summary of generalized least squares models of greenhouse gas flux (N_2O, CO_2, and CH_4) with t-statistics and corresponding p-values indicating the probability that a given coefficient estimate is equal to zero. Note that soil collar was retained as an explanatory variable only for N_2O because its inclusion reduced the model's residual sum of squares as determined by the log likelihood ratio, whereas including the effect of collar did not improve the CO_2 or CH_4 model fits.

Greenhouse Gas Flux Models				
N_2O (mg N_2O-N m^{-2} d^{-1})$^{1/3}$				
	Coefficient	**Standard Error**	**t-value**	**p-value**
Intercept	0.309	0.111	2.774	0.0094*
Temperature	-0.005	0.029	-0.181	0.8579
HRT	-0.057	0.017	-3.444	0.0017*
Influent N	-0.116	0.135	-0.856	0.3986
Collar (middle)	-0.198	0.157	-1.259	0.2177
Collar (right)	-0.218	0.157	-1.388	0.1754
CH_4 (mg CH_4-C m^{-2} d^{-1})$^{1/3}$				
	Coefficient	Standard Error	t-value	p-value
Intercept	1.354	0.187	7.244	<0.0001*
Temperature	0.113	0.039	2.926	0.0064*
HRT	0.069	0.017	3.972	0.0004*
Influent N	-0.094	0.158	0.557	0.5572
CO_2 ln(mg CO_2-C m^{-2} d^{-1})				
	Coefficient	**Standard Error**	**t-value**	**p-value**
Intercept	8.415	0.092	91.923	<0.0001*
Temperature	0.091	0.024	3.759	<0.0001*
HRT	-0.091	0.014	-6.679	<0.0001*
Influent N	-0.710	0.111	-6.378	<0.0001*

4.5 Discussion

4.5.1 Nutrient Removal

Average N removal efficiency (8.4%) and bed-normalized mass removal rates (0.41 +/- 0.10 g NO_3^--N m^{-3} d^{-1}) for this denitrifying bioreactor are substantially lower than the target removal efficiency range of 25-45% and the mean removal rate of 4.7 g NO_3^--N m^{-3} d^{-1} reported for denitrifying beds based on 27 individual units (Addy et al., 2016). However, removal rates were within the range reported for three tile drain bioreactors in the Maryland Coastal Plain, 0.21 to 5.36 g NO_3^--N m^{-3} d^{-1}, and just below the corresponding removal efficiency range of 9.0-62%. Performance was also comparable, although somewhat weaker, in a ditch diversion bioreactor also located in the Maryland Coastal Plain, where removal rates averaged 0.97 g NO_3^--N m^{-3} d^{-1} and N load reduction was 25% (Christianson et al., 2017). Recall that for consistency with the literature removal rates are reported here on the basis of total bed volume, but due to suboptimal hydraulic utilization of the bed, an average of only 50% of the bed volume was saturated and actively treating drainage waters. Thus, if removal rates increase from -0.93-1.58 g NO_3^--N m^{-3} d^{-1} on the basis of total bed volume to -1.76-5.23 g NO_3^--N m^{-3} d^{-1} on the basis of saturated bed volume. Apart from occurrences of N export (negative removal rates), removal for actively bed volume very closely corresponds to removal rates observed by Rosen and Christianson (2017), and brings average removal to nearly 1 g NO_3^--N m^{-3} d^{-1}, in line with Christianson et al. (2017). Additionally, observed N removal rates can be further explained by average influent concentrations, HRT, and bed age, all of which were found to be statistically significant controls on N removal in bioreactors in a recent a recent meta-analysis by Addy et al. (2016). Conditions in this bioreactor would be classified as low influent (< 10 mg NO_3^--N l^{-1}) with

an average concentration of 4.37 NO_3^--N l^{-1}, typically within the mid-range 6-20 h HRT category, and with a bed age exceeding 13 mo. This meta-analysis showed that N removal rates tended to increase with HRT, although the 6-20 h category was not significantly different from the >20 category, increase with higher influent concentrations, and decrease after 13 mo to a rate thought to be representative of long term performance, 13-24 mo and >24 mo categories not being significantly different. While HRTs 6-20 h corresponded to average N removal rates similar to the overall aver of 4.7 g NO_3^--N m^{-3} d^{-1} for denitrifying beds, the low influent N category averaged only 2.4 g NO_3^--N m^{-3} d^{-1} and the beds with ages 13-24 mo averaged 2.6 g NO_3^--N m^{-3} d^{-1} (Addy et al., 2016). Within this context, observed N removal was still lower but closer to expected rates, and low N loading, only 4.86 g NO_3^--N m^{-3} d^{-1}, is thought to be the dominant constraint.

Findings of Addy et al. (2016) emphasize the importance of N limitation as a control on N removal in denitrifying bioreactors and suggest that N-limited conditions persist at higher influent concentrations than previously reported (Addy et al., 2016). N-limited conditions within a bioreactor are often defined by effluent < 0.5 mg l^{-1} (e.g., van Driel et al., 2006), but this meta-analysis found that N removal rates were correlated with influent concentration and significantly differed between high (>30 mg N l^{-1}), intermediate (10-30 mg N l^{-1}), and low (<10 mg N l^{-1}) categories (Addy et al., 2016). Thus, it is suspected that N-limited conditions persisted during the observation period, except during temperature-limited conditions during the winter, as evidenced by the linear relationship between removal rate and influent concentrations (Table 3, figure 2a). The significant interaction effect between influent concentration and HRT, where for a given influent concentration the removal rate decreases as HRT increases, provides

further evidence for N-limited conditions. For constant influent concentration, as flow increases and thus HRT decreases, N loading to the bioreactor increases; if the bioreactor N removal rate is zero-order, as has been encountered (Hua et al., 2016; Warneke et al., 2011e), bed concentration decreases linearly with reaction time (analogously to effluent concentration decreasing linearly with HRT), and removal rate remains constant independently of HRT. However, if removal rate is first-order due to N-limitation, bed concentration decreases asymptotically, and the removal rate decreases as HRT increases, as captured by the GLS linear model (Figure 2a). Notably, though loading was significantly lower during the growing season, mean removal rates not significantly different for the non-growing season, indicating that cooler temperatures became rate limiting, overwhelming the effect of increased influent concentration.

The dominance of N-limited conditions in this bioreactor provides a unique assessment of bioreactor performance under consistently low N loading. Although the low loading rates were the result of three years of continuous soy cultivation, with no fertilizer application the season prior to bioreactor installation and during the first two years of use, and clearly not representative of the typical corn-soy rotation, this study provides important insight into field-scale bioreactor performance at the lower boundary of N inputs. Understanding performance under low N loading is relevant not only to situations where fertilization does not occur, but, perhaps more importantly, informs expectations for N removal efficiency in bioreactors used in conjunction with drainage water management, which alone can reduce N losses from the field by 17-80% (Skaggs et al., 2010).

N export in tile drainage was quite low at 10.0 kg ha^{-1} yr^{-1} (Table1) compared to the 31.4 kg ha^{-1} yr^{-1} reported by Christianson et al. (2013) as representative of Midwestern drainage N loading. Additionally, the distribution of N loading throughout the year constrained removal more severely than would be predicted by the average loading rate of, expressed on the basis of bioreactor volume as 4.86 +/- 1.52 g NO_3^--N m^{-3} d^{-1}, decreasing sharply during the growing season to 1.96 +/- 0.65 g NO_3^--N m^{-3} d^{-1}; even nearing complete removal during the growing season would result in relative underperformance as judged by mass removal rate. Previous work in the Midwest has noted the increased N loading and drainage volume occurring in the spring coincide with low N removal due to decreased residence times and lower temperature, creating a "design and operational challenge" (Christianson et al., 2013).

Other factors likely contributed to suppressing removal rates, specifically low pH conditions and suboptimal bed dimensions. Bed pH averaged 5.3, reflecting the acidic soils typical of the Atlantic Coastal Plain. The inhibition of denitrification at below optimal pH 7-8 is well established (Mateju et al., 1992), but the effect of pH on N removal could not be distinguished. Quantifying and potentially compensating for suppression of removal rates in locations with acid soils like the Atlantic Coastal Plain will require regionally-specific investigation. These acid soils may play a role in the relatively low average removal rates reported for bioreactors in the Maryland Coastal Plain (Christianson et al., 2017; Rosen and Christianson, 2017). Additionally, the bed length to width ratio of 1:1.1, constrained by site characteristics, deviates substantially from the recommended minimum 1:5 to avoid preferential flow (Christianson et al., 2013b). Preferential flow results in dead zones that reduce the effective volume of the bioreactor and cause calculations of theoretical HRT to

overestimate residence times. Calculated HRT values averaged 11 h, but observed removal rates correspond to the averages for HRT < 6 in the Addy et al. (2016) meta-analysis, 0.7 g m^{-3} d^{-1} (95% CI 0.3-1.3), suggesting hydraulic inefficiency may be constraining.

Removal of P was not observed, corroborating findings of Christianson et al. (2011) in laboratory tests and Pluer et al. (2016) in field-scale bioreactors that biochar addition did not enhance P removal. This conflicts with results of a laboratory batch study (Bock et al., 2015), which appears to have limited relevance to field-scale, flow-through systems. Note that different biochars were used in each of these studies, highlighting the considerable variability in biochar properties.

4.5.2 Greenhouse gas emissions

On 13 dates January through October 2016, N_2O emission factors, proportion of NO_3^- removed released as N_2O, ranged -1.8-7.0% for individual measurements and 1.0-2.3% averaging measurements from the three collars. The overall average emission factor was 0.20% and the median only 0.02%, substantially less than the 0.75% determined by the IPCC for agricultural NO_3^- inputs. Although maximum emission factor of 7% observed is the higher than typically reported, most flux measurements yielded emission factors below those reported in the literature. Warneke et al. (2011) reported an average loss of 1% as removed NO3- -N emitted as N_2O-N from the bed surface and an additional 3.3% exported dissolved in the effluent. Elgood et al. (2010) and Moorman et al. (2010) also quantified dissolved N_2O in bioreactor effluent, reporting 0.6% and 0.84% of removed NO_3 -N lost as N_2O, respectively. These analyses of dissolved N_2O export emphasize the potential significance of bioreactors as sources of GHGs even with low emissions from the bed surface. However, the range measured

flux rates, -0.60-19.7 mg N_2O-N m^{-2} d^{-1}, was similar to those dissolved in the effluent of a stream-bed bioreactor and normalized to bed area, -5.4-14.6 mg N_2O-N m^{-2} d^{-1}, and to those reported to represent agricultural soils, 0.1-15 mg N_2O-N m^{-2} d^{-1} (Elgood et al., 2010). Nearly 90% of measured fluxes were within the range reported by Woli et al. (2010) of 0.24-3.12 mg N_2O-N m^{-2} d^{-1}, which the authors considered to be negligible in a tile-fed woodchip bioreactor averaging N removal rates of 6.4 g N m^{-3} d^{-1}. Measured CH_4 fluxes (-0.03-308 mg CH_4-C m^{-2} d^{-1}) were within the range observed by Elgood et al. (2010), -2.6 to 1236 mg CH_4-C m^{-2} d^{-1}, who likewise observed the highest CH_4 production in the warmer summer months (Figure 3b), and noted the similarity to CH_4 fluxes for peatland soils (0.2-423 mg CH_4-C m^{-2} d^{-1}, Lai, 2009). With respect to CO_2, as noted by Schipper et al. (2010), the substrate used in the bioreactor would have decayed and released CO_2 had it been used elsewhere, and thus does not contribute to net CO_2 emissions. Therefore, although individual measurements resulted in high N2O emission factors, and both N_2O and CH_4 contributed significantly to total greenhouse gas emissions from the bed as determined by their carbon dioxide equivalent fluxes, GHG emissions form this particular bioreactor did not raise serious concern.

4.6 Conclusion

The concurrence of the lowest influent N concentrations and periods of no flow with seasonally high temperatures enabling the highest potential rates of denitrification exacerbated the effect of low influent concentration on removal (Figure 1). Additionally, low bed pH and suboptimal bed dimensions may have suppressed removal. However, N mass removal rates (0.41 g NO_3^--N m^{-3} d^{-1}) and efficiency (8.4%) correspond to the low end of reported performance in bioreactors within the Atlantic Coastal Plain region and elsewhere where

influent concentrations are low or residence times are short. The addition of biochar was not successful in removing P, as no statistically significant difference between influent and effluent concentrations was observed. Although effect of biochar on N_2O emissions could not be determined from this study, mitigating the effects of low pH may be important for bioreactor applications in areas with acidic agricultural drainage waters given that ratio N_2:N_2O produced during denitrification is known to decrease with soil pH (Liu et al., 2010).

Understanding the effect of in-bed conditions that limit N removal of GHG emissions and how they are derived from field conditions will help adapt bioreactor designs to a wider range of agricultural systems and geographic regions. Although denitrifying bioreactors becoming important tools for managing agricultural nonpoint source pollution in the Midwest, their performance in other agriculturally important areas in the United States, such as the Mid-Atlantic, is only beginning to be tested. In addition to installation and monitoring of new bioreactors to develop regionally-specific nutrient removal efficiencies, considering how regional differences typically translate to the field scale and how they impact known in-bed controls on N removal (e.g. pH) can help identify differences in design, implementation, and performance requiring further investigation or consideration. Although bioreactor N removal efficiency is highly variable and effectiveness relies on site-specific design, regional difference in artificial drainage networks, cropping systems, soil types, and hydrologic regimes can inform assessment of bioreactor utility and cost-effectiveness in the Mid-Atlantic.

4.7 Acknowledgements

This work was funded by the USDA Natural Resources Conservation Service through a Conservation Innovation Grant.

4.8 References

Addy, K., Gold, A.J., Christianson, L.E., David, M.B., Schipper, L.A., Ratigan, N.A., 2016. Denitrifying bioreactors for nitrate removal: a meta-analysis. J. Environ. Qual. 45(3):873–881. doi:10.2134/jeq2015.07.0399

Bock, E., Smith, N., Rogers, M., Coleman, B., Reiter, M., Benham, B., Easton, Z.M., 2015. Enhanced nitrate and phosphate removal in a denitrifying bioreactor with biochar. J. Environ. Qual. 44(2):605-613. doi:10.2134/jeq2014.03.0111

Bock, E.M., Coleman, B., Easton, Z.M., 2016. Effect of biochar on nitrate removal in a pilot-scale denitrifying bioreactor. J. Environ. Qual. 45(3):762-771. doi:10.2134/jeq2015.04.0179

Burke, P.M., Hill, S., Iricanin, N., Douglas, C., Essex, P., Tharin, D., 2002. Evaluation of preservation methods for nutrient species collected by automatic samplers. Environ. Monit. Assess. 80(2):149–173. doi:10.1023/A:1020660124582

Christianson, L.E., Bhandari, A., Helmers, M.J., 2011a. Pilot-scale evaluation of denitrification drainage bioreactors: reactor geometry and performance. J. Environ. Eng. 137(4):213–220. doi:10.1061/(ASCE)EE.1943-7870.0000316

Christianson, L.E., Bhandari, A., Helmers, M.J., 2011b. Potential design methodology for agricultural drainage denitrification bioreactors. World Environmental and Water Resources Congress 2011. American Society of Civil Engineers, Reston, VA, pp. 2740–2748. doi:10.1061/41173(414)285

Christianson, L.E., Hedley, M., Camps, M., Free, H., Saggar, S., 2011c. Influence of biochar amendements on denitrificaiton bioreactor performance. Report. Massey University.

Christianson, L.E., Christianson, R., Helmers, M., Pederson, C., Bhandari, A., 2013a. Modeling and calibration of drainage denitrification bioreactor design criteria. J. Irrig. Drain. Eng. 139(9): 699–709. doi:10.1061/(ASCE)IR.1943-4774.0000622

Christianson, L.E., Helmers, M., Bhandari, A., Moorman, T., 2013b. Internal hydraulics of an agricultural drainage denitrification bioreactor. Ecol. Eng. 52:298–307. doi:10.1016/j.ecoleng.2012.11.001

Christianson, L.E., Lepine, C., Sibrell, P.L., Penn, C., Summerfelt, S.T. 2017. Denitrifying woodchip bioreactor and phosphorus filter pairing to minimize pollution swapping. Water Res. 121, 129–139. doi:10.1016/J.WATRES.2017.05.026

Collier, S.M., Ruark, M.D., Oates, L.G., Jokela, W.E., Dell, C.J., 2014. Measurement of greenhouse gas flux from agricultural soils using static chambers. J. Vis. Exp. 90:e52110. doi:10.3791/52110

David, M.B., Flint, C.G., Gentry, L.E., Dolan, M.K., Czapar, G.F., Cooke, R.A., Lavaire, T., 2015. Navigating the socio-bio-geo-chemistry and engineering of nitrogen management in two illinois tile-drained watersheds. J. Environ. Qual. 44(2):368-381. doi:10.2134/jeq2014.01.0036

De Klein, C.A.M., Harvey, M.J., 2012. Nitrous oxide Chamber Methodology Guidelines--Version 1.1. Global Reserch Alliance on Agricultural Greenhouse Gases. Available: <https://globalresearchalliance.org/wp-content/uploads/2015/11/Chamber_Methodology_Guidelines_Final-V1.1-2015.pdf> (accessed December 10, 2017)

Dinnes, D.L., Karlen, D.L., Jaynes, D.B., Kaspar, T.C., Hatfield, J.L., Colvin, T.S., Cambardella, C.A., 2002. Nitrogen management strategies to reduce nitrate leaching in tile-drained Midwestern soils. Agron. J. 94:153–171.

Duran, B.E.L., Kucharik, C.J., 2013. Comparison of Two Chamber Methods for Measuring Soil Trace-Gas Fluxes in Bioenergy Cropping Systems. Soil Sci. Soc. Am. J. 77:1601. doi:10.2136/sssaj2013.01.0023

Easton, Z.M., Rogers, M., Davis, M., Wade, J., Eick, M., Bock, E., 2015. Mitigation of sulfate reduction and nitrous oxide emission in denitrifying environments with amorphous iron oxide and biochar. Ecol. Eng. 82:605-613. doi:10.1016/j.ecoleng.2015.05.008

Elgood, Z., Robertson, W.D., Schiff, S.L., Elgood, R., 2010. Nitrate removal and greenhouse gas production in a stream-bed denitrifying bioreactor. Ecol. Eng. 36:1575–1580. doi: 10.1016/j.ecoleng.2010.03.011

Gelmen, A., Hill, J., 2007. Data Analysis Using Regression and Multilevel/Hierarchical Models. Cambridge University Press, New York, NY. p 46.

Ghane, E., Ranaivoson, A.Z., Feyereisen, G.W., Rosen, C.J., Moncrief, J.F., 2016. Comparison of contaminant transport in agricultural drainage water and urban stormwater runoff. PLOS One. 11(12):e0167834. doi:10.1371/journal.pone.0167834

Hartz, T., Smith, R., Cahn, M., Bottoms, T., Bustamante, S.C., Tourte, L., Johnson, K., Coletti, L., 2017. Wood chip denitrification bioreactors can reduce nitrate in tile drainage. Calif. Agric. 71(1):41–47. doi:10.3733/ca.2017a0007

Healy, R.W., Striegl, R.G., Russell, T.F., Hutchinson, G.L., Livingston, G.P., 1996. Numerical evaluation of static-chamber measurements of soil—atmosphere gas exchange: identification of physical processes. Soil Sci. Soc. Am. J. 60(3):740-747. doi:10.2136/sssaj1996.03615995006000030009x

Hua, G., Salo, M.W., Schmit, C.G., Hay, C.H., 2016. Nitrate and phosphate removal from agricultural subsurface drainage using laboratory woodchip bioreactors and recycled steel byproduct filters. Water Res. 102:180-189. doi:10.1016/j.watres.2016.06.022

IA EPA. 2015. Illinois nutrient loss reduction strategy. Springfield, IL. http://www.epa.illinois.gov/assets/iepa/water-quality/watershed-management/nlrs/nlrs-final-revised-083115.pdf (accessed 11 Dec. 2017).

IDALS. 2014. Iowa nutrient reduction strategy: A science and technology-based framework to assess and reduce nutrients to Iowa waters and the Gulf of Mexico. Iowa Department of Agriculture and Land Stewardship, Iowa Department of Natural Resources, and Iowa State

University. http://www.nutrientstrategy.iastate.edu/ (accessed 11 Dec. 2016).

Ikenberry, C.D., Soupir, M.L., Schilling, K.E., Jones, C.S., Seeman, A., 2014. Nitrate-nitrogen export: magnitude and patterns from drainage districts to downstream river basins. J. Environ. Qual. 43(6):2024-2033. doi:10.2134/jeq2014.05.0242

IPCC, 2007. Contribution of Working Groups I, II, and III to the Fourth Assessment Report of the Intergovernmental Panel on Climate Change. Core Writinng Team, Pachauri, R.K. and Reisinger, A. (Eds.)

Kladivko, E.J., Van Scoyoc, G.E., Monke, E.J., Oates, K.M., Pask, W., 1991. Pesticide and nutrient movement into subsurface tile drains on a silt loam soil in Indiana. J. Environ. Qual. 20(1):264-270. doi:10.2134/jeq1991.00472425002000010043x

Kutzbach, L., Schneider, J., Sachs, T., Giebels, M., Nykänen, H., Shurpali, N.J., Martikainen, P.J., Alm, J., Wilmking, M., 2007. CO_2 flux determination by closed-chamber methods can be seriously biased by inappropriate application of linear regression. Biogeosciences 4, 1005–1025.

Lai, D.Y.F., 2009. Methane dynamics in northen peatlands: a review. Pedosphere. 19(4):409-421. doi: 10.1016/S1002-0160(09)00003-4

Liu, B., Mørkved, P.T., Frostegård, Å., Bakken, L.R., 2010. Denitrification gene pools, transcription and kinetics of NO, N_2O and N_2 production as affected by soil pH. FEMS Microbiol. Ecol. 72(3):407–417. doi:10.1111/j.1574-6941.2010.00856.x

Livingston, G.P., Hutchinson, G.L., Spartalian, Kevork, N.D. Trace gas emission in chambers: a non-steady-state diffusion model. Soil Sci. Soc. Am. J. 70:1459-1469. doi:10.2136/sssaj2005.0322

Mateju, V., Cizinska, S., Krejci, J., Janock, T., 1992. Biological water denitrificaiton - a reivew. Enzyme Microb. Technol. 14(3):170–183. doi:10.1016/0141-0229(92)90062-S

MN PCA. 2014. The Minnesota nutrient reduction strategy. Minnesota Pollution Control Agency, St. Paul, MN. https://www.pca.state.mn.us/sites/default/files/wq-s1-80.pdf (accessed 11 Dec. 2016).

Moorman, T.B., Parkin, T.B., Kaspar, T.C., Jaynes, D.B., 2010. Denitrification activity, wood loss, and N_2O emissions over 9 years from a wood chip bioreactor. Ecol. Eng. 36:1567–1574. doi: 10.1016/j.ecoleng.2010.03.012

Partheeban, C., Karkl, G., Khand, K.B., Kjaersgaard, J., Hay, C., Troolen, T., 2014. Calibration of AgriDrain control structure by using generalized "V" notch weir equation for flow measurement. Western South Dakota Hydrology Conference. https://www.researchgate.net/publication/276832543_Calibration_of_AgriDrain_control_structure_by_using_generalized_V_notch_weir_equation_for_flow_measurement (accessed 12 Dec. 2016).

Pluer, W.T., Geohring, L.D., Steenhuis, T.S., Walter, M.T., 2016. Controls influencing the

treatment of excess agricultural nitrate with denitrifying Bioreactors. J. Environ. Qual. 45(3):772-778. doi:10.2134/jeq2015.06.0271

R Core Team, 2017. R: A language and environment for statistical computing. R Foundation for Statistical Computing, Vienna, Austria. http://www.R-project.org/

Rosen, T., Christianson, L., 2017. Performance of denitrifying bioreactors at reducing agricultural nitrogen pollution in a humid subtropical coastal plain climate. Water 9(2): [112]. doi:10.3390/w9020112

Schipper, L.A., Robertson, W.D., Gold, A.J., Jaynes, D.B., Cameron, S.C., 2010b. Denitrifying bioreactors—An approach for reducing nitrate loads to receiving waters. Ecol. Eng. 36:1532–1543. doi:10.1016/j.ecoleng.2010.04.008

Skaggs, R., Youssef, M., Gilliam, J., Evans, R., 2010. Effect of controlled drainage on water and nitrogen balances in drained lands. Trans. ASABE. 53(6):1843-1850. doi: 10.13031/2013.35810

Soil Survey Staff, Natural Resources Conservation Service, United States Department of Agriculture. Web Soil Survey. Available online at the following link: https://websoilsurvey.sc.egov.usda.gov/ (accessed 6 April 2017).

USDA NASS, 2012 Census of Agriculture, Ag Census Web Maps. Available at: www.agcensus.usda.gov/Publications/2012/Online_Resources/Ag_Census_Web_Maps/ Overview/Warneke, S., Schipper, L.A., Bruesewitz, D.A., Baisden, W.T., 2011a. A comparison of different approaches for measuring denitrification rates in a nitrate removing bioreactor. Water Res. 45(14):4141–4151. doi:10.1016/j.watres.2011.05.027

USDA-NRCS. 2015. Conservation practice standard denitrifying bioreactor code 605 (605-CPS-1). USDA-NRCS, Washington, DC.

Warneke, S., Schipper, L.A., Bruesewitz, D.A., McDonald, I., Cameron, S., 2011a. Rates, controls and potential adverse effects of nitrate removal in a denitrification bed. Ecol. Eng. 37:511–522. doi:10.1016/j.ecoleng.2010.12.006

Warneke, S., Schipper, L.A., Matiasek, M.G., Scow, K.M., Stewart Cameron, Bruesewitz, D.A., McDonald, I.R., 2011b. Nitrate removal, communities of denitrifiers and adverse effects in different carbon substrates for use in denitrification beds. Water Res. 45(17):5463–5475. doi:doi: 10.1016/j.watres.2011.08.007

Williams, M.R., King, K.W., Fausey, N.R., 2015. Drainage water management effects on tile discharge and water quality. Agric. Water Manag. 148:45-51. doi:10.1016/j.agwat.2014.09.017

Woli, K.P., David, M.B., Cooke, R.A., McIsaac, G.F., Mitchell, C.A., 2010. Nitrogen balance in and export from agricultural fields associated with controlled drainage systems and denitrifying bioreactors. Ecol. Eng. 36:1558–1566. doi:10.1016/j.ecoleng.2010.04.024

5.0 CONCLUSIONS

5.1 Summary

Denitrifying bioreactors hold promise for managing agricultural drainage in the Mid-Atlantic, but challenges remain with respect to adapting designs for large subsurface drainage networks to the ditch drainage systems and small, targeted tile drain systems typical of this region. Growing interest in denitrifying bioreactors has expanded the application geographically, spurred active efforts in substrate engineering (Christianson and Schipper, 2016), and a renewed focus on mitigating unintended impacts of bioreactors related to pollution swapping. Motivated by the success of bioreactors in mitigating N export from agricultural systems in the US Midwest, opportunities to expand bioreactor application operationally and geographically were investigated. Each section of this document has provided context, approaches, and analyses to support the advancement of bioreactor technology to improve environmental outcomes. Substrate engineering to enhance biologically mediated N removal was investigated in Section 2, controls on production of the harmful greenhouse gases (GHGs) and additional opportunities for substrate engineering were explored in Section 3, and performance of one of the first denitrifying bioreactors implemented in the Mid-Atlantic Coastal Plain was evaluated in Section 4.

The pilot study demonstrated that biochar has the potential to enhance NO_3^--N removal in woodchip DNBRs receiving sufficiently NO_3^--N-enriched influent at concentrations (5-10 mg NO_3^--N l^{-1}) likely to be encountered in agricultural drainage. By achieving a given level of removal with a shorter residence time than a woodchip bed, biochar amendment could either allow for smaller bed designs or the treatment of larger flows with high NO_3^--N concentrations.

An economic analysis of the costs and N removal benefits from woodchip and biochar-amended bioreactor developed with removal efficiencies predicted by the model developed during this pilot study indicated that if these predictions represent field performance, biochar amendment could be a cost-effective means to boost N removal (DeBoes et al., 2017). However, considerable uncertainty in the magnitude of the effect of biochar on N removal within the context of the pilot study remains and, as emphasized by Christianson et al. (2016), the effect of wood-based biochars on N removal in bioreactors must be validated at the field scale. Further motivation to investigate the performance of biochar-amended bioreactors was supplied by a laboratory batch experiment suggesting that these wood-based biochars increase P removal and reduced nitrous oxide (N_2O) emissions relative to woodchips alone (Bock et al., 2015). Indeed, with agricultural drainage also recognized as important sources of P export (Gentry et al., 2007) and agricultural sources representing approximately 6% of total anthropogenic N_2O emissions (IPCC, 2007), leveraging denitrifying bioreactors to address these pollutants presents a natural opportunity.

With a growing interest in managing pollution trade-offs within denitrifying bioreactors (Christianson and Schipper, 2016), a controlled laboratory experiment with horizontal flow-through bioreactor columns was used to test the effect of pine-feedstock biochar on GHGs N_2O, methane (CH_4), and carbon dioxide (CO_2). Biochar amendment was found to substantially increase N_2O and CO_2 flux compared to woodchips alone across the range of hydraulic residence times (HRTs 3,6, and 12 h) and influent concentrations (4.5 and 16.1 mg NO_3^--N l^{-1}) tested, with fluxes increasing with longer residence times, and for N_2O, with increased N loading. While CH_4 fluxes across all media types tested (woodchips, 10% biochar, 30% biochar)

were negligible, N_2O fluxes contributed an average of over 20% of the total global warming potential produced by the columns. The data suggest that higher rates of biochar may increase GHG fluxes, posing a caution to evaluating the potential benefits of N removal with biochar amendment without a mass-balance approach to determine the fate of removed N.

Biochar amendment to woodchip bioreactors would not be recommended without prior verification of a specific biochar's effects on GHG emissions and better understanding of the mechanisms involved. Adding additional complication, the variability of biochar materials as a function of feedstock and pyrolysis process (mainly temperature and oxygen levels) and how these characteristics affect properties relevant to the yet-to-be determined mechanism influencing denitrification and other biochemical processes resulting in nutrient removal or GHG production should be considered. The freshness of the carbon media (both woodchips and biochar) used in this study also constrains the transferability of the results, because recent work has shown that the ability of biochar to enhance N removal may erode over months to years (Pleur et al., 2016). Consequently, the laboratory study is unlikely to be predictive of long-term performance, this conclusion being supported by a recent bioreactor meta-analysis by Addy et al. (2016) substantiating that laboratory experiments produce significantly higher rates of N removal than field-experiments. While the tightly controlled conditions of a laboratory likely favor higher rates of removal over the more variable conditions of the field, this decrease in performance over time for both woodchips and biochar suggests that more labile components of the bioreactor media temporarily sustain higher removal rates. Perhaps the increase in GHG emissions with biochar amendment would also decrease over time as the more labile components are consumed. The effect of biochar amendment on both N removal and GHG

emissions must be further investigated before a determination can be made regarding the benefits or detriments of its application.

In addition to exploring opportunities to enhance bioreactor performance with biochar, the aim of this work was to investigate the potential to use denitrifying bioreactors to address water quality problems in the Chesapeake Bay watershed. Although denitrifying bioreactors becoming important tools for managing agricultural nonpoint source pollution in the Midwest, their performance in other agriculturally important areas in the United States, such as the Mid-Atlantic, remains largely untested. A field-scale study of a woodchip bioreactor amended with 17% pine-feedstock biochar (same material as column study) installed in the Atlantic Coastal Plain provided insight into potential opportunities and challenges for bioreactors in this region. The main distinguishing characteristic of this installation was the atypically low N loading as a result of continuous soy cultivation without fertilizer application in the drainage area, on average 10.0 kg ha yr^{-1}, which resulted an average N removal rate on the lower boundary of those reported in the literature, 0.41 g N m^{-3} d^{-1}. N removal was likely also constrained by additional factors including low pH, substantial periods of no flow during the growing season, and a ~1:1 length to width ratio deviating from the recommended maximum of 1:5. However, low influent N concentrations and loading, particularly during the growing season when elevated temperatures allow higher potential denitrification rates, was the dominant cause of low removal. Significant P removal was not observed. Greenhouse gas fluxes were driven by CO_2, which increased with temperature and as influent N or HRT decreased. However, N_2O and CH_4 both contributed significantly to total GHG emissions at times suggesting that incomplete denitrification was significant, potentially due to low pH, and overly lengthy HRTs sometimes

enabled methanogenesis. These findings form one of the first bioreactor applications in the Mid-Atlantic Coastal Plain provide a useful information for establishing regionally-specific nutrient removal rates for denitrifying bioreactors. Additionally, this work provides a unique assessment of performance under consistently low N loading, which has relevance to soy cultivation in rotation cropping, or use of bioreactors in conjunction with drainage water management, which in itself can be very effective at reducing N export (Skaggs et al., 2010).

Understanding the effect of the in-bed conditions that limit N removal and increase GHG production and how they are derived from field conditions will help adapt bioreactor designs to a wider range of agricultural systems and geographic regions. Considering the regional differences at the field scale and how they impact known in-bed controls on N removal can identify differences in design, implementation, and performance requiring further investigation or consideration. Although bioreactor N removal efficiency is highly variable and their effectiveness relies on site-specific design, regional difference in artificial drainage networks, cropping systems, soil types, and hydrologic regimes can inform assessment of bioreactor utility and cost-effectiveness in the Mid-Atlantic.

5.2 Future Work

As research relating to denitrifying bioreactors continues to gain momentum, and the controls on performance are identified, focus will shift to identifying approaches for cost-effective implementation and adapting designs to a wider range of applications. Although some experiments with biochar and other organic carbon media have shown some promise with respect to increasing N removal rates, little of this work has been successfully translated to the field scale with questions remaining about longevity in the field and mechanisms of action.

Early efforts to refocus on the physical design of bioreactors are expanding the horizon and show perhaps the most promise for increasing the impact of bioreactors (Christianson et al., 2017). Adapting the traditional tile drain bioreactor design to ditch drainage networks, overcoming shallow water tables and low gradients, and more effectively treating low N loads in small tile drain systems has the potential to yield substantial water quality benefits in the Chesapeake Bay watershed where surface drainage of agricultural land predominates. However, opportunities to improve performance through substrate engineering remain, such as for mitigating the effects of low pH, which can limit N removal and increase N_2O production. As more holistic evaluation of bioreactor performance includes consideration of GHG emissions and other harmful byproducts, understanding of the controls and mechanisms of GHG export should be refined. Though denitrifying bioreactors are becoming important tools for managing agricultural nonpoint source pollution, exciting opportunities to improve their performance and expand their application await.

5.3 References

Addy, K., Gold, A.J., Christianson, L.E., David, M.B., Schipper, L.A., Ratigan, N.A., 2016. Denitrifying bioreactors for nitrate removal: a meta-analysis. J. Environ. Qual. 45(3):873–881. doi:10.2134/jeq2015.07.0399

Bock, E., Smith, N., Rogers, M., Coleman, B., Reiter, M., Benham, B., Easton, Z.M., 2015. Enhanced nitrate and phosphate removal in a denitrifying bioreactor with biochar. J. Environ. Qual. 44(2):605-613. doi:10.2134/jeq2014.03.0111

Bock, E.M., Coleman, B., Easton, Z.M., 2016. Effect of biochar on nitrate removal in a pilot-scale denitrifying bioreactor. J. Environ. Qual. 45(3):762-771. doi:10.2134/jeq2015.04.0179

Christianson, L.E., Schipper, L.A., 2016. Moving denitrifying bioreactors beyond proof of concept: introduction to the special section. J. Environ. Qual. 45(3):757-761. doi:10.2134/jeq2016.01.0013

Christianson, L.E., Lepine, C., Sibrell, P.L., Penn, C., Summerfelt, S.T. 2017. Denitrifying woodchip bioreactor and phosphorus filter pairing to minimize pollution swapping. Water Res. 121,

129–139. doi:10.1016/J.WATRES.2017.05.026

DeBoe, G., Bock, E., Stephenson, K., Easton, Z., 2017. Nutrient biofilters in the Virginia Coastal Plain: nitrogen removal, cost, and potential adoption pathways. J. Soil Water Conserv. 72(2): 139–149. doi:10.2489/jswc.72.2.139

Gentry, L.E., David, M.B., Royer, T.V., Mitchell, C.A., and K.M. Starks. 2007. Phosphorus transport pathways to stream in tile-drained agricultural watersheds. J. Environ. Qual. 36:408-415. doi:10.2134/jeq2006.0098

Skaggs, R., Youssef, M., Gilliam, J., Evans, R., 2010. Effect of controlled drainage on water and nitrogen balances in drained lands. Trans. ASABE. 53(6):1843-1850. doi:10.13031/2013.35810